IMPROVEMENT AND ECONOMIC ANALYSIS OF BIO-HYDROGENATED DIESEL PRODUCTION FOR PRODUCING BIO-JET FUEL

Miss Nattamon Munkong

A Thesis Submitted in Partial Fulfillment of the Requirements
for the Degree of Master of Engineering in Chemical Engineering
Department of Chemical Engineering
FACULTY OF ENGINEERING
Chulalongkorn University
Academic Year 2019

การปรับปรุงและการประเมินความคุ้มค่าทางเศรษฐศาสตร์ของการผลิตไบโอไฮโดรจีเนตดีเซลเพื่อผลิตเชื้อเพลิงเครื่องบินชีวภาพ

น.ส.นัทธมน มั่นคง

วิทยานิพนธ์นี้เป็นส่วนหนึ่งของการศึกษาตามหลักสูตรปริญญาวิศวกรรมศาสตรมหาบัณฑิต
สาขาวิชาวิศวกรรมเคมี ภาควิชาวิศวกรรมเคมี
คณะวิศวกรรมศาสตร์ จุฬาลงกรณ์มหาวิทยาลัย
ปีการศึกษา 2562

Thesis Title	IMPROVEMENT AND ECONOMIC ANALYSIS OF BIO-HYDROGENATED DIESEL PRODUCTION FOR PRODUCING BIO-JET FUEL
By	Miss Nattamon Munkong
Field of Study	Chemical Engineering
Thesis Advisor	Professor Dr. SUTTICHAI ASSABUMRUNGRAT
Thesis Co Advisor	Assistant Professor Dr. Suksun Amornraksa

Accepted by the FACULTY OF ENGINEERING, Chulalongkorn University in Partial Fulfillment of the Requirement for the Master of Engineering

..... Dean of the FACULTY OF ENGINEERING

(Professor Dr. SUPOT TEACHAVORASINSKUN)

THESIS COMMITTEE

..... Chairman

(Dr. PARAVEE VAS-UMNUAY)

..... Thesis Advisor

(Professor Dr. SUTTICHAI ASSABUMRUNGRAT)

..... Thesis Co-Advisor

(Assistant Professor Dr. Suksun Amornraksa)

..... Examiner

(Professor Dr. BUNJERD JONGSOMJIT)

..... External Examiner

(Assistant Professor Dr. Lida Simasatitkul)

นัทธมน มั่นคง : การปรับปรุงและการประเมินความคุ้มค่าทางเศรษฐศาสตร์ของการผลิตไบโอไฮโดรจีเนตดีเซลเพื่อผลิตเชื้อเพลิงเครื่องบินชีวภาพ. (IMPROVEMENT AND ECONOMIC ANALYSIS OF BIO-HYDROGENATED DIESEL PRODUCTION FOR PRODUCING BIO-JET FUEL) อ.ที่ปรึกษาหลัก : ศ. ดร.สุทธิชัย อัสสะบำรุงรัตน์, อ.ที่ปรึกษาร่วม : ผศ. ดร.สุขสันต์ อมรรักษา

งานวิจัยนี้ศึกษาการปรับปรุงกระบวนการผลิตไบโอไฮโดรจีเนตดีเซล (BHD) เพื่อผลิตเชื้อเพลิงเครื่องบินชีวภาพเป็นผลิตภัณฑ์ทางเลือก ไบโอไฮโดรจีเนตดีเซลผลิตจากน้ำมันปาล์มด้วยการใช้ตัวเร่งปฏิกิริยา NiMo/*Y*-Al_2O_3 ในขณะที่เชื้อเพลิงเครื่องบินชีวภาพผลิตจากปฏิกิริยาไฮโดรแครกกิ้งด้วยตัวเร่งปฏิกิริยา NiAg/SAPO-11 โดยใช้ BHD เป็นวัตถุดิบ แล้วตามด้วยกระบวนการแยกที่เหมาะสม การประเมินกระบวนการที่ปรับปรุงแล้วถูกจำลองโดยใช้โปรแกรม Aspen Plus และการเปรียบเทียบกับกระบวนการผลิต BHD ซึ่งเป็นกรณีฐานจะถูกอธิบายและพิจารณาในงานวิจัยนี้ ผลจากงานวิจัยพบว่ากระบวนการผลิต BHD สามารถปรับปรุงได้โดยการเพิ่มส่วนไฮไดรแครกกิ้ง/ไอโซเมอร์ไรซ์เซชั่นเข้ากับกระบวนการปัจจุบัน ผลิตภัณฑ์ของกระบวนการหลังปรับปรุง คือเชื้อเพลิงเครื่องบินชีวภาพที่มีส่วนประกอบหลักเป็นออกตะเดกเคน 280,000 บาร์เรลต่อปี และไบโอดีเซลที่มีส่วนผสมหลักเป็นเพนตะเดกเคน 230,000 บาร์เรลต่อปี ค่าความร้อนสูง (HHV) ที่ 15 องศาเซลเซียสของเชื้อเพลิงเครื่องบินชีวภาพได้เท่ากับ 43.53 เมกะจูลต่อกิโลกรัม สัดส่วนผลิตภัณฑ์โดยรวมของโรงงานผลิตเชื้อเพลิงเครื่องบินชีวภาพ/ไบโอดีเซล คือ 37.7% และ 29.7% โพรเพนเป็นผลพลอยได้ของกระบวนการและมีความบริสุทธิ์ที่ 91.73 เปอร์เซ็นต์โมล ในการประเมินความคุ้มค่าทางเศรษฐศาสตร์ พบว่าเงินทุนคงที่ของโรงงานผลิตเชื้อเพลิงเครื่องบินชีวภาพ/ไบโอดีเซลเพิ่มเป็นสองเท่าของโรงงานผลิต BHD และต้นทุนการผลิตเพิ่มขึ้น 17 เปอร์เซ็นต์จากการใช้ไฮโดรเจนที่มากขึ้น 52 เปอร์เซ็นต์ จากการเพิ่มกำลังการผลิตของโรงงานผลิตเชื้อเพลิงเครื่องบินชีวภาพ/ไบโอดีเซลพบว่าโครงการมีความเป็นไปได้ทางเศรษฐศาสตร์โดยมี IRR 29.07 เปอร์เซ็นต์

สาขาวิชา	วิศวกรรมเคมี	ลายมือชื่อนิสิต .....
ปีการศึกษา	2562	ลายมือชื่อ อ.ที่ปรึกษาหลัก .....
		ลายมือชื่อ อ.ที่ปรึกษาร่วม .....

6170936721 : MAJOR CHEMICAL ENGINEERING

KEYWORD: bio-hydrogenated diesel, bio-jet fuel, biodiesel, economic analysis

Nattamon Munkong : IMPROVEMENT AND ECONOMIC ANALYSIS OF BIO-HYDROGENATED DIESEL PRODUCTION FOR PRODUCING BIO-JET FUEL. Advisor: Prof. Dr. SUTTICHAI ASSABUMRUNGRAT Co-advisor: Asst. Prof. Dr. Suksun Amornraksa

In this study, process improvement of bio-hydrogenated diesel (BHD) production to produce jet fuel as an alternative product was carried out. The BHD was produced from palm oil with NiMo/*Y*-Al_2O_3 catalyst, while the bio-jet fuel was produced by catalytic cracking of the BHD product using NiAg/SAPO-11 catalyst, followed by appropriate separations. Process simulation by using Aspen Plus program was performed to evaluate the improved process. A comparison with a base case BHD production process was also demonstrated and discussed. It was found that a conventional existing BHD process can be improved by plugging in a hydrocracking/isomerization unit to process. The product of the modified plant was 280 thousand barrel per year bio-jet fuel having the main composition of octadecane and 230 thousand barrel per year biodiesel having the main composition of pentadecane. The higher heating value (HHV) at 15 degree celsius of the bio-jet fuel is found to be 43.53 MJ/kg. The overall product yield of bio-jet fuel/biodiesel plant was 37.7% and 29.7%. The propane by-product obtained was 91.73 %mol in purity. In economic analysis, the fixed capital investment of the bio-jet/biodiesel plant was two times higher than the original BHD plant and the manufacturing cost was increased by 17%, resulting from the increase of 52% hydrogen consumption. By increasing plant capacity, the project was feasible with 29.07% of IRR.

Field of Study:	Chemical Engineering	Student's Signature .....
Academic Year:	2019	Advisor's Signature .....
		Co-advisor's Signature .....

ACKNOWLEDGEMENTS

It is a pleasure to thank those who made this thesis possible. Firstly, I am heartily thankful to my advisor, Professor Dr. Suttichai Assabumrungrat, and co-advisor, Assistant Professor Dr. Suksun Amornraksa, for giving me the opportunity to do this research. They also provided insight and expertise that greatly assisted this research.

I would like to thank my thesis committee, Dr. Paravee Vas-umnuay, Professor Dr. Bunjerd Jongsomjit, and Assistant Professor Dr. Lida Simasatitkul, for their vision and great suggestions to fulfill my research. I am extremely grateful for Dr. Amata Anantpinijwatna and Dr. Pongtorn Charoensuppanimit, who educated me on the methodology and guidance on simulation to figure out the problem during the research study.

I gratefully acknowledge the Center of Excellence in Catalysis and Catalytic Reaction Engineering, Department of Chemical Engineering, Faculty of Engineering, Chulalongkorn University, for the support of Aspen Plus program.

Finally, I would like to thank my caring and loving family and friends who always support and understand me during the rough time of the study. It was a great comfort knowing that they were willing to provide encouragement for me. It was helpful to complete this thesis successfully.

Nattamon Munkong

TABLE OF CONTENTS

Page

LIST OF TABLES

Page

LIST OF FIGURES

Page

CHAPTER 1 INTRODUCTION

1.1 Motivation

Human activities have been recognized as one of the root causes of global warming. Scientific evidence indicates that the rising of carbon dioxide (CO_2) levels in the atmosphere is related to the increasing of average global temperature over the past 60 years. The level of CO_2 in the atmosphere has increased from 270 to 400 ppm from 1850 to 2010. The amount of CO_2 emission from anthropogenic is 63% of major greenhouse gases, and most of them are emitted by the burning of fossil fuel [1, 2]. Global energy consumption has become greater along with population growth, economic growth, and technological process. In 2014, world primary energy consumption reached about 12.93 billion tons of standard oil equivalent, which includes coal 30.0%, petroleum 32.6%, and natural gas 23.7% [2]. By examination, population growth accelerates energy demand, which is projected to be doubled by 2050 [3]. This growth will lead to the depletion of energy sources, and the world will face an energy supply shortage in the coming years. The transportation sector is the primary source of energy consumption, which mainly uses gasoline and diesel [3]. Therefore, researchers are currently finding alternative and renewable fuels to meet up the future energy demand.

Presently, the world trend is focusing on biofuel as an alternative source for the transportation sector. Comparatively, there are three advantages of biofuel over petroleum fuel. Firstly, biofuel is a renewable resource that can be easily extracted from biomass. Secondly, fewer toxic compounds are released into the atmosphere during the combustion process. Thirdly, biofuel is a CO_2 neutral energy source as the released CO_2 emission is absorbed during cultivation [4, 5]. Moreover, using biodiesel in a diesel engine has been proved that it can enhance diesel engine power while specific fuel consumption decreases [3].

Biofuel can be divided into three generations. The 1st generation is bioethanol produced by fermentation of starch or sugar, and biodiesel produced by transesterification of vegetable oils from food crops. The 2nd generation is bioethanol and biodiesel produced from non-food raw material such as biomass by appropriate conversion technologies, i.e., biochemical and thermochemical conversion processes. The 3rd generation is biodiesel from microalgae and seaweed [4, 6]. Petroleum diesel can be replaced with biodiesel fuels due to similarity in chemical structure, although it has lower volumetric heat capacity. Nowadays, there are two ways to produce biodiesel. A conventional route is transesterification of triglyceride to produce fatty acid methyl esters (FAME), which is a major constituent of biodiesel. This method produces glycerol as a by-product. Another interesting route is a deoxygenation process such as hydrodeoxygenation (HDO), decarbonylation (DCO), and decarboxylation (DCO_2) [6]. In this

process, renewable feedstock containing triglycerides and fatty acids reacts with H_2 gas at a high temperature ranging between 270-420 ℃ and operating pressure between 15-80 bars. Then, the obtained products are isoparaffin-rish diesel, containing C_{15} –C_{18} hydrocarbon. This product is also known as 'bio-hydrogenated diesel' (BHD) or 'green diesel'. Propane, carbon dioxide, and water are also produced as by-products by this process [7-9]. The deoxygenated iso-paraffin diesel helps increase the cetane number of the fuel because it contains long-chain paraffins which have the best ignition quality characteristics among hydrocarbons. In addition, it has better oxidation stability due to its low content of chemically-bond oxygen [10, 11].

It is interesting to note that the process for producing BHD can also produce jet fuel, C_9-C_{18} hydrocarbons because triglyceride based vegetable oil can be directly converted into cyclo-paraffin and aromatic components. In terms of hydrocarbon mole ratio, the jet fuel produced by this process has good flow properties, good thermal stability, and low freezing point, which can meet the requirement of aviation fuel properties [12]. Therefore, using triglycerides as feedstock for producing alternative jet fuel is possible and attractive.

The hydrodeoxygenation process is an essential step for converting bio-based feedstocks to deoxygenated fuel, which is compatible with conventional petroleum-based fuel. The process is usually carried out under high pressure and high temperature in the presence of a suitable catalyst. From a study on the hydrodeoxygenation of crude palm oil, degummed palm oil, and palm fatty acid distillate, sulfided NiMo/γ-Al_2O_3 catalyst was found to be suitable for triglyceride feedstock [7]. The operating condition for hydrotreating of palm oil examined was at a temperature between 370-460 ℃ and H_2 pressure between 550-925 psig. After the reaction complete, by-product gases, mainly propane, were separated in a flash drum. The alkane products were distilled in a distillation column, followed by a hydrocracking process to cut off long chain length carbon [8, 11].

For large scale production of the deoxygenated fuel, an economic assessment was done by using process simulation and techno-economic analysis to estimate the capital cost and operating cost. It was found that a stand-alone hydrodeoxygenation plant required a high investment cost in order to build new infrastructure and facilities [10]. Also, almost 98% of the total operating cost was contributed from the feedstock, catalyst, and hydrogen usages [11]. Therefore, the process is not suitable for small scale production. The first industrial-scale plant for the production of renewable diesel with a capacity of 170,000 tons/year is Neste Oil's Porvoo oil refinery [13]. The bio-based fuel products are diesel, gasoline, and jet fuel range, which depend on the type of feedstock, catalyst, and operating conditions. Due to the complexity of the process and the requirements to handle the flexible type of feedstocks, this technology still

requires a very high investment cost, which can only be compensated by the high capacity of the plant only [10].

This study aims to upgrade the existing process of biodiesel production to produce bio-jet fuel as an alternative product. To overcome the economic limitation of stand-alone hydroprocessing plant, the same infrastructure of the existing plant will be used, with some modifications. The operating conditions are adjusted in order to produce the two products. Process optimization, as well as other operating costs, will be performed.

1.2 Research objective

1.2.1 To study and improve bio-hydrogenated diesel production to produce jet fuel range hydrocarbon as an alternative product.

1.2.2 To do a feasibility study of the industrial-scale process

1.3 Research scopes

1.3.1 The study is conducted by process simulation using Aspen plus V9 program.

1.3.2 Crude palm oil is used as bio-based feedstock.

1.3.3 The operating conditions of the study are temperature between 370-460°C and pressure between 550-925 psig.

1.3.4 NiMo/γ-Al_2O_3 is used as a catalyst.

1.3.5 Product composition from simulation results is compared to literature's data.

1.4 Expected benefits

This research provides insights for the improvement of biofuel energy production in commercial scale and utilization of the by-product of the bio-hydrogenated process to minimize the operating cost.

CHAPTER 2 FUNDAMENTALS AND LITERATURE REVIEWS

This chapter provides related theoretical background as well as a literature review of previous works in the field of bio-hydrogenated diesel production and bio-jet fuel production.

2.1 Fundamentals

2.1.1 Bio-hydrogenated diesel

Bio-hydrogenated diesel (BHD) or green diesel is different from traditional biodiesel. It is one of the renewable fuel-producing from hydro-processing of bio-based feedstocks, which are chemically not ester-based [11]. Bio-based feedstocks enriched with triglycerides are common crude material for BHD production. Triglycerides and fatty acids are converted to straight-chain alkane ranging from n-C_{15} to n-C_{18}, which are in diesel fuel range and have a higher cetane number than conventional biodiesel [7]. BHD production requires the presence of a suitable catalyst and hydrogen to eliminate oxygen in the fatty acid molecule. The renewable feed is introduced to a catalytic hydrodeoxygenation reactor to react with hydrogen at moderate to high reaction conditions [14]. The unsaturated oils in the feed are hydrogenated to saturated oils. It is then followed by hydrogenolysis to convert saturated triglyceride and fatty acid to free fatty acid (FFA), by removing propane and then releasing oxygen by hydrodeoxygenation (HDO), decarbonylation (DCO) and decarboxylation (DCO_2). The by-products are propane, water, and carbon dioxide [11].

The BHD is the 2nd generation biodiesel, while the 1st generation is the ester-based biodiesel obtained by the conventional transesterification of edible or non-edible oil. During transesterification, hydrolysis of the ester bond between glycerol and the fatty acid chain was occurred, followed by esterification with alcohol, generally methanol. The product from this process is called fatty acid methyl esters (FAME), which is a major component of biodiesel [4]. The main routes that are used to produce biofuels from natural triglycerides are demonstrated in Figure 1 [14].

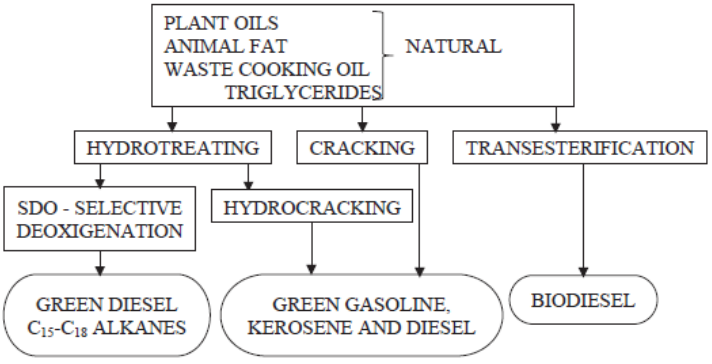

Figure 1 Main routes for treatment of natural triglycerides

Some properties of BHD are better than conventional biodiesel, such as low oxidative stability. The properties of BHD, traditional biodiesel, and ultra-low sulfur diesel are compared and illustrated in Table 1 [11].

Table 1 Properties of BHD, biodiesel and Ultra-low sulfur diesel.

	BHD	**Biodiesel**	**Ultra-low sulfur diesel**
Sulfur (ppm)	<10	<10	46
LHV (MJ/kg)	44	38	42.7
Cloud point (°C)	-20	-5	-12
Distillation (°C) (10-90%)	265-320	340-355	264-329
Cetane number	>80	50	53.9
Oxygen (%)	0	11	0
Density at 15 °C (kg/m^3)	780	880	840
Viscosity at 40 °C (mm^2/s)	2.5	4.1	2.5
Aromatics (wt%)	0	0	24.4
Stability	Good	Marginal	Good

2.1.2 Reaction involves in hydroprocessing [12], [14]

The triglycerides of plant oil, for example, tripalmitin, triolein, tristrearin and trilinolein, can be converted into BHD by catalytic hydrotreating. Unsaturated triglycerides are hydrogenated to saturated ones and then broken down from one triglyceride molecule into three fatty acid molecules by hydrogenolysis. After that, the fatty acid can go through one of three different pathways, i.e., hydrodeoxygenation (HDO), decarbonylation (DCO), or decarboxylation (DCO_2) to produce the BHD. In the HDO pathway, oxygen is removed from the fatty acid molecule in the presence of a metal catalyst. The product from this reaction is n-alkanes that have the same number of carbon as the interrelated fatty acids. The DCO removes oxygen by releasing CO, while the DCO_2 removes CO_2 from the free fatty acid molecules. The resultant straight-chain alkane products will have one less carbon atom than the initial fatty acid. Possible reactions involving the three pathways for BHD processing are given in the next sections.

a) Hydrogenation and hydrogenolysis

Unsaturated or double bond triglycerides are converted to saturated fatty acids by hydrogenation. It is crucial to decrease the degree of unsaturated bond in the based oil as it affects chemical stability and reactivity during the deoxygenation reaction, which leads to the formation of different n-alkane products. In the view of the chemical property, a saturated fatty

acid is better in terms of oxidative stability. Moreover, the hydrogen consumed by this process is depended on the number of double bond in based oil. Figure 2 shows the hydrogenation pathway of triglyceride, it is then followed by hydrogenolysis to convert saturated triglyceride to free fatty acid (FFA) by removing propane.

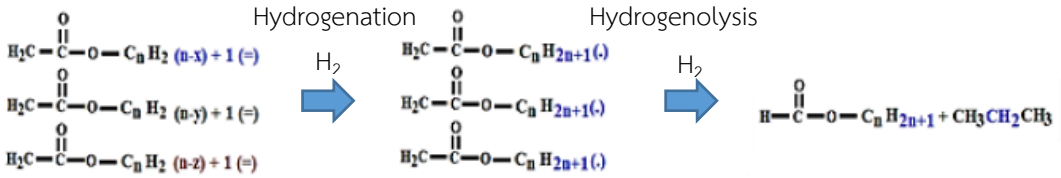

Figure 2 Hydrogenation pathway of triglyceride.

b) Hydrodeoxygenation (HDO)

The conversion of fatty acid undergoing hydrodeoxygenation eliminates oxygen by converting it into water (H_2O). Its advantage is that the n-alkane product will have several carbon atoms equal to the primary fatty acid, as shown in equation (1). The HDO reaction pathway with tristerin as a model compound is illustrated by Figure 3.

$$C_nH_{2n}O_2 + 3H_2 \longrightarrow C_nH_{2n+2} + 2H_2O \quad (1)$$

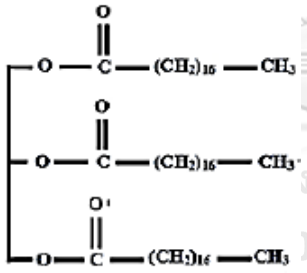

$$+ 12H_2 \longrightarrow 3CH_3 - (CH_2)_{16} - CH_3 + C_3H_8 + 6H_2O$$

Figure 3 Hydrodeoxygenation of tristearin

c) Decarbonylation (DCO)

Removal of carbonyl group in pressurized hydrogen condition to derive n-alkane product with one carbon atom lower than the fatty acid feed is called decarbonylation (DCO). This reaction gives carbon monoxide (CO) and water molecules as by products, as shown in equation (2). Formic acid is an intermediate that is released during DCO_2 reaction which can then be decomposed to n-alkane by dehydration to release CO and H_2O.

$$C_nH_{2n}O_2 + H_2 \longrightarrow C_{n-1}H_{2n} + CO + H_2O \quad (2)$$

d) Decarboxylation (DCO_2)

Decarboxylation (DCO_2) is pointed out to the elimination of oxygen in the fatty acid chain by removal of carboxyl group in the form of carbon dioxide (CO_2), as shown in equation (3). The carboxylic acid and unsaturated glycerol di-fatty ester are derived from triglyceride. They are hydrogenated to release fatty acid and form n-alkane hydrocarbon, which one carbon atom lower than the original compound. The benefit of the DCO_2 pathway is that hydrogen is not required to convert a carboxylic acid to normal paraffin and CO_2. The overall reaction to convert tristerin into normal paraffin by DCO and DCO_2 is demonstrated in Figure 4.

$$C_nH_{2n}O_2 \longrightarrow C_{n-1}H_{2n} + CO_2 \quad (3)$$

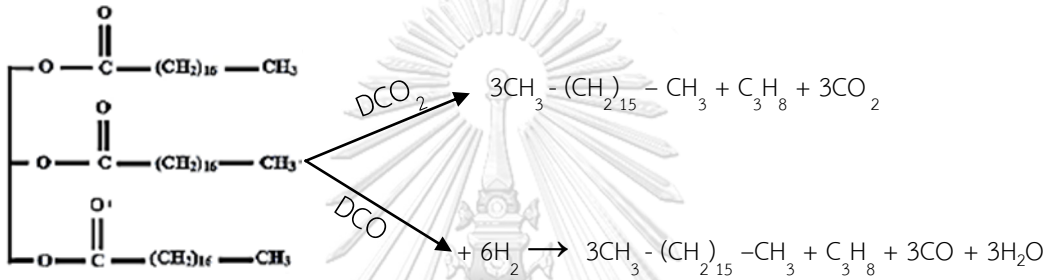

Figure 4 DCO and DCO_2 of tristearin

e) Cracking and isomerization

Hydrocracking of long chain paraffin, as shown in equation (4), is a common process in petroleum refinery. Cracking reaction converts high-boiling point constituent hydrocarbons to valuable fuel such as gasoline and jet fuel, which is C_9 to C_{15} hydrocarbon chains. On the other hand, isomerization reaction, as shown in equation (5), converts straight-chain alkanes into branched-chain alkanes. A straight-chain molecule is transformed into a branched molecule with the same atoms, but different in arrangement. The new molecule is known as isomers. Thereby, hydrocracking and isomerization can be used to enhance the HDO process to improve fuel properties' standard such as cetane number, cold flow properties and freezing point.

$$\text{Long chain paraffin} \longrightarrow \text{Lighter hydrocarbon} \quad (4)$$

$$n\text{-}C_nH_{2n+2} \longrightarrow i\text{-}C_nH_{2n+2} \quad (5)$$

f) Gas phase reactions

The gases product from HDO, DCO, and DCO_2 include H_2O, CO_2, and CO, can further react with H_2 in the gas phase. The reaction of CO and CO_2 is called methanation, as shown in equation (6) and (7), respectively. Another reaction that can be occurred is water-gas-shift, as

shown in equation (8). In summary, the possible reaction pathway of triglycerides hydroprocessing of vegetable oils can be depicted in Figure 5. [14]

$$CO + 3H_2 \longrightarrow CH_4 + H_2O \quad (6)$$

$$CO_2 + 4H_2 \longrightarrow CH_4 + 2H_2O \quad (7)$$

$$CO + H_2O \longrightarrow H_2 + CO_2 \quad (8)$$

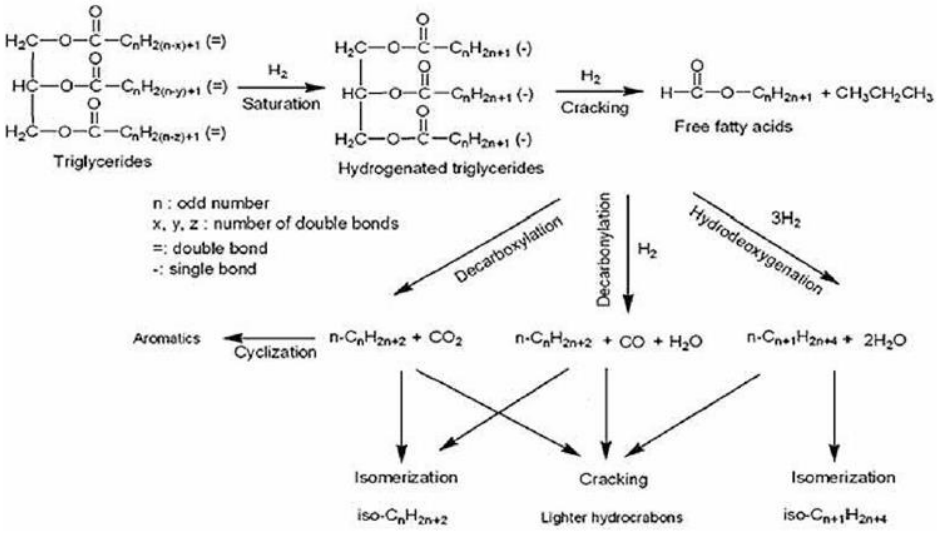

Figure 5 Possible reaction pathway of triglycerides hydroprocessing of vegetable oils

2.2 Literature reviews

Currently, there are some refineries developing technologies for the production of bio-hydrogenated diesel and liquid aviation fuels. Many researchers are working on a renewable source, catalyst type, and operating conditions to obtain the highest product yield. Much research also focuses on process design and optimization of the BHD production process to make the process more feasible. This section gives the conclusion of previous researches, including related topics mentioned earlier.

Palm oil is the most promising renewable source for BHD production in Thailand. For edible oil processing, crude palm oil (CPO) is typically treated to remove impurity such as phospholipids and phosphatides by precipitation called degumming process. The degummed palm oil (DPO) is then bleached to dispose of pigment, trace metals, and other undesirable impurities. The bleached product is called bleached palm oil (BPO). After that, reefing and deodorization steps are applied. The product from this step is refined, bleached, deodorized palm oil (RBDPO) with palm fatty acid distillate (PFAD) as a by-product [7, 9]. Table 2 reveals the fatty acids containing in palm oil [14]. Kiatkittipong et al [7] studied BHD operating conditions with different palm oil feedstocks, including CPO, RBDPO, and PFAD over commercial 5 wt% Pd/C and

synthesized NiMo/γ-Al_2O_3. The results showed that the phospholipid-free palm oil was helpful for the BHD process as it did not interfere with the reaction or caused catalyst poison. The highest diesel yield at 81% was obtained from PFAD when using the Pd/C catalyst, followed by DPO and CPO, with the yield 70% and 51%, respectively. Despite the greater diesel yield of PFAD and DPO, it was concerned that the degumming process consumes higher energy in industrial-scale production. So, CPO might be more reasonable. Furthermore, comparing the catalyst activity, the NiMo/γ-Al_2O_3 catalyst was more suitable for triglyceride feedstock while Pd/C was favored by free fatty acid feedstock.

Table 2 Palm oil fatty acids composition

Fatty acids		Composition (wt%)
Unsaturated	Oleic	36-44
	Linoleic	9-12
Saturated	Palmitic	39.3 - 47.5
	Stearic	3.5 - 6

The optimum operating parameters of hydroprocessing of CPO with Pd/C catalyst were also studied by Kiatkittipong et al [7]. The effect of reaction time on CPO conversion to liquid product is demonstrated in Figure 6 . It can be concluded that the conversion of CPO and diesel yield rise with higher reaction time. However, after 3 hours of reaction, the conversion was increased slightly to 69% while diesel yield was lower. It is because long-chain hydrocarbon was cracked into lighter products. In addition, CPO conversion and diesel yield strongly depended on temperature. From Figure 7, it can be seen that a higher temperature resulted in increasing in CPO conversion and diesel yield. The highest yield was obtained at 400 ℃. Above this reaction temperature, diesel range product was cracked to lighter fractions. By changing the pressure from 20 to 60 bar, CPO conversion and diesel yield were increased, and the diesel yield reached the maximum at 40 bar.

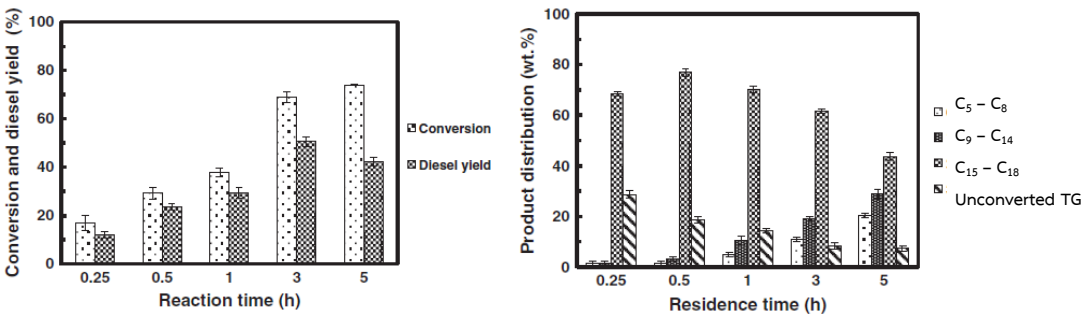

Figure 6 Conversion, diesel yield and product distribution from hydroprocessing of CPO feedstock using Pd/C catalyst with varying reaction time at 400 ℃ and 40 bar

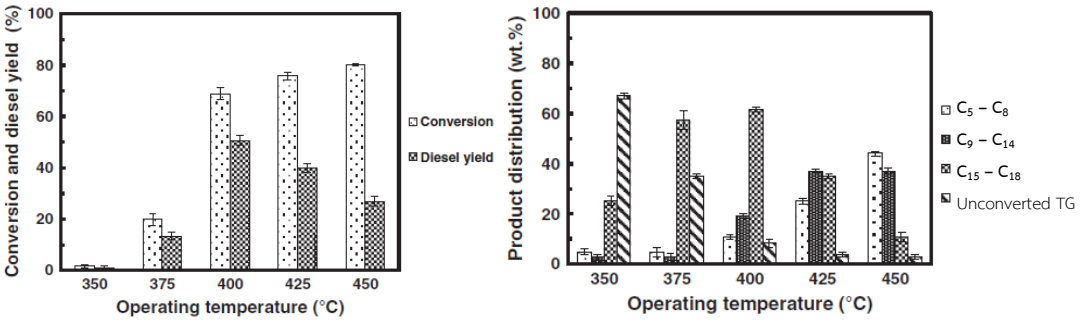

Figure 7 Conversion and diesel yield from hydroprocessing of CPO feedstock using Pd/C catalyst with varying temperature at 3 hours reaction time and 40 bar

Dominant liquid products produced from Pd/C catalyst were n-pentadecane (n-C_{15}), and n-heptadecane (n-C_{17}) whiles NiMo/γ-Al_2O_3 catalyst gives n-hexadecane (n-C_{16}) and n-octadecane (n-C_{18}) because of the difference of reaction pathway. The NiMo/γ-Al_2O_3 catalyst has a higher degree of HDO than Pd/C. On the contrary, DCO and DCO_2 were the main reaction pathway of Pd/C. The result was consistent with Hsu et al [11] which performed the lab-scale test for hydroprocessing of CPO in the presence of NiMo/γ-Al_2O_3. Table 3 represents the liquid product composition with various process conditions involving temperature, pressure, WHSV (weight hourly space velocity), and H_2 to oil ratio. It can be seen that the main product of NiMo/γ-Al_2O_3 catalyst is the n-hexadecane (n-C_{16}). From Figure 8, the increasing temperature promotes cracking reaction as indicated by the increasing of n-C_8 to n-C_{14} concentration. Moreover, DCO and DCO_2 reaction pathway trends to rise, which can be seen by the increase of CO and CO_2 concentration in the gaseous product.

Table 3 Liquid product composition (%wt) and product appearance with various process condition

Parameter	T (C)	P (psig)	WHSV (h^{-1})	H_2-to-oil ratio	n-C_8-n-C_{14} (wt%)	n-C_{15} (wt%)	n-C_{16} (wt%)	n-C_{17} (wt%)	n-C_{18} (wt%)	n-C_{19}-n-C_{20} (wt%)	Liquid color
Temperature	370	800	2	750	20.02	14.37	45.74	3.79	12.63	3.43	Yellow
	400	800	2	750	37.31	12.09	37.05	2.38	7.86	3.28	Yellow
	430	800	2	750	53.32	11.88	26.05	1.53	4.03	3.16	Light Green
	460	800	2	750	59.93	13.10	18.42	1.25	2.47	4.80	Light Green
Pressure	430	550	2	750	42.95	18.32	20.68	13.14	2.52	2.36	Brown
	430	675	2	750	58.55	11.83	20.79	1.72	3.22	3.85	Light Green
	430	800	2	750	53.32	11.88	26.05	1.53	4.03	3.16	Light Green
	430	925	2	750	53.10	13.42	21.73	5.89	2.7	3.13	Light Green
WHSV	430	800	1	750	43.60	17.31	26.78	2.78	5.82	3.69	Brown
	430	800	2	750	53.32	11.88	26.05	1.53	4.03	3.16	Light Green
	430	800	3	750	50.36	11.66	27.86	1.58	4.77	3.74	Light Green
	430	800	4	750	50.62	12.28	27.89	1.55	4.09	3.54	Light Green
H_2-to-oil ratio	430	800	2	500	48.71	16.11	24.24	2.66	4.31	3.95	Yellow
	430	800	2	750	53.32	11.88	26.05	1.53	4.03	3.16	Light Green
	430	800	2	1000	41.06	13.06	34.37	1.76	5.53	4.19	Clear
	430	800	2	1250	44.55	12.98	30.59	2.37	5.95	3.54	Clear

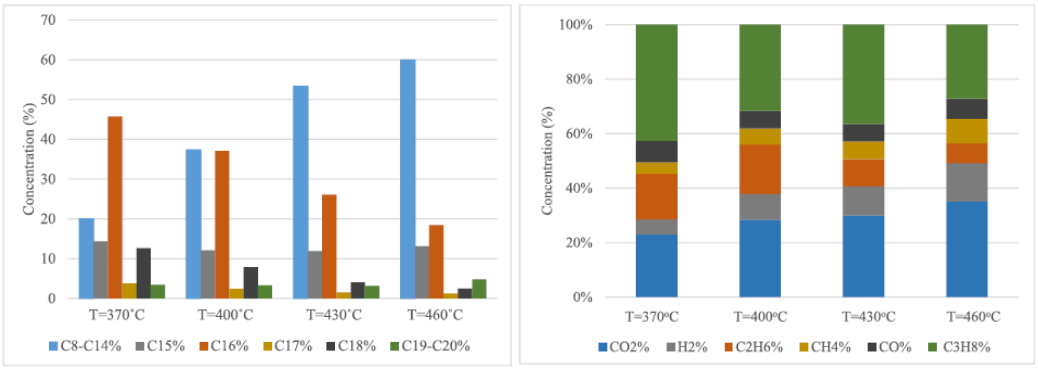

a) Liquid phase product b) Gas phase product

Figure 8 Effects of reaction temperature on liquid and gas product compositions

Srifa et al and Hsu et al [8, 11] also reported that high pressure was favored by HDO pathway as a reason of better H_2 solubility in oil and larger adsorption of H_2 on the catalyst surface. This can be noticed by higher n-C_{16}, and n-C_{18} concentration in product whiles lower n-C_{15} and n-C_{17} fraction as demonstrated in Figure 9. For the gaseous product composition, propane is cracked to ethane and methane at higher pressure due to above-mentioned causes.

The hydrogen volumetric feed corresponded to oil volumetric feed is defined as H_2 to oil ratio. The result from Srifa et al. and Hsu et al [8, 11] showed that larger H_2 to oil ratio enhanced HDO, DCO, DCO_2. This can be seen by Figure 10 that all product concentrations were higher at a higher amount of H_2 dissolve to oil. The highest yield was at 1000-1500 (Ncm^3/cm^3)

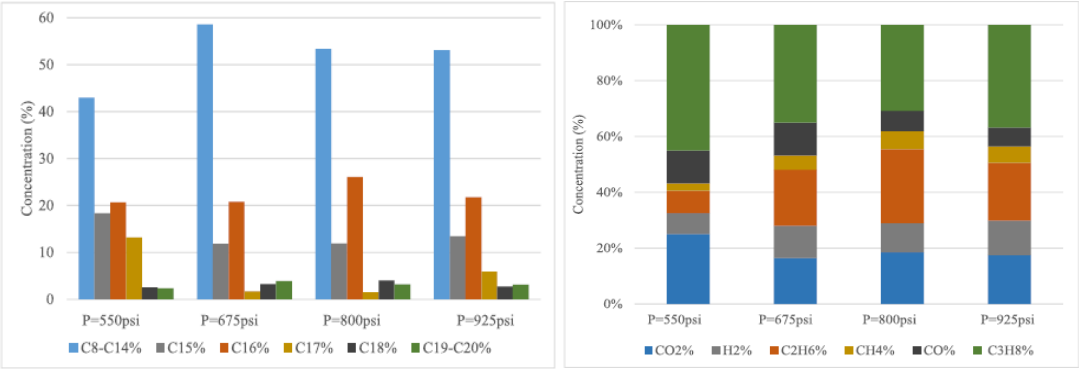

a) Liquid phase product *b) Gas phase product*

Figure 9 Effects of reaction pressure on liquid and gas product compositions

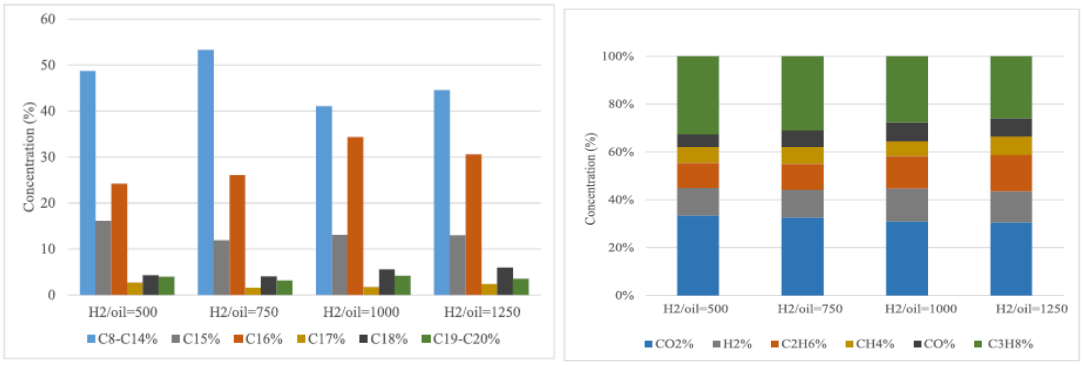

Figure 10 Effects of H_2 to oil ratio on liquid and gas product compositions

Recently, researchers are interested in producing jet fuel range hydrocarbons, C_9-C_{18}, from triglyceride based vegetable oil via hydroprocessing and hydrocracking/ isomerization processes. The alternative jet fuel is called "bio-jet fuel" because its properties are comparable with conventional jet fuel. The class of jet fuel is divided by its properties according to the ASTM standard. For example, jet fuel such as Jet A and Jet A-1 is used in a commercial airplane while Jet A-5 and JP-8 are used in military aircraft. There are other physicochemical properties of alternative jet fuel that must be considered as following [12],

1) Higher heating values (HHV), which is measured by using a bomb calorimeter; and defined as the amount of heat released when fuel is combusted. The heat of condensation of the water is included in the total measured heat. In general, the minimum limit of the heating value of 42.8 MJ/kg is recommended for jet fuel.

2) Kinematic viscosity. The fuel flow property is depended on kinematic viscosity. The range within 8 - 8.5 mm^2/s at -20 °C is favored by jet fuel as ASTM standard. This property is essential to the atomization and fuel injector system in the aviation engine. The high viscosity may damage the engine and cause incomplete combustion. The researcher [15] revealed that deoxygenation reaction could improve fuel viscosity because it can remove oxygen molecule from triglyceride then the intermolecular boundaries of hydrogen bonds was decreased.

3) Fuel density for jet fuel is ranged from 775 to 840 kg/m^3. It is dependent on temperature. Fuel density decreases when the temperature is increased. The studies [16] on the effect of temperature on deoxygenated triglyceride fuel showed that the density was slightly changed from 775 to 785 kg/m^3 when the temperature was changed.

4) Flash point is the property for describing combustion phenomena. It indicates the lowest temperature at which a liquid can give off vapor to form an ignitable mixture in air near the surface of the liquid under an external flame. The lower the flash point, the easier the ignition of fuel. According to the ASTM standard, the minimum flash point for jet fuel is 38 °C. The higher flash point is preferable for jet fuel applications due to safety reasons.

5) Freezing point of a fuel is the temperature at which a liquid fuel becomes a solid hydrocarbon at lower temperature conditions. As reported by the ASTM standard, the Jet A fuel specification is at -40 ℃, while Jet A-1 is at -47 ℃. It is heavily dependent on the number of carbon and n-paraffins portion in fuel. The freezing point can be lower by reducing n-paraffin fraction in triglyceride based jet fuel products.

6) Aromatic contents has a strong effect to engine's power, which is necessary characteristics for jet fuel. In general, jet fuel consists of aromatic content about 5-25% depending on the type of oil. Researcher reported [12] that the aromatics content of alternative jet fuel from vegetable oil complies with the commercial jet-fuel standard. Some studies [17] also reported that the minimum aromatic content is set at 8% for the reason of the seal contraction, which will increase when the aromatic content is less than 8% and cause leakage in the engine system. However, the fuel with higher aromatic content will result in lower net heat of combustion and decreasing the freezing point.

Other important properties of jet fuel are the total acid number of fuel and smoke point. The total acid number is related to the corrosion problem in the aviation engine, so jet fuel must keep the total acid number less than 0.1 mg KOH/g. The smoke point is the temperature at which fuel begins to produce soot and is determined by the maximum flame height that fuel combusts without smoke. The soot formation tends to increase when C/H and C/O ratio are increased. Moreover, it is related to aromatic content because higher aromatic content will increase C/H ratio. It then will generate more soot that is referred to as a lower smoke point. Table 4 shows the comparison of various conventional jet fuel and alternative jet fuel from hydroprocessed esters and fatty acids (HEFA).

Table 4 Comparison of various conventional jet fuel and alternative jet fuel

Properties	HEFA	Jet A-1	Jet A	JP-8
Higher heating values (MJ/kg)	42.8	42.8	43.28	42.8
Viscosity (mm^2/s) at -20 ℃	8.0	8.0	8.0	8.0
Density (kg/m^3) at 15 ℃	730-770	775-840	775-840	755-840
Flash point (℃). min	38	38	38	38
Freezing point (℃), max	-40 to -47	-47	-40	-47
Final BP (℃)	250	300	300	300
Total acidity, (mg KOH/g)	0.015	0.1	0.1	0.015
Aromatics (wt%)	26.5 (vol%)	18.0	18.5	13.5
Smoke point (mm)	NM	25	25	25

C.-H. Lin, et al [18] studied jet fuel production by using crude palm oil as a feedstock. The first process was hydroprocessing of CPO to produce alkane hydrocarbons in the diesel fuel range. NiMo-S/γ-Al_2O_3 was selected as the hydroprocessing catalyst. The produced alkanes were then used as raw material for producing jet fuel by hydrocracking/isomerization over the NiAg/SAPO-11 catalyst. In their study, the effect of the reaction temperature, pressure, and liquid hourly space velocity (LHSV) on carbon distribution and isomer-to-normal alkane ratio (I to N ratio) and aromatics content were investigated. It was revealed in Figure 11 that the higher temperature decreased the composition of C_{15} to C_{18} and increased of C_8 to C_{14} alkane due to the increasing of cracking severity. When the cracking temperature was 360 °C, the carbon distribution of the cracked products was in the same range of jet fuel. Also, it was found that the isomerization reaction increased with increasing temperature.

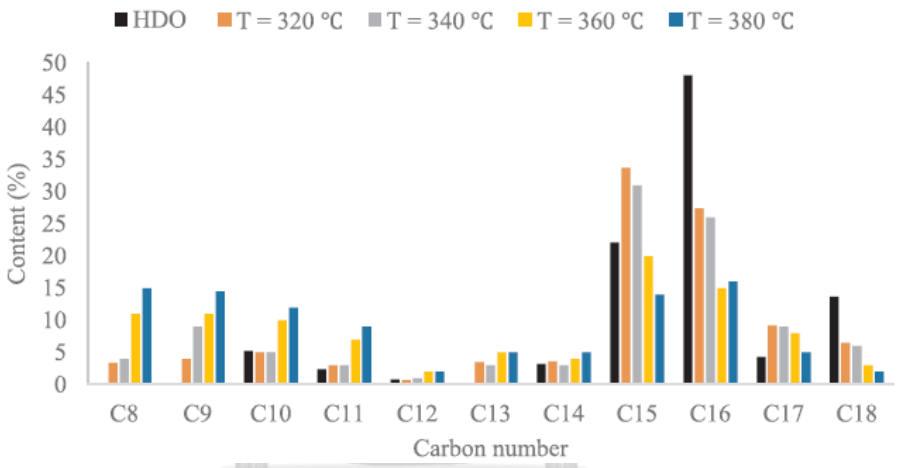

Figure 11 Distribution of carbon numbers at various temperature (pressure of 3 MPa, LHSV of 1 h^{-1} and the H_2/oil molar ratio of 13.6)

In terms of reaction pressure, it was found that increasing the reaction pressure resulted in increase in the lighter hydrocarbons contents. It was because the higher pressure increases the collision probability of the dissociated hydrogen and the alkycarbenium ion, which led to faster reaction completion and higher catalytic efficiency. Moreover, higher pressure increased isomer yield, as already mentioned.

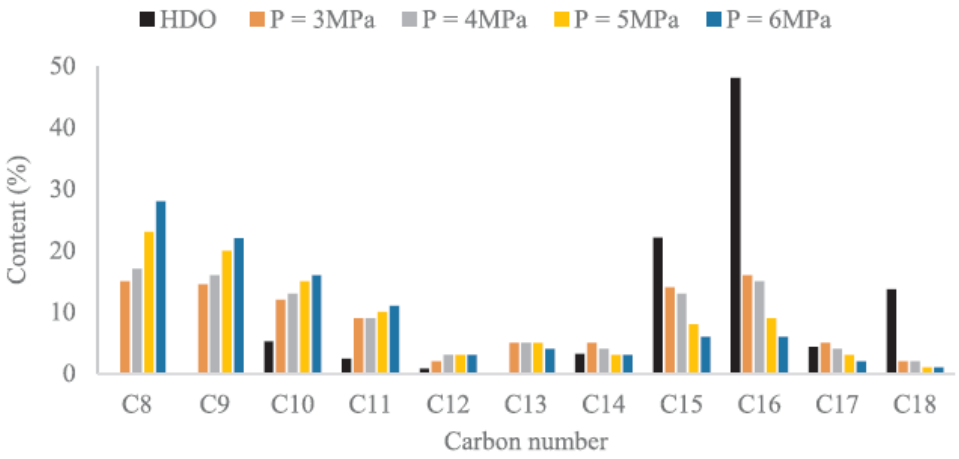

Figure 12 Distribution of carbon numbers with various pressures (temperature of 380 °C, LHSV of 1 h^{-1} and H_2/oil molar ratio of 13.6).

In terms of aromatics content, which is an important factor in enhancing the flash point property of jet fuel, it was found that the aromatics content could be increased by increasing temperature and decreasing pressure, as shown in Figure 13 and Figure 14. In conclusion, they recommended the reaction temperature at 360 °C, the pressure of 3 MPa, the LHSV of 1 h^{-1}, and the hydrogen/oil molar ratio of 13.6 were the optimal condition for hydrocracking/isomerization over the NiAg/SAPO-11 catalyst. The final alkane product obtained had aromatic content of 9%, which was sufficient to meet the jet fuel specifications.

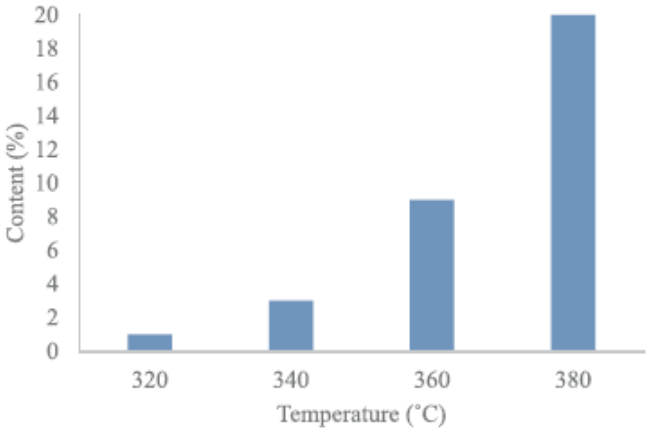

Figure 13 The content of aromatics at various temperatures.

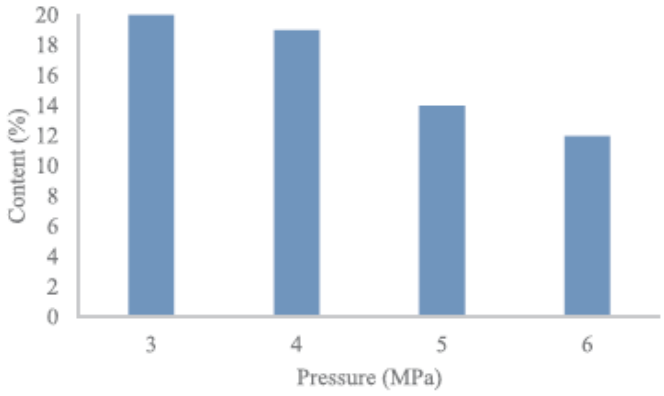

Figure 14 The content of aromatics at various pressures

In the view of the industrial scale, the simulation and techno-economic analysis study was investigated. Plazas-González et al [14] studied the process modeling of BHD production from palm oil with NiMo/γ-Al_2O_3 catalyst to determine the optimal operating condition by using Aspen Plus® 7.3 software. The model used to predict the gas-liquid equilibrium of triglycerides at high pressure was Peng Robinson with RK-Aspen. The composition of palm oil entering the reactor is 37% triolein, 48.6% tripalmitin, 10% trilinolein, and 4.4% tristearin. Table 5 presents the reactions used for simulation in the equilibrium reactor. The process flow diagram for this study is shown in Figure 15. Palm oil and hydrogen introduced to the reactor at 300 ℃ and 40 bar. After the reaction completes, the product was separated in a high-pressure separation column, which separated the gas component at the top of the column. The liquid product leaving at the bottom of the column enters the second column operated at low pressure to obtain a purified product of n-hexadecane and n-octadecane as the main product. Light gaseous product leaving at the top of the column was then sent to separate H_2 as by-product gas. To find the optimal operating condition for separation, sensitivity analysis is applied. The pressure selected for CS-1 column is 40 bar to obtain acceptable amount of propane, major portion of gas-phase product, and H_2 to recycle. The selected temperature for CS-1 was set at 200 ℃. Above this and propane recovery will be lower. For the liquid phase product leaving from the bottom of CS-1, it was found that the higher temperature of CS-1 causes a higher fraction of n-C_{16} and n-C_{18}. For CS-2 column, the conditions were chosen at atmospheric pressure and 60 ℃ because recovery fraction was lower as temperature increased. The purity of BHD product was achieved at 97% with the composition of 52.9% n-C_{18}, 44.2% n-C_{16}, 1% H_2O, 1% n-C_{17}, and 0.7% n-C_{15} from this study.

Table 5 Reaction included in Plazas-González et al simulation

No.	Stoichiometric reaction	Type
1	Triolein + $3H_2 \rightleftharpoons$ 3 oleic acid + propane	Initial reactions
2	Tripalmitin + $3H_2 \rightleftharpoons$ 3 palmitic acid + propane	
3	Trilinolein + $3H_2 \rightleftharpoons$ 3 linoleic acid + propane	
4	Tristearin + $3H_2 \rightleftharpoons$ 3 stearic acid + propane	
5	Oleic acid + $H_2 \rightleftharpoons$ stearic acid	Hydrogenation
6	Linoleic acid + $2H_2 \rightleftharpoons$ stearic acid	
7	Stearic acid $\rightleftharpoons$ n − C_{17} + CO_2	Decarboxylation
8	Palmitic acid $\rightleftharpoons$ n − C_{15} + CO_2	
9	Oleic acid $\rightleftharpoons$ C_{17}= + CO_2	
10	Stearic acid + $H_2 \rightleftharpoons$ n − C_{17} + CO + H_2O	Decarbonylation
11	Palmitic acid + $H_2 \rightleftharpoons$ n − C_{15} + CO + H_2O	
12	Oleic acid + $H_2 \rightleftharpoons$ C_{17}= + CO + H_2O	
13	Stearic acid + $3H_2 \rightleftharpoons$ n − C_{18} + $2H_2O$	Reduction
14	Palmitic acid + $3H_2 \rightleftharpoons$ n − C_{16} + $2H_2O$	
15	Oleic acid + $3H_2 \rightleftharpoons$ C_{18}= + H_2O	
16	Stearic acid + $2H_2 \rightleftharpoons$ octadecan-1-ol + H_2O	Alcohol formation
17	Palmitic acid + $2H_2 \rightleftharpoons$ hexadecan-1-ol + H_2O	

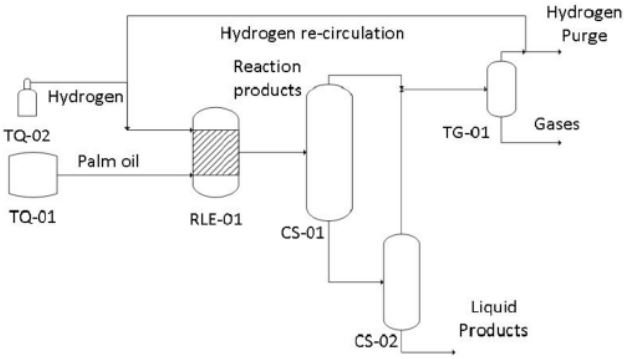

Figure 15 Process flow diagram for BHD production from palm oil

Hsu et al [11] worked on the process simulation and techno-economic analysis of hydroprocessing of crude palm oil. The production cost at the capacity of 600 tonnes per day was estimated. The minimum diesel selling price was calculated when altering materials cost, plant capacity, operating conditions, and catalysts (Pd/C and NiMo/γ-Al_2O_3.). The simulation was

carried out by Aspen plus program using the NRTL model. Raw materials were fed and reacted in 5 consecutive reactors using RStioc. The 1st reactor is where hydrogenation occurs. Unsaturated triglyceride was converted to saturated triglyceride. Then, they were converted to a fatty acid with hydrogenolysis reaction in the 2nd reactor, and propane was removed by this reaction. HDO, DCO, and DCO_2 were developed in 3rd, 4th and 5th reactor, respectively, as depicted in Figure 16 (reactions actually happen in one reactor),. Propane was separated in flash drum. The straight-chain alkane product was distillate in a distillation column where renewable diesel was removed at top of column. The heavy components at the bottom were then sent to hydrocracking reactor to cut long-chain hydrocarbons. After that, they were distilled in the distillation column. Renewable diesel product was mixed with the 1st column distillate. By techno-economic assessment, the selling price was proposed to be 1.72 dollars/liter. It was found that increasing plant capacity from 600 tonnes to 2,000 tonnes per day will decrease in selling price by 1 cent per liter. The NiMo/γ-Al_2O_3 catalyst could help reduction in selling price in comparison with the Pd/C catalyst.

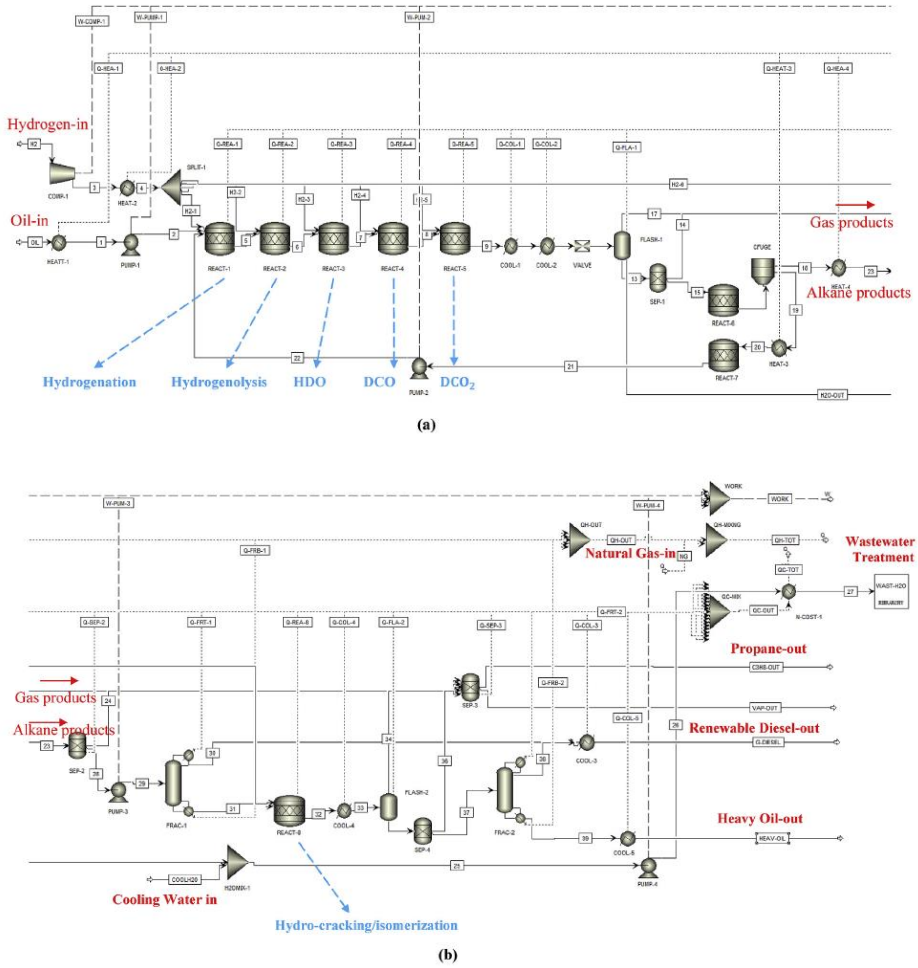

Figure 16 Process model for BHD production. (a) First part; (b) second part.

The technologies for converting non-edible oil, such as jatropha oil, are also interesting. Wang [19] studies the economics of a bio-refinery process for producing hydro-processed renewable jet fuel (HRJ) from jatropha oil by using Aspen plus simulation program and techno-economic analysis. The HRJ processing is demonstrated in Figure 17, which is similar to the BHD process. Chemical components found in jatropha oil are mainly fatty acid with 14 to 20 carbon atoms, as listed in Table 6. Wang [19] chose operating conditions at 360 °C, and 3 MPa over Pt/Al_2O_3 catalyst for hydroprocessing reactor, whereas hydro-isomerization and cracking reactor occurred at 355 °C and 600 psig using $Pt/HZSM\text{-}22/g\text{-}Al_2O_3$ as a catalyst.

Jet fuel requires more specific properties being a high flash point, good cold flow properties. Thereby, hydrocracking and hydro-isomerization unit are added to the process, followed by distillation to separate the mixed product to light gasses, naphtha, jet fuel, and diesel. The product separation train usually consists of 4 distillation columns, as shown in Figure 18. By simulation and techno-economic analysis, the minimum jet fuel selling price (MJSP) produced from jatropha oil is $5.74/gal based on the plant capacity of 2,400 metric tonnes of feedstock per day.

Table 6 Composition of Jatropha oil

Fatty acid composition	Percent by weight
Myristic acid C14:0	0.1
Palmitic C16:0	14.2
Palmitoliec C16:1	0.7
Margaric C17:0	0.1
Stearic C18:0	7.0
Oleic C18:1	44.7
Linoleic C18:2	32.8
Linolenic C18:3	0.2
Arachidic C20:0	0.2

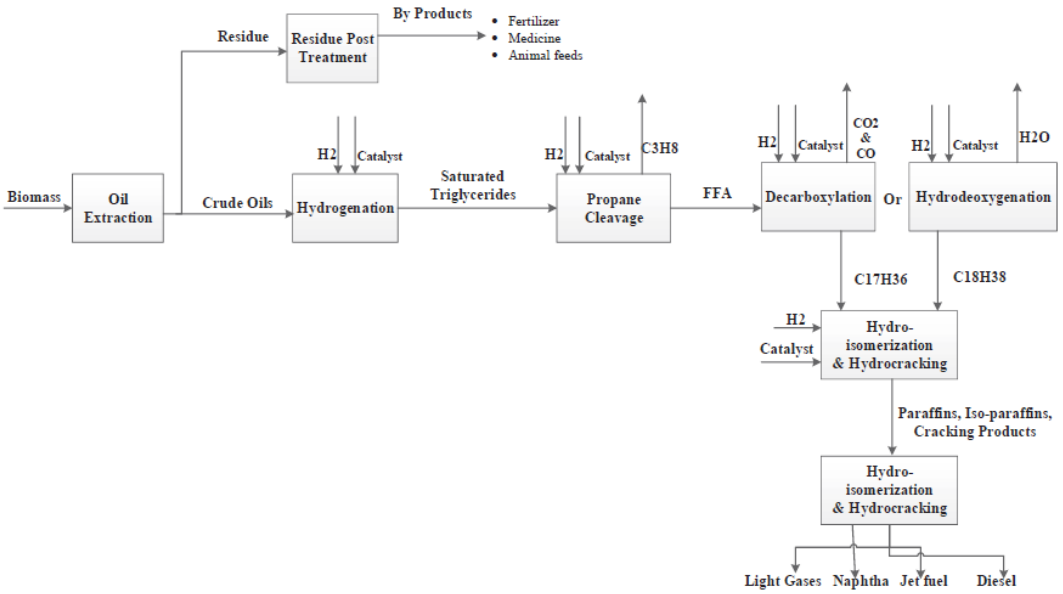

Figure 17 Hydro-processed renewable jet (HRJ) process.

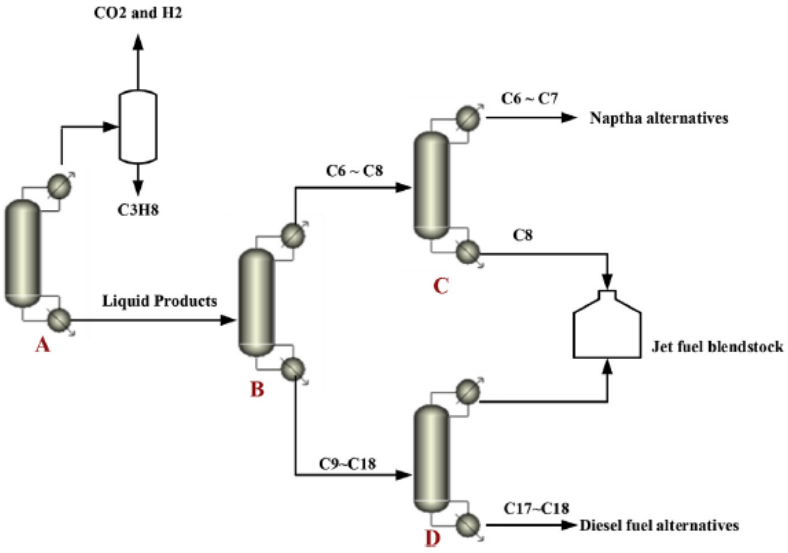

Figure 18 Distillation process to separate bio-fuel.

CHAPTER 3 METHODOLOGY

In this chapter, the procedure for process simulation and economics analysis of BHD and Bio-jet fuel production are provided and described. It includes validation of the BHD process then improved process by isomerization and hydrocracking unit for producing two main products include BHD and Bio-jet. Process design and equipment sizing was also performed. The economics analysis was estimated to study the feasibility of the process.

3.1 Validation of BHD process

In this step, palm oil composition and reaction conditions such as temperature, pressure, and H_2 to oil ratio from Hsu et al [11] experiment are the input for simulation. Process simulation is conducted by Aspen plus V9 program. Since the system contains hydrocarbons and mildly polar mixture and processes are dealing with high pressure and high temperature, Peng Robinson is selected for the thermodynamics model. Peng Robinson model described equilibrium behavior in the liquid phase and vapor phase by Equation of State. Some model parameter such as binary parameters is determined by the regression method including in Aspen plus V9 tools.

The main reaction taking place in the BHD production are hydrogenation, hydrogenolysis, HDO, DCO, DCO_2, respectively, as shown in Table 7. The reactor used in this simulation consisted of six consecutive R-Stoic reactors. The last reactor is for methanation, water-gas shift and cracking (Reaction actually occur in one reactor). The conversion of each reaction was varied and the product composition were adjusted by using design spec tool in Aspen plus V9. The composition of both phase is compared to Hsu et al [11] lab scale result. The BHD process is validated when the deviation of simulation result and lab scale result are less than 3%.

3.2 Improving of BHD process

The previously produced BHD is sent to a hydrocracker unit to convert it to a jet fuel product. The reaction condition and catalyst used for the simulation of the hydro cracking unit are obtained from C.-H. Lin et al [18] experiment, which studied the production of jet fuel from CPO. For validation of the hydrocracking process, the simulation result is compared with the result of C.-H. Lin et al. research. In their study, CPO was converted to BHD by deoxygenation reaction in a present of NiMo-S/γ-Al_2O_3 catalyst. BHD was then used as raw material for producing jet fuel by hydrocracking/isomerization over the NiAg/SAPO-11 catalyst. BHD composition were 14% C_{15}, 56% C_{16}, 5% C_{17}, 25% C_{18}.

Table 7 Reaction used in simulation

No.	Reaction path way	Reaction
1	Hydrogenation	Triglyceride + H_2 $\longrightarrow$ Sat-Triglyceride + $2H_2O$
2	Hydrogenolysis	Sat-Triglyceride + H_2 $\longrightarrow$ Fatty acid+ C_3H_8
3	Hydrodeoxygenation	$C_nH_{2n}O_2 + 3H_2$ $\longrightarrow$ $C_nH_{2n+2}+ 2H_2O$
4	Decarbonylation	$C_nH_{2n}O_2+ H_2$ $\longrightarrow$ $C_{n-1}H_{2n} + CO + H_2O$
5	Decarboxylation	$C_nH_{2n}O_2$ $\longrightarrow$ $C_{n-1}H_{2n} + CO_2$
6	Methanation	$CO + 3H_2$ $\longrightarrow$ $CH_4 + H_2O$ $CO_2 + 4H_2$ $\longrightarrow$ $CH_4 + 2H_2O$
7	Water-gas shift	$CO + H_2O$ $\longrightarrow$ $H_2 + CO_2$
8	Cracking	Long chain paraffin $\longrightarrow$ Lighter hydrocarbon

3.3 Process design and Equipment sizing

Simplified process flow diagram for BHD and jet fuel production in this work proposed as in Figure 19. Firstly, palm oil and hydrogen were reacted in deoxygenation reactor then mixed-product stream obtained from the deoxygenation reactor are sent to a flash drum to remove light gas components such as H_2, CO_2, and C_3H_8. The BHD product exited at the bottom of the flash drum is sent to a cracking unit to produce a liquid mixture containing C_8-C_{20} hydrocarbon. Finally, it is introduced to distillation unit to separated liquid mixture by selective boiling point. In the view of aviation fuel properties' requirement, the higher heating values (HHV) is used for defined the specification of product. According to ASTM standard, the minimum limit of heating value of 42.8 MJ/kg is recommended for jet fuel.

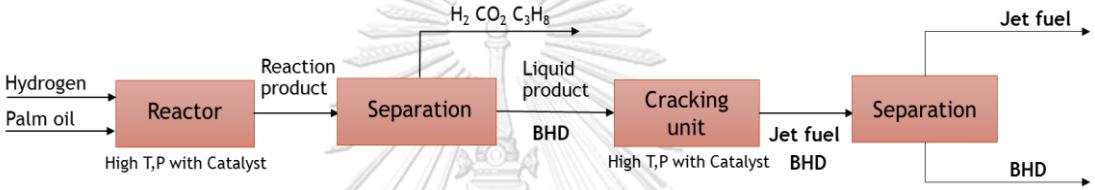

Figure 19 Simplified process diagram for BHD and jet fuel production

After the process flowsheet was developed, material and energy balances can be calculated from Aspen plus V9. That information will later use for plant equipment sizing and determine the capacities needed for the cost correlations in economic evaluation. Principally, the required data are flow rate, temperature, pressures, and heat duties. The equipment was sized by Aspen plus together with sizing procedures from Lorenz T. Biegler and team method [20]. Basis calculations for equipment sizing are as following,

Countercurrent shell and tube heat exchanger, the total area of heat exchanger can be calculated from

$$Q = UA\Delta T_{lm} \tag{9}$$

where heat duty (Q) is known by energy balance from simulation, the log mean temperature (ΔT_{lm}) is given by

$$\Delta T_{lm} = [(T_1 - t_2) - (T_2 - t_1)]/ln\{(T_1 - t_2)/(T_2 - t_1)\} \tag{10}$$

Reactor volume is estimated by WHSV (Weight Hourly Space Velocity), and LHSV (Liquid Hourly Space Velocity) obtained from Hsu et al [11] and C.-H. Lin, et al [18] research. Sizing of vessels, distillation column, compressors, and pump was computed from Aspen Plus.

3.4 Economic analysis and feasibility study

In this section, the economic analysis was performed using methods from Turton R. and the team [21]. It includes evaluation of capital cost and manufacturing costs associated with direct and indirect cost. Firstly the calculation was based on plant capacity at 75 thousand bbl/y of bio-jet fuel follow Elias Martinez-Hernandez, el al research [22] then the capacity was expanded to 4 times of based case plant to comply with existing commercial biodiesel plant in Thailand namely, Bangchak Petroleum Public Co., Ltd, Sun Tech Palm Oil Co., Ltd, Patum Vegetable Oil Co., Ltd.[23]. The estimating procedures to obtain a new plant capacity is six-tenths rule method recommended by Turton R. and team method [21] as equation (11) with n set to 0.6. It can be used to scale up or down to new plant capacity.

$$\frac{C_a}{C_b} = \left(\frac{A_a}{A_b}\right)^n \tag{11}$$

where A = Equipment cost attribute, C= Purchased cost, n = Cost exponent

Subscription: *a* refers to equipment with the required attribute

B refers to equipment with the base attribute

The revenue of the bio-jet fuel process is calculated from two main product streams, including bio-jet fuel and BHD, and propane as a by-product. In the case of BHD plant, only one main product, BHD, and by-product, propane, were taken into account. Two processes were compared in terms of economic by applying Net Present Value (NPV), Internal Rate of Return (IRR), and Pay Back Period. The sensitivity analysis of IRR to product price and investment cost was also examined.

CHAPTER 4 RESULT AND DISCUSSION

4.1 Bio-hydrogenated diesel (BHD) production process

4.1.1 Validation of thermodynamics model

The mixtures in this research contain hydrocarbons, light gases, such as carbon dioxide, hydrogen, and other mildly polar non-ideal chemicals. Thus, Peng Robinson (PENG-ROB) property method was selected for the thermodynamic model. This property method is particularly suitable in the high temperature and high-pressure regions, such as in hydrocarbon processing applications. For accurate results of vapor-liquid equilibrium (VLE) or liquid-liquid equilibrium (LLE) calculations, the binary parameters in Aspen Physical Property System built-in binary parameters (PRKBV) were uses to describe binary interaction. Moreover, the Data Regression System also used to determine the binary parameters from experimental phase equilibrium data (usually binary VLE data), for example, pentadecane and carbon dioxide system.

Figure 20 showed the evaluation of thermodynamics model. Experimental data from NIST data bank in aspen tools were compared with the predictions obtained from thermodynamics model. The result can be concluded that the PENG-ROB is capable of describing the pentadecane and carbon dioxide system. The binary parameters PRKBV/1 from regression was 0.0686.

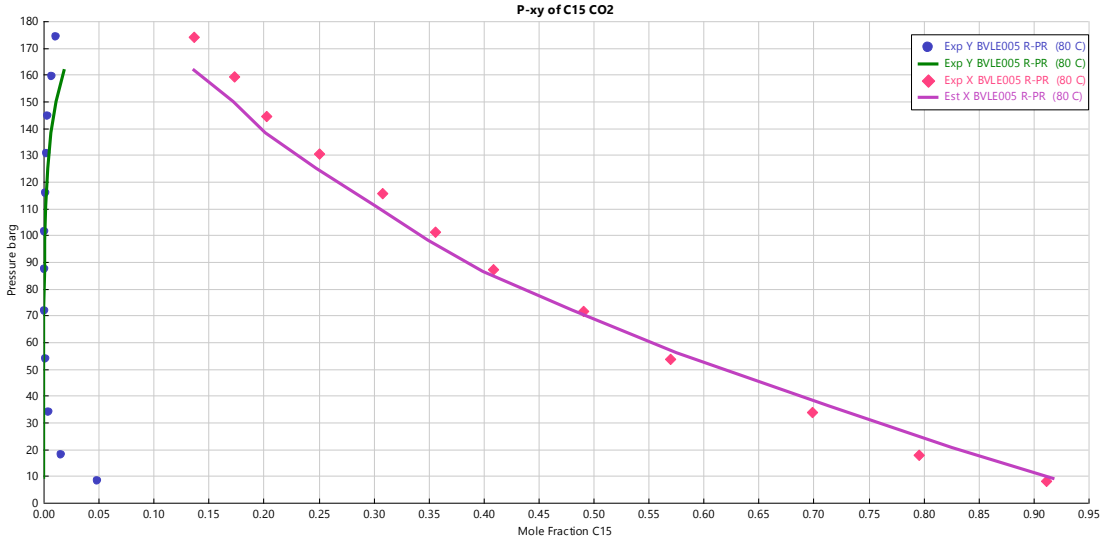

Figure 20 Phase behavior of pentadecane and carbondioxide at pressure 10 to160 barg.

4.1.2 Validation of BHD process

Crude palm oil (CPO) is used as a model compound for this study. The composition of CPO is obtained from work by Hsu et al [11], which studied the BHD process of palm oil in a lab-scale experiment, and is shown in Table 8. NiMo/γ-Al_2O_3 is used as a catalyst for deoxygenation reaction. The reactions occur at temperature of 370 °C and pressure of 55.2 barg. Raw material feed follows H_2/Oil ratio, 254.3 Ncm^3/cm^3

Table 8 Crude palm oil composition

Component	Percent by weight (%)
Tripalmitin (16:0), $C_{51}H_{98}O_6$	44
Tristearin (18:0), $C_{57}H_{110}O_6$	4
Triolein (18:1), $C_{57}H_{104}O_6$	40
Trilinolein (18:2), $C_{57}H_{98}O_6$	10
Triarachidin (20:0), $C_{63}H_{122}O_6$	2

A process flow diagram of the BHD production process is shown in Figure 21 adapted from a study of process simulation by Hsu et al. Liquid palm oil at 2,108 kg/h feed rate was heated from 30 to 370 °C by E-101 and transferred to the reactor, D-101, (all reactions occurred in one reactor). The pressure was raised up to reaction temperature at 55.2 bag by P-101. Excess hydrogen stream in the vapor phase was introduced to the reactor by compressor, C-101, and then heated up by E-102 to react with palm oil with H_2 to oil ratio at 550 Ncm^3/cm^3. Main reaction pathway was Hydrogenation, Hydrogenolysis, HDO, DCO, DCO_2, cracking and methanation. All reaction stoichiometry is based on palm oil compositions as shown in Table 8 and explained in Appendix A. Product mixed stream at a mass flow rate of 2,196 kg/h leaving from the reactor was cooled down to 50 °C by E-103 before entering a flash drum. Deoxygenated product from BHD reactor was sent to flash drum to separate light gas from liquid phase product which operates at 40 °C, 8.52 barg and water also separated.

The simulation results of BHD process are shown in Figure 22. It can be seen that the n-alkane products in liquid phase contain n-C_8 to n-C_{14}, n-C_{15} to n-C_{18}, and n-C_{19} to n-C_{20}, and the highest concentration is n-C_{16}. For the gas phase product, propane was found to have the highest concentration, which is the by-product from hydrogenolysis reaction during the conversion of saturated triglyceride to free fatty acid molecule. By comparing the simulation result with the product compositions from a report by Hsu et al., it was found that the difference was less than 3%. Therefore, the simulation of BHD production is valid

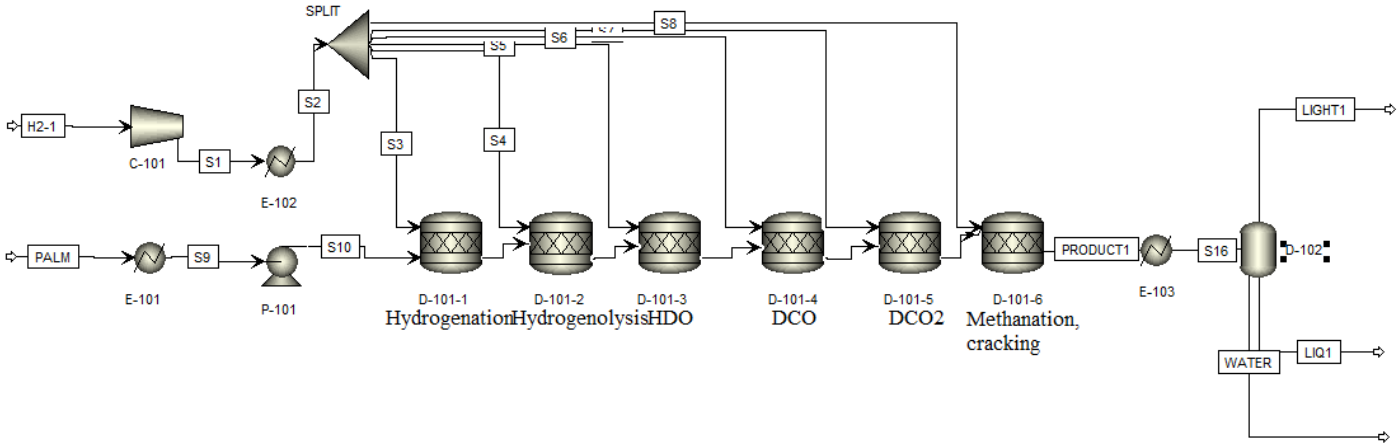

Figure 21 BHD process including deoxygenation section and flash drum for separate gas product and water from liquid product.

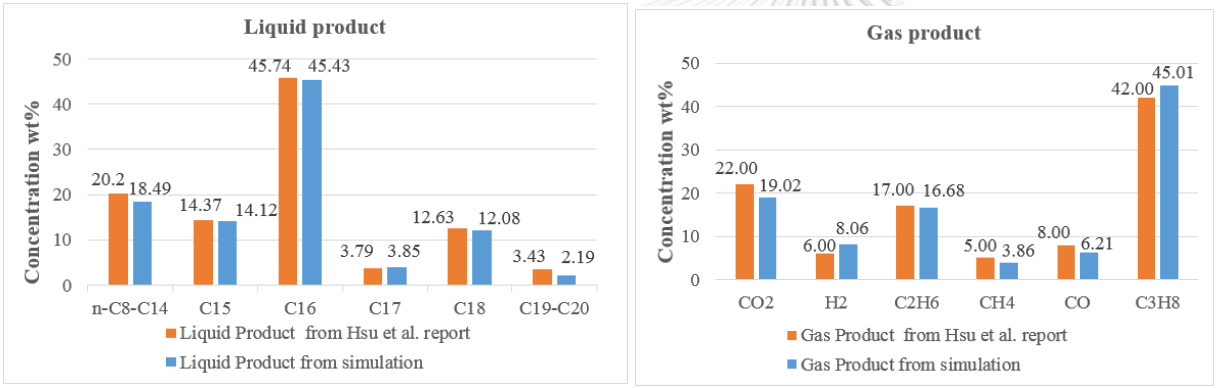

a) Liquid product b) Gas product

Figure 22 Product distribution of BHD process after separated with flash drum at operating condition of 40 °C and 8.52 barg.

a) Liquid product b) Gas product

The distribution of deoxygenation reaction pathway was also calculated based on mole balance. Hydrodeoxygenation (HDO) ratio is defined as the mole of n-alkane with even number of carbon to total mole of fatty acid in the reactant. Decarbonylation/decarboxylation (DCO/DCO_2) is defined as the mole of n-alkane with odd number of carbon to total mole of fatty acid in the reactant. DCO and DCO2 reaction could be separately estimated by the composition of gas product. DCO reaction releases carbon monoxide while DCO_2 releases carbon dioxide. The calculation is expressed in the following equation:

$$\%HDO = \frac{mole\ of\ n{-}alkane\ with\ even\ number\ in\ product}{total\ mole\ of\ fatty\ acid\ (n{-}C_{15}to\ n{-}C_{20}\ in\ reactant)} \quad (12)$$

$$\%DCO = \frac{mole\ of\ n{-}alkane\ with\ odd\ number\ in\ product\ with\ CO\ release}{total\ mole\ of\ fatty\ acid\ (n{-}C_{15}to\ n{-}C_{20}\ in\ reactant)} \quad (13)$$

$$\%DCO_2 = \frac{mole\ of\ n{-}alkane\ with\ odd\ number\ in\ product\ with\ CO2\ release}{total\ mole\ of\ fatty\ acid\ (n{-}C_{15}to\ n{-}C_{20}\ in\ reactant)} \quad (14)$$

The result of the mole balance is shown by the percentage of reaction pathways, as seen in Table 9. Crude palm oil principally consists of tripalmitin and triolein. Thus, the main composition of the product was C_{16} and C_{18} n-alkane. Because NiMo/γ-Al_2O_3 catalyst was used, the major reaction was hydrodeoxygenation which provides 30% of n-C_{16} and 37.3% of n-C_{18}. The deoxygenation behavior on NiMo/γ-Al_2O_3 catalyst was explained in Kiatkittipong et al. [7] and Srifa et al [8] report. Hydrogen consumption was also determined by equation (15). In the case of BHD process, hydrogen consumption was 0.052 kg/kg product.

$$Hydrogen\ consumption = \frac{Total\ hydrogen\ feed\ to\ reactor}{Product} \quad (15)$$

Table 9 The distribution of deoxygenation pathway of crude palm oil

Reaction pathway	% mol
HDO C_{16}	30.0%
HDO C_{18}	37.3%
HDO C_{20}	1.5%
DCO C_{15}	3.3%
DCO C_{17}	9.4%
DCO C_{19}	0.4%
DCO_2 C_{15}	13.0%
DCO_2 C_{17}	5.1%
DCO_2 C_{19}	0.0%
Sum	100.0%

4.2 Improving of BHD process and validation of bio-jet fuel production from BHD

The BHD product was used as a raw material for bio-jet fuel. It was sent to a hydrocracker/isomerization unit where the long-chain hydrocarbon (n-C_{16} to n-C_{20}) are converted into a lighter fraction. The process was catalytic hydrocracking and was experimented by C.-H. Lin et al [18]. The reaction conditions and catalyst used for the simulation of hydrocracking unit is interpreted in Table 10. In their study, CPO was converted to BHD by deoxygenation reaction in a present of NiMo-S/γ-Al_2O_3 catalyst. The BHD composition were 14% n-C_{15}, 56% n-C_{16}, 5% n-C_{17}, 25% n-C_{18}.

Table 10 Reaction condition and catalyst for hydrocracking process

Parameter	Condition	Unit
Catalyst	NiAg/SAPO-11	-
Temperature	360	℃
Pressure	29	barg
H_2/Oil ratio	13.6	Molar ratio

Firstly, the simulation of the hydrocracking reaction was executed by applying BHD composition from research by C.-H. Lin et al. After the hydrocracking reaction was validated, the BHD composition from this research will be applied. Table 11 and Table 12 show the comparison of crude palm oil and BHD composition of C.-H. Lin et al and this research. The BHD composition depends on the source of crude palm oil which had a different triglyceride component.

Table 11 The comparison of crude palm oil of C.-H. Lin, et al research and this research

Composition (wt%)	Crude palm oil	
	Paper based data	Simulation based data
Tripalmitic (C16:0)	49.8	44.0
Tristearic (C18:0)	3.6	4.0
Trioleic (C18:1)	36.2	40.0
Trilinoleic (C18:2)	7.9	10.0
TriArchidic (C20:0)	0.0	2.0
Total	97.5	100.0

Table 12 The comparison of BHD composition of C.-H. Lin, et al research and this research

Composition (wt%)	Hydro-processed alkanes	
	Paper-based data	Simulation-based data
n-C_{15}	14.00	14.29
n-C_{16}	56.00	45.97
n-C_{17}	5.00	3.90
n-C_{18}	25.00	12.22
Total	100.00	76.38

Due to the complexity of cracking reactions, the stoichiometry are unknown. So, possible reactions for n-alkane cracking are assumed. All reaction is simulated by R-Equil model reactor to find a reaction that gives product compositions that match with the compositions of C.-H. Lin et al report. R-Equil model reactor was performed based on simultaneous phase and chemical equilibrium by stoichiometric calculation. The temperature approach to equilibrium for reactions was specified at 0 °C for this simulation. After that, the resultant reactions were used as input for R-Stoic reactor model. The conversion is varied until product composition is valid with less than 3% difference from the laboratory result. Table 13 shows the reactions and conversion obtained from R-Equil and R-Stoic simulation, and Figure 23 was the validation data of cracking reaction.

Table 13 Cracking reaction and conversion from simulation

No.	Reaction	Conversion
1	$C_{15}H_{32} + H_2 \longrightarrow C_{13}H_{28} + C_2H_6$	0.372
2	$C_{15}H_{32} + 3H_2 \longrightarrow C_8H_{18} + 2C_2H_6 + C_3H_8$	0.100
3	$C_{15}H_{32} + 2H_2 \longrightarrow C_{11}H_{24} + C_3H_8 + CH_4$	0.050
4	$C_{16}H_{34} + H_2 \longrightarrow 2C_8H_{18}$	0.110
5	$C_{16}H_{34} + 2H_2 \longrightarrow C_{10}H_{22} + 2C_3H_8$	0.229
6	$C_{16}H_{34} + 2H_2 \longrightarrow C_{12}H_{26} + 2C_2H_6$	0.063
7	$C_{16}H_{34} + H_2 \longrightarrow C_{15}H_{32} + CH_4$	0.213
8	$C_{16}H_{34} + 2H_2 \longrightarrow C_{11}H_{24} + C_3H_8 + C_2H_6$	0.151
9	$C_{17}H_{36} + H_2 \longrightarrow C_8H_{18} + C_9H_{20}$	0.836
10	$C_{17}H_{36} + H_2 \longrightarrow C_{14}H_{30} + C_3H_8$	0.860
11	$C_{18}H_{38} + H_2 \longrightarrow C_{10}H_{22} + C_8H_{18}$	0.120
12	$C_{18}H_{38} + H_2 \longrightarrow 2C_9H_{20}$	0.334
13	$C_{18}H_{38} + H_2 \longrightarrow C_{17}H_{36} + CH_4$	0.440

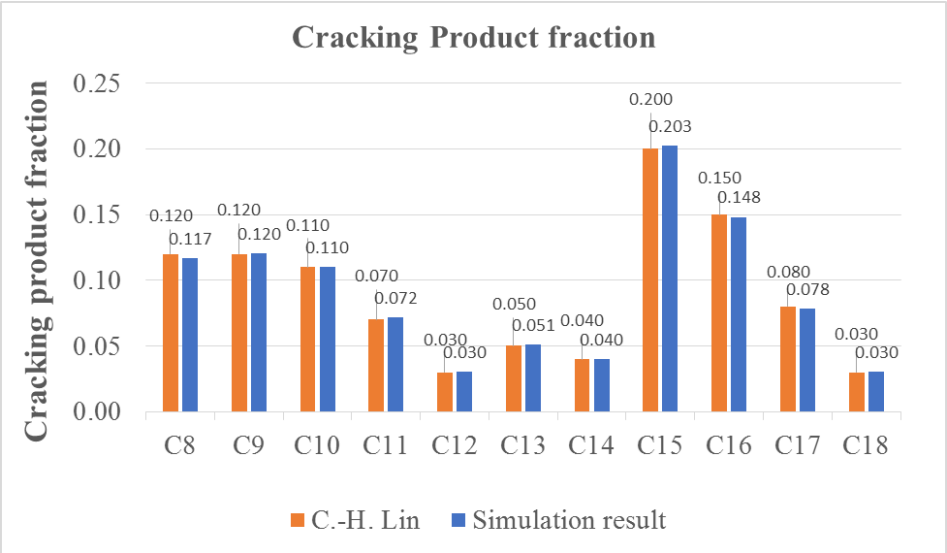

Figure 23 Cracking product composition at 360 °C, 29 barg

The cracking product composition of n-C_8 and n-C_9 was increased because the cracking of long-chain hydrocarbon is typically symmetric cracking. In other words, the cracking occurs in the middle of the hydrocarbon chain [18, 22, 24]. Therefore, the cracking product fraction was similar to jet fuel. It can be seen that the highest percentage of composition was n-C_{15} because the conversion of cracking reaction of n-C_{15} was lower than n-C_{16}, n-C_{17} and n-C_{18}. According to Figure 23, the difference in simulation result and C.-H. Lin work was less than 3%. Therefore, the cracking reaction and conversion shown in Table 13 can be used for simulation.

Isomerization converts n-paraffins to iso-paraffins. In C.-H. Lin et al. studies, isomerization was spontaneously occurred together with hydrocracking reaction over the NiAg/SAPO-11 catalyst, and the bio-jet fuel product obtained had 9% of aromatic content. It was compiled with the commercial jet fuel standard, which reported that the minimum aromatic content is set at 8% [12]. For the isomerization reaction, the simulation was run by the R-Stioc reactor model. The stoichiometry and fractional conversion were required input. The fractional conversion was calculated based on isomerization to normal alkane ratio (I-to-N ratio), which was 1.5 at 360 °C, 29 barg as reported by C.-H. Lin et al. experiment. The isomerization reaction is shown in equation (16) and isomerization content was derived by equation (17).

$$C_nH_{2n+2} \longrightarrow \text{iso-}C_nH_{2n+2} \quad (16)$$

$$\text{Isomerization content} = 1.5 \text{ n-alkane content} \quad (17)$$

According to equation 16, all of isomerization reaction conversion was found to be 0.6, and the major isomerization product was assumed to be a mono-branched cracking product for C_{8+} hydrocarbons [24]. The entire possible reaction is expressed in Appendix B.

4.3 Process design and Equipment sizing

4.3.1 Jet fuel production process from BHD

Subsequently, the validated hydrocracking unit is then plugged into BHD process. Deoxygenated product from BHD reactor was sent to the hydrocracking/isomerization unit, which was simulated by two R-Stioc reactor model. However, it is actually operated in one reactor at D-201. The liquid product leaving from flash drum was heated by E-201. The temperature was risen from 43 to 360 °C at the reaction condition. The other input stream was hydrogen which also heated up from ambient temperature to the same condition. Hydrocracking/Isomerization occurred at 360 °C, 29 barg giving product composition as shown in Figure 24. The cracking product was cooled down to 50 °C by E-203 then its pressure was reduced at the flash drum, D-202. A liquid stream (S18), containing several light gases such as H_2, CO, CO_2 CH_4, C_2H_6 and C_3H_8, was partially vaporized in D-202 at temperature of 50 °C and pressure of 20 barg. Because of the large pressure drop, part of the fluid vaporized. It resulted in two phases: a vapor phase, enriched in the more volatile components (light gas), and a liquid phase, enriched in the less volatile components (n-C_{8+}). The light gas was taken off overhead, while the liquid (LIQ4) was drained at the bottom of the drum. The vapor fraction was controlled at 0.768 to minimize the amount of octane (C_8H_{18}) loss, and 98.59% of octane was recovered. It can be seen that the products are in the jet fuel range. The product compositions mainly contained 9.83% of n-pentadecane, 8.51% of i-pentadecane and 6.62% of n-hexadecane and 5.67% of i-hexadecane. The product was then introduced to the separation unit to separate the liquid mixture by selective boiling point.

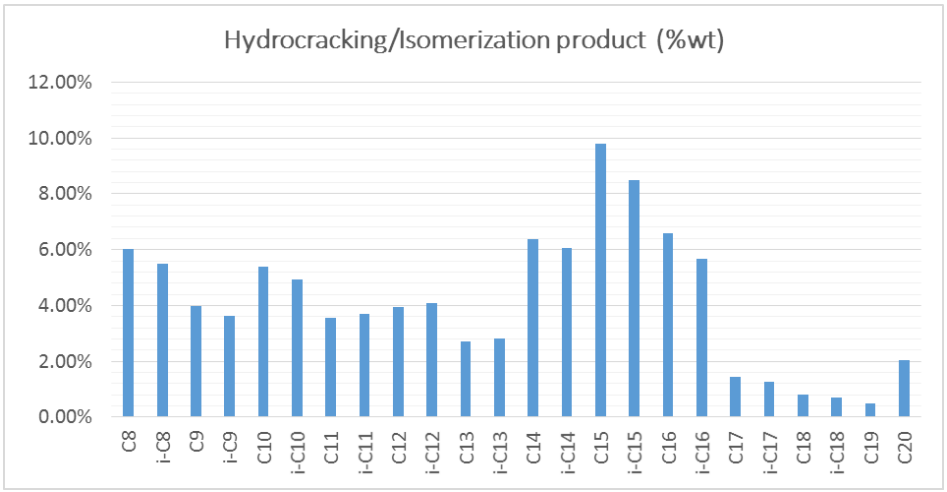

Figure 24 Product distribution leaving from hydrocracking/Isomerization reactor.

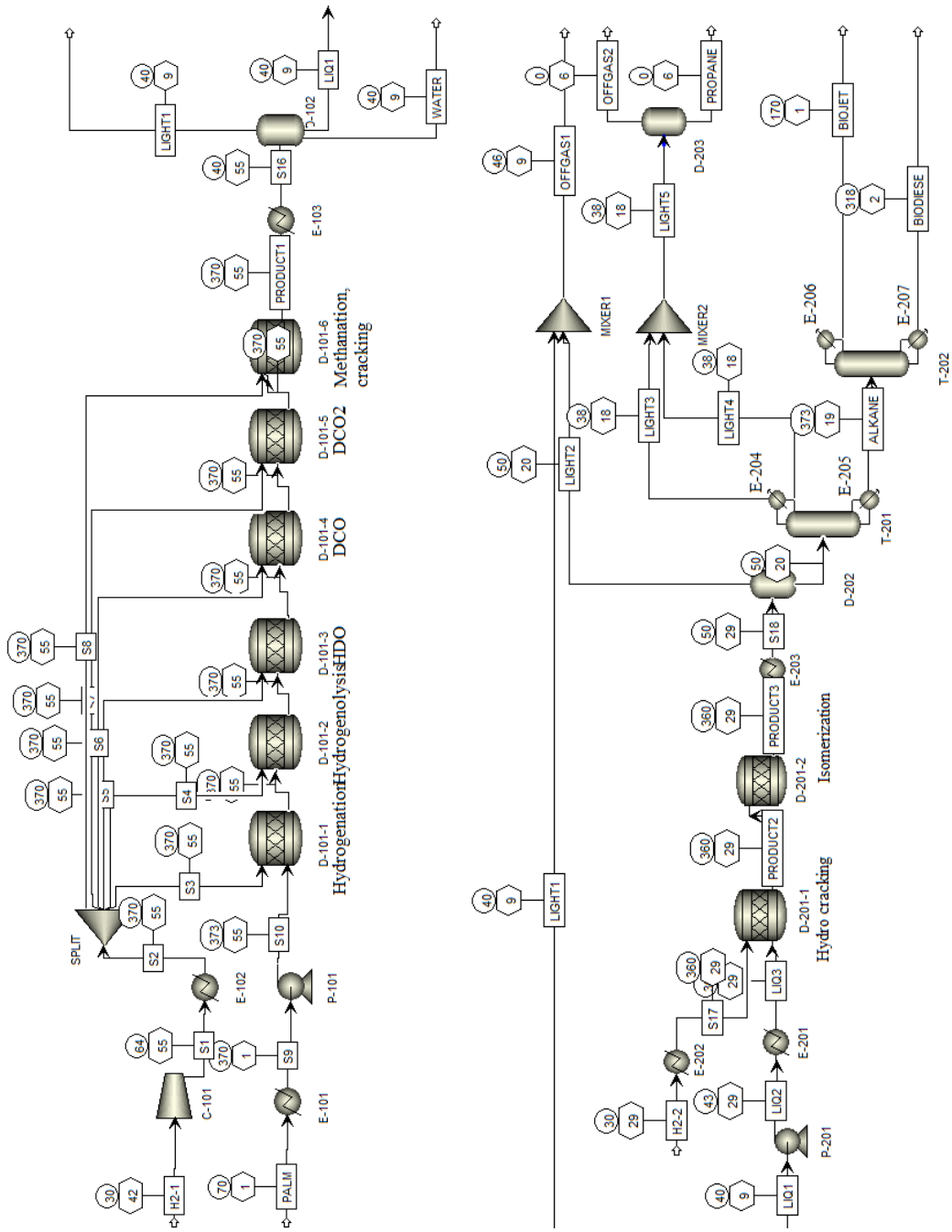

Figure 25 BHD process and hydrocracking unit for produce bio-jet fuel

In the separation section, two columns with countercurrent multiple-contact stages were used. The first column was stabilizer column and the second column was distillation column. The bottom product of flash drum (D-202) 1,542.10 kg/h, still contained some of the light gas components which have a mass flow rate of 57.37 kg/h. A stabilizer column (T-201) was preferred to remove light material from a heavy key stream. The overhead product and the bottom product were cut between propane and 2-methyl heptane (i-C_8H_{18}). The overhead product stream contained 2.40 kg/h of water, so the simulation was run by Radfrac model. The condenser valid phase was vapor-liquid-dirty water which had one vapor distillate and one liquid distillate where the water was decanted then went into the distillate. The distillate rate was set at 1.483 kmol/h resulting in mole recovery of propane in distillated stream (light3) 80% and mole recovery of 2-methyl heptane in the bottom stream (alkane) 99.99% including water content 1,503 ppm. Figure 26 and Figure 27 show the outlet stream of T-201 column. Two distillate streams were enriched with propane. It was purified in the flash drum (D-203) where pressure was reduced from 18 to 5.5 barg, and the temperature was cooled down to 0 °C due to vaporization. The purity of liquid propane was optimized at 91.73% mol.

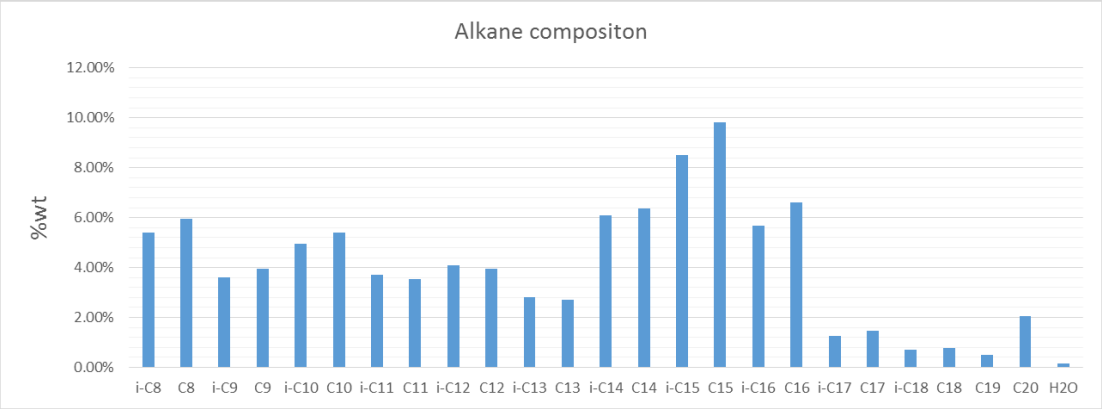

Figure 26 Bottom product stream (alkane) leaving from stabilizer column

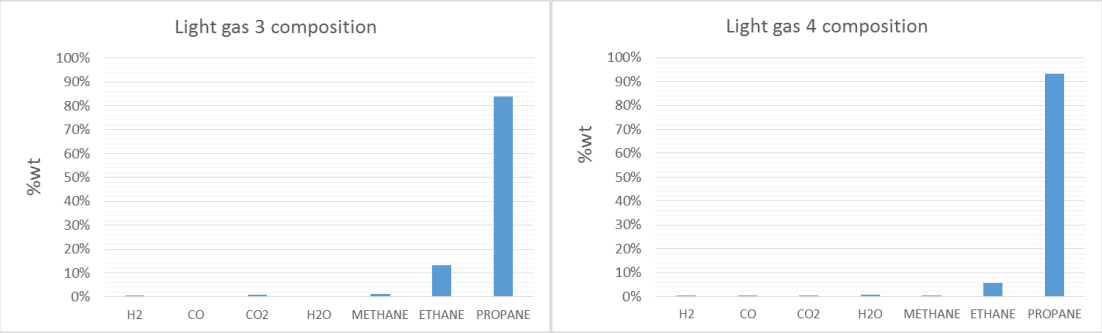

a) Vapor distillated b) Liquid distillated

Figure 27 Overhead product stream (light 3 and light 4) leaving from stabilizer column

The bottom product of the stabilizer column was alkane having composition ranging from C_8 to C_{20} at the flow rate of 1,487.03 kg/h. It was then introduced to the distillation column (T-202) to separate alkane mixture to bio-jet fuel and biodiesel fuel. In fractional distillation, a cut point was the temperature defined by a boundary between the two products. In this research, a cut point was determined at n-tetradecane (n-$C_{14}H_{30}$) having a boiling point temperature at 253.58 °C. Column T-202 was performed by Radfrac model. The condenser used was a total condenser. Distillate stream was drawn from the column in the liquid phase at 5.937 kmol/h. It was optimized using a design spec tool in Aspen plus to achieve the minimum HHV of bio-jet being 42.8 MJ/kg [12]. Mass recovery fraction of n-pentadecane in the bottom product was specified at 0.9999, and the adjusted parameter was distillate rate. After optimized, the HHV at 15 °C of bio-jet fuel and biodiesel from Aspen plus were found to be 43.53 MJ/kg and 31.34 MJ/kg, respectively. Two product streams were 854.68 kg/h of jet fuel leaving at the top of the column and 632.36 kg/h of biodiesel leaving at the bottom of the column. The overall product yield of bio-jet fuel production from BHD was shown in Table 14. It can be seen that off-gas, which is containing H_2, CO, CO_2 and light hydrocarbon, was 25.09% of the total product. It can be utilized by use as a heat source of the furnace.

The composition of bio-jet fuel in Figure 28 shows that the highest component of bio-jet fuel was n-octadecane (n-C_8H_{18}) and their isomer. It can be explained by cracking reaction that occurs in the middle of n-hexadecane (n-$C_{16}H_{34}$) and n-heptadecane (n-$C_{17}H_{36}$) which then isomerized to i-octadecane (i-C_8H_{18}). In the case of biodiesel composition in Figure 29, the major components were n-pentadecane (n-$C_{15}H_{32}$) and their isomer because it had low conversion during cracking reaction.

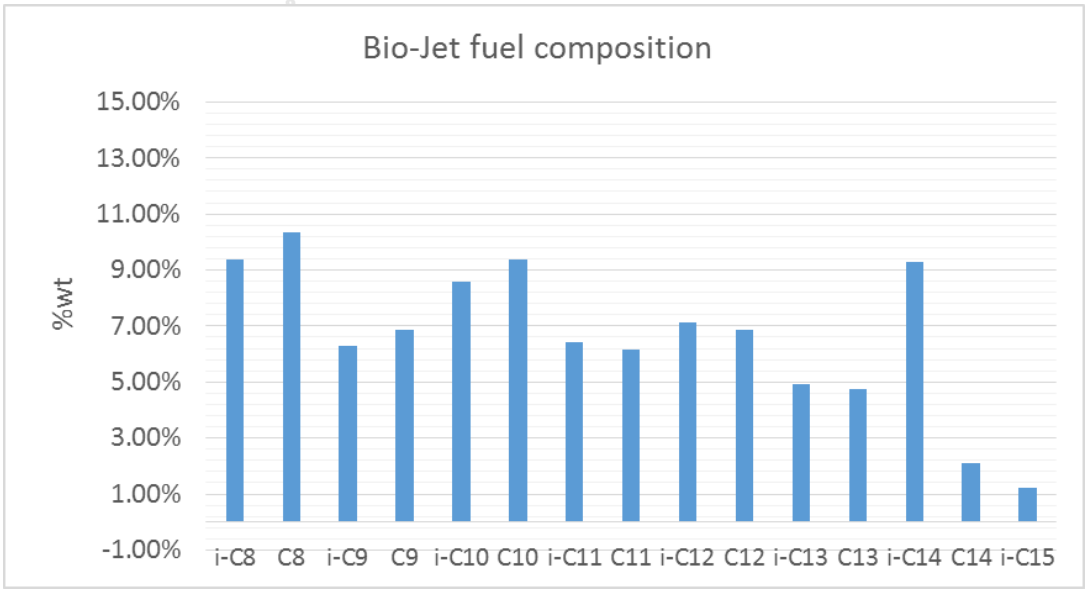

Figure 28 Bio-jet fuel composition

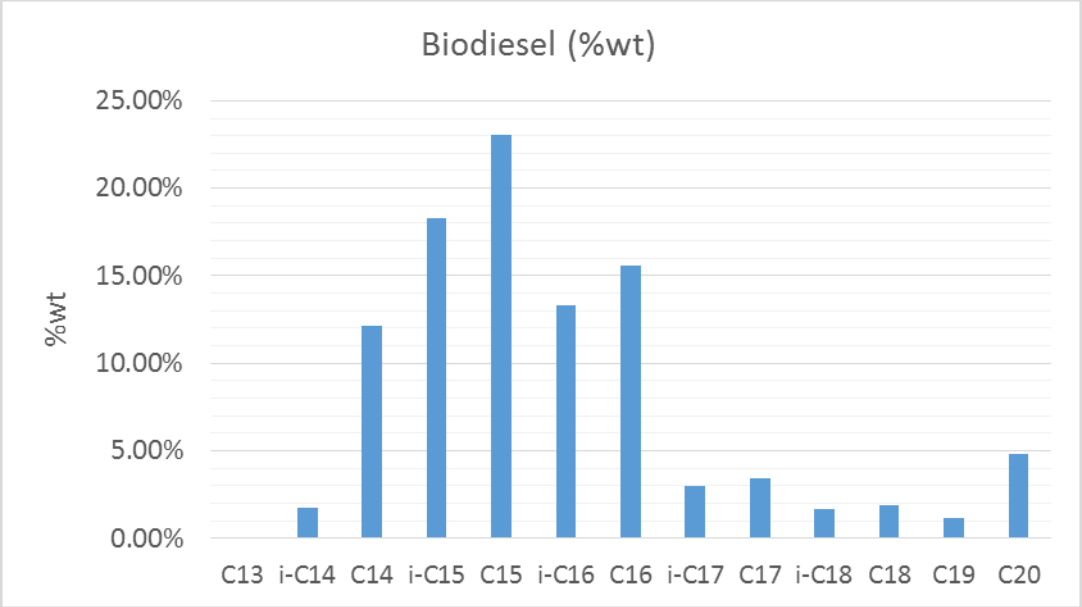

Figure 29 Biodiesel composition

Table 14 Overall product yield of bio-jet fuel/biodiesel process

Product	Mass flow rate (kg/h)	% product yield
Bio-jet	854.68	37.70%
Biodiesel	632.36	27.90%
Propane	6.68	0.29%
off-gas	568.78	25.09%
water	204.29	9.01%
	2,266.78	100.00%

In the view of hydrogen consumption of bio-jet fuel/biodiesel process, it was calculated at 0.107 kg/kg product, which was 52% more than BHD based case process. It was because of the higher hydrogen required for cracking reaction. The data is expressed in Table 15.

Table 15 Comparison of hydrogen consumption of base case and improvement case

Process	Main product	Hydrogen consumption (kg/kg product)
BHD production (Base case)	BHD	0.052
Bio-jet fuel/biodiesel process	Biodiesel and bio-jet fuel	0.107

4.3.2 Equipment design and sizing

Knowing the material and energy balance of process flow sheet, equipment size can be determined. Main equipment in the BHD production plant (based case) and bio-jet fuel/biodiesel plant (improvement case) was reactor, column, furnace, heat exchanger, flash drum, pump and compressor. A number of the equipment for both processes were shown in Table 16. The equipment was sized by aspen plus together with sizing procedures from Lorenz T. Biegler and team method [20]. Firstly the calculation was based on plant capacity at 75,000 bbl/y of bio-jet fuel following Elias Martinez-Hernandez, el al research [22].

Table 16 Main equipment of BHD process and bio-jet fuel/biodiesel process

Equipment	BHD process	Bio-jet fuel/biodiesel process
Reactor	1	2
Column	-	2
Furnace	2	6
Heat exchanger	1	4
Flash drum	1	3
Pump	1	4
Compressor	1	1

a) Reactor

In Hsu et al [11] experiment, NiMo/γ-Al_2O_3 is used as a catalyst for deoxygenation reaction. 5-gram catalyst was loaded in fixed bed reactor. The catalyst bed volume is roughly 184 cm^3 and total volume of the reactor is approximately 283 cm^3. In this study, the reactor size was estimated by those experimental data and used WHSV of 3 h^{-1} for computing the actual weight of the catalyst within the reactor.

The product from the deoxygenation reaction experiment was used as raw material for hydrocracking and isomerization process for producing a jet fuel-ranged product. The experiment was proposed by C.H. Lin et al [18]. NiAg/SAPO-11 was chosen as a catalyst and using a fixed bed reactor with a total volume of approximately 51 cm^3. Catalyst weight was reported as 5 grams, and LHSV was 1 h^{-1}. All parameters used for reactor sizing and process simulation in the deoxygenation process and hydrocracking/isomerization process was presented in Table 31. To determine the actual size of the reactor, mass flow rate and volume flow rate of raw material were used. Table 17 shows the result of the calculation. Principally, the packed bed reactor was selected to handle gas-liquid reaction with long-lifetime catalyst, which is not regenerated frequently. However, for large scale of production, the resistance of mass transfer of gas reactant

through gas-liquid interphase and then to the surface of solid catalyst should be considered. Hydrogen must first dissolve into palm oil (liquid phase), then both reactant must diffuse or move to the catalyst surface for reaction to occur. For a high reaction conversion, a trickle bed reactor can be a satisfying option [25].

Table 17 Actual size of the reactor and their operating condition

Parameters	Unit	Deoxygenation process	hydro-cracking/ isomerization process
Catalyst		NiMo/γ-Al_2O_3	NiAg/SAPO-11
Temperature	°C	370	360
Pressure	barg	55.2	29
H_2/Oil ratio		254.3 (Ncm^3/cm^3)	13.6 (Molar ratio)
WHSV	h^{-1}	3	-
LHSV	h^{-1}	-	1
Mass flow of raw material	kg/h	2,107.72	1,729.09
Volume flow rate of raw material	m^3/h	1.79	3.93
Volume of catalyst bed	m^3	25.85	2.55
Total reactor volume	m^3	39.79	3.93
Catalyst weight	kg	702.57	387.73
Net heat of duty (Sum of all reactor)	kcal/h	-543,484.25	-11,682.63

b) Column

There are 2 columns in the separation section of bio-jet fuel/biodiesel process. One is a stabilizer column (T-201), and another one is a distillation column (T-202). Their size, condenser and reboiler heat duty estimated by Aspen plus. Distillate rate, reflux ratio and the number of stages were estimated by performing DSTWU column model and define a cut point of distillation. The calculation result was shown in Table 18, while the detail of the calculation was shown in Appendix C2. The column temperature profile was shown in Figure 30 and Figure 31. It can be seen that the temperature of T-201 reboiler was higher than T-202 because the column pressure of T-201 was increased. The type of tray in both towers was a sieve tray. By considering cost, sieve-type was more reasonable comparing to a valve tray, which is about 20% higher, and bubble-cap tray, which is almost double of sieve-type tray [26]

Table 18 Actual size of column and their configuration

	Unit	Stabilizer column	Distillation column
Height	m	14.63	37.19
Diameter	m	0.61	0.91
Condenser pressure	barg	18	1
Column pressure drop	barg	0.5	0.5
Number of stage		14	40
Internal		Sieve tray	Sieve tray
Distillate rate	kmol/h	1.483	5.9373
Reflux ratio		2	5
Condenser heat duty	kW	-12.43	-571.67
Reboiler heat duty	kW	411.33	372.96

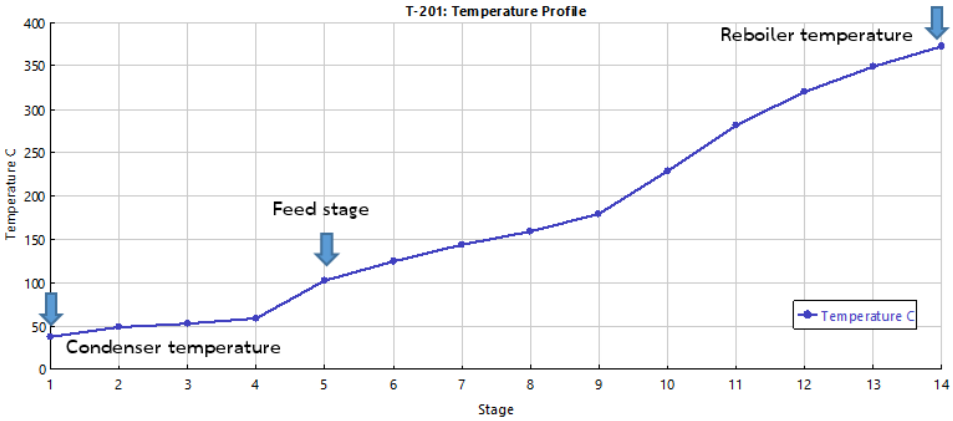

Figure 30 Stabilizer temperature profile and feed location

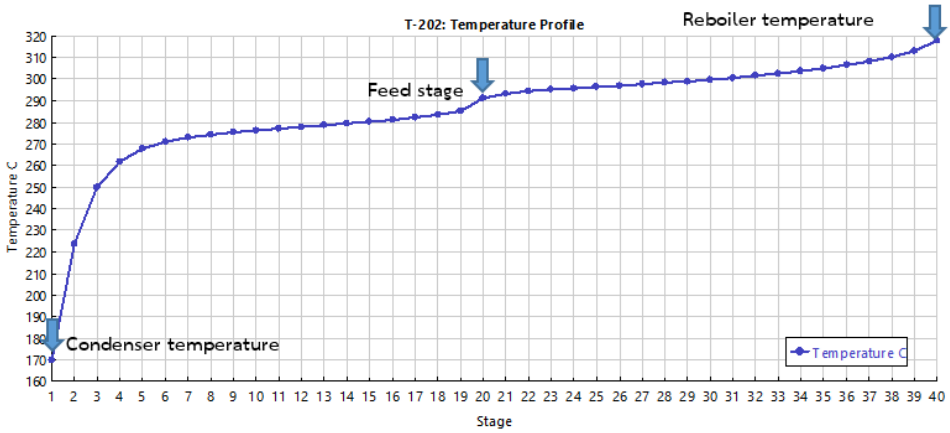

Figure 31 Distillation column temperature profile and feed location

c) Furnace and heat exchanger

The main reactions in this research were deoxygenation reaction, cracking reaction and isomerization. They occurred at a high temperature between 360-370 °C. By considering utility requirement, high-pressure steam is supplied at 41 barg, 254 °C, which is insufficiency for heating [21]. Thus, a non-reactive furnace was selected for heating equipment. For cooling product stream, a fixed tube heat exchanger was used except E-204, which was double pipe heat exchanger due to small heat transfer area. Furnace and heat exchanger were listed in Table 19 and Table 20.

Table 19 Heating equipment in BHD plant

Equipment	Type	Heat duty (kW)	Heat transfer area (m^2)
E-101	Furnace	469	-
E-102	Furnace	110	-
E-103	Fixed tube heat exchanger	671	24

Table 20 Heating equipment in bio-jet fuel/biodiesel plant

Equipment	Type	Heat duty (kW)	Heat transfer area (m^2)
E-101	Furnace	469	n/a
E-102	Furnace	110	n/a
E-103	Fixed tube heat exchanger	671	24
E-201	Furnace	427	n/a
E-202	Furnace	94	n/a
E-203	Fixed tube heat exchanger	566	37
E-204	Double pipe Heat exchanger	13	4
E-205	Furnace	412	n/a
E-206	Fixed tube heat exchanger	572	26
E-207	Furnace	373	n/a

d) Flash drum

Flash drum is a process vessel which allows vapor fraction in vapor-liquid mixture to separate in low-pressure condition. The volume of the flash drum was calculated based on a five-minute liquid holdup time with an equal volume added for vapor flows [20] The detail was shown in Appendix C. The result of the calculation was showed in Table 21.

Table 21 Flash drum sizing

	D-102	D-202	D-203
Volume (m^3)	3	14	3
Type	Vertical vessel	Vertical vessel	Vertical vessel

e) Pump/Compressor

Pump and compressor size determined by shaft power. The data was obtained from Aspen plus as Table 22.

Table 22 pump and compressor sizing

	C-101	P-101	P-201	P-203 (Stabilizer reflux pump)	P-203 (Distillation reflux pump)
Power (kW)	13	13	5	1	2

4.4 Economic analysis and feasibility study

According to mass and energy balance, evaluation of fixed capital cost and manufacturing costs was performed. The BHD plant with capacity of 120,229 bbl/y was compared with bio-jet and biodiesel plant with total capacity 127,595 bbl/y. Calculation basis and assumptions for the feasibility study were listed in Table 23. The raw material used for both plants were crude palm oil and hydrogen, and their price were obtained from world market price [27, 28]. The catalyst was assumed to be replaced every five years and its price was estimated by chemical composition based on laboratory analysis. Manufacturing cost and labor cost were based on Turton and team method [21]. To calculate revenue of the project, product prices must be known. Bio-jet and biodiesel prices were obtained from other research [22]. Also, the sensitivity analysis of prices was executed. Propane was sold as a by-product of bio-jet and biodiesel plant, and its purity was 91.73 %mol. Propane price was 0.17 USD/liter given by US Energy Information Administration [29]. In the case of BHD plant, propane purity was only 69.62% mol. Therefore, there was no purification unit added to purify propane in this research. Thus, propane was not be taken into account in BHD plant case. The evaluation of the total capital cost of both plants considered direct project expenses, including equipment free onboard cost, materials required for installation and labor cost to install equipment and material, and indirect project expenses namely, freight/insurance/taxes, construction overhead and contractor engineering expenses. This study used a bare module costing technique to estimate the cost of a new chemical plant [21]. It represented the sum of direct and indirect costs in base case

condition being carbon steel (CS) as a unit fabrication material and unit operated at near-ambient pressure. Then, the material of construction factor, F_m, and pressure factor, F_p, were multiplied to find the bare module cost (C_{BM}) of equipment in actual plant condition. The comparison between BHD plant with bio-jet/biodiesel plant was shown in Table 24. The fixed capital investment (FCI), cost of operating labor (C_{OL}), Cost of utilities (C_{UT}), Cost of waste treatment (C_{WT}) and Cost of raw materials (C_{RM}) were interpreted. The economic analysis of both cases was also considered.

Table 23 Parameter and assumption for feasibility study

Parameter	Unit	Value
Operating hour	h/y	7920
Plant life time	year	15
Product Capacity	bbl/y	
- BHD plant		120,229
- Bio-jet/biodiesel plant		69,967 and 57,628
Interest rate (MLR)	%	5.58
Exchange rate	baht/USD	32.61
Equipment cost as year		2017
Contingency		18%
Raw material cost		
- Crude palm oil	USD/kg	0.56
- Hydrogen	USD/kg	1
- NiMo-S/γ-Al_2O_3	USD/kg	4.38
- NiAg/SAPO	USD/kg	114.74
Utility cost and labor cost		
- Electricity	USD/kW	0.06
- Fuel (natural gas)	$/GJ	11.1
- Process water	USD/1,000 kg	0.067
- Chemical cost for cooling water	USD/1,000 kg	0.156
- Waste water treatment cost	USD/1000 m^3	56
- Labor (for 2000 hour-year) [21]	USD	52,900
Parameter for revenue calculation		
Bio-jet price	USD/liter	1.21
Biodiesel price	USD/liter	0.92
Propane price	USD/liter	0.17

Table 24 Cost estimation and economic analysis of BHD plant and bio-jet fuel/biodiesel plant

Parameters	Unit	BHD Plant	Bio-jet fuel/biodiesel plant
Fixed capital investment (FCI)	MB	145.96	431.67
Bare module cost		122.28	361.65
Contingency		22.01	65.10
Interest during construction		1.66	4.92
Manufacturing cost (COM)	MB/Y	508.70	595.75
Cost of raw materials (C_{RM})		328.68	347.17
Cost of utilities (C_{UT})		8.37	13.70
Cost of waste treatment (C_{WT})		2.98	2.98
Cost of operating labor (C_{OL})		23.73	27.38
Other direct/Indirect cost		144.96	204.53
Project benefit (Average 15 year)	MB/Y	458.82	571.53
Net benefit		458.63	570.99
Net profit before tax		41.59	64.56
Net profit after tax		32.82	50.32
EBITDA		55.38	101.17
Feasibility study			
NPV	MB	128.24	99.79
IRR	%	27.24	16.90
Payback period		5 Year 9 Month	7 Year 4 Month

By comparing the fixed capital investment, the bio-jet fuel/biodiesel plant was two times higher than BHD plant, as a result of higher investment in cracking/isomerization unit and separation. Manufacturing cost was increased 17%, caused by raw material expenditure, because the bio-jet fuel/biodiesel plant consumed more hydrogen in cracking/isomerization reaction. In the view of project revenue, bio-jet fuel/biodiesel plant can maximize the benefit to 571.53 MB per year while BHD plant was 458.82 MB per year because the bio-jet fuel price was higher than BHD. According to the feasibility study, considering NPV, IRR and payback period, BHD plant is still more attractive for investment with the IRR 27.24% while bio-jet fuel/biodiesel plant was only 16.90%. For insight feasibility study of bio-jet fuel/biodiesel plant, the cash flow diagram was plotted in Figure 32. The net cash flow of first 3 years was negative because the project was in the construction period. This study sets to be 3 years for construction and benefit was fully generated at the third year. Positive cash flow was 101.25 MB from third to thirteenth years. The replacement cost of catalyst for every five years was distributed into a yearly cost. In the

fourteenth year, the net cash flow included a salvage value estimated from a depreciation of equipment based on 15 years of the project lifetime. The straight-line depreciation method (SL) was calculated to 28.78 MB per year. An equal amount of depreciation was charged each year over the depreciation period starting from year 0 to 14th.

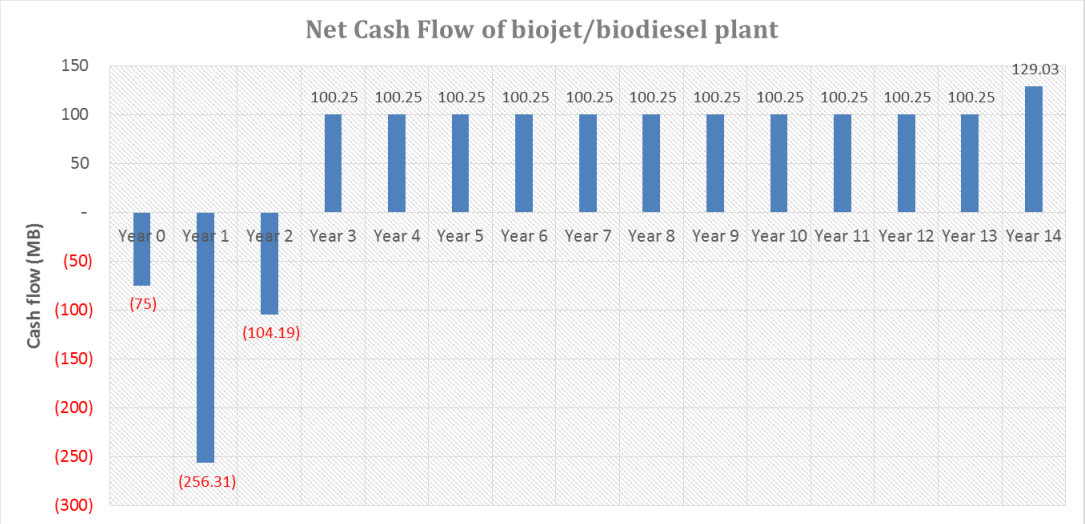

Figure 32 Net cash flow diagram of bio-jet fuel/bio diesel plant.

According to the fluctuation of the price of investment cost and product, the sensitivity study was examined. The fixed investment cost and bio-jet fuel/biodiesel prices were varied, then IRR was determined and shown in *Table 25* and *Table 26.* The bio-jet fuel price can have a significant effect on feasible of the project. IRR was increased when the bio-jet fuel price increases and fixed investment cost dwindle. The maximum IRR obtained was at 54.1% when the bio-jet fuel price was 2.01 USD/liter and the fixed investment cost was 432.67 MB. If the bio-jet fuel price is below 1.21 USD/liter, IRR cannot be determined because of negative values on the net profit and entire net cash flow [30]. In the case of biodiesel price, the same scenario of the project was described. IRR was maximized at 35.8% when biodiesel price was 1.32 USD/liter, and fixed investment cost was 432.87 MB. There was some allowance of biodiesel price fluctuation. It can be lower to 0.72 USD/liter, which still obtained positive IRR.

Table 25 Sensitivity study of Total fixed investment and bio-jet fuel price

			Bio- jet fuel price (USD/liter)				
			0.41	**0.81**	**1.21**	**1.61**	**2.01**
		16.9%	**-0.8**	**-0.4**	**0**	**0.4**	**0.8**
Total Fixed Assets Investment (MB)	**388**	**-10%**	N/A	N/A	18.9%	38.9%	54.1%
	410	**-5%**	N/A	N/A	17.9%	37.2%	52.0%
	432	**0%**	N/A	N/A	**16.9%**	35.7%	50.1%
	453	**5%**	N/A	N/A	16.0%	34.4%	48.4%
	475	**10%**	N/A	N/A	15.2%	33.1%	46.7%

*N/A mean that IRR cannot be determine because the entire net cash flow was negative. Numerical value of IRR can range from -100% < IRR < infinity [30]

Table 26 Sensitivity study of Total fixed investment and biodiesel price

			Biodiesel price (USD/liter)				
			0.52	**0.72**	**0.92**	**1.12**	**1.32**
		16.9%	**-0.4**	**-0.2**	**0**	**0.2**	**0.4**
Total Fixed Assets Investment (MB)	**388**	**-10%**	-20.8%	7.2%	18.9%	28.0%	35.8%
	410	**-5%**	-20.7%	6.5%	17.9%	26.7%	34.3%
	432	**0%**	-20.6%	5.8%	**16.9%**	25.5%	32.9%
	453	**5%**	-20.5%	5.2%	16.0%	24.4%	31.6%
	475	**10%**	-20.5%	4.6%	15.2%	23.4%	30.3%

Principally, the plant capacity was the main effect of fixed capital investment; thus, the concept of economy of scale was applied. The bio-jet fuel/biodiesel plant capacity was expanded to 4 times of the base case to comply with existing commercial biodiesel plant in Thailand [23]. The estimating procedures to obtain a new plant capacity is six-tenths rule method recommended by Turton R. and team method [21]. Figure 33 and Figure 34 illustrated the effect of plant capacity on fixed capital investment and IRR, seeing that when plant capacity increased, fixed investment cost was also increased. Even though the cost was doubled, the IRR was increased. By specifying new plant capacity at 510,381 bbl/y (Bio-jet 279,870 bbl/y and biodiesel 230,511 bbl/y), fixed capital investment cost was estimated to be 831.79 MB, and IRR was 29.07% because of the lower cost of equipment per unit of capacity.

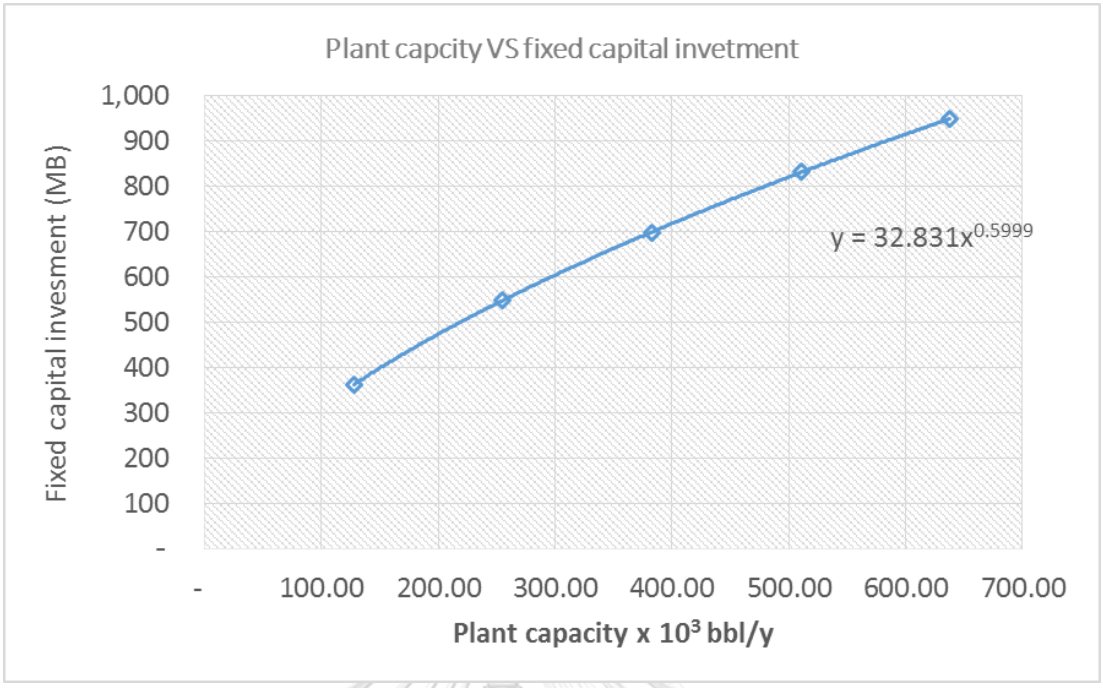

Figure 33 Effect of plant capacity on fixed capital cost

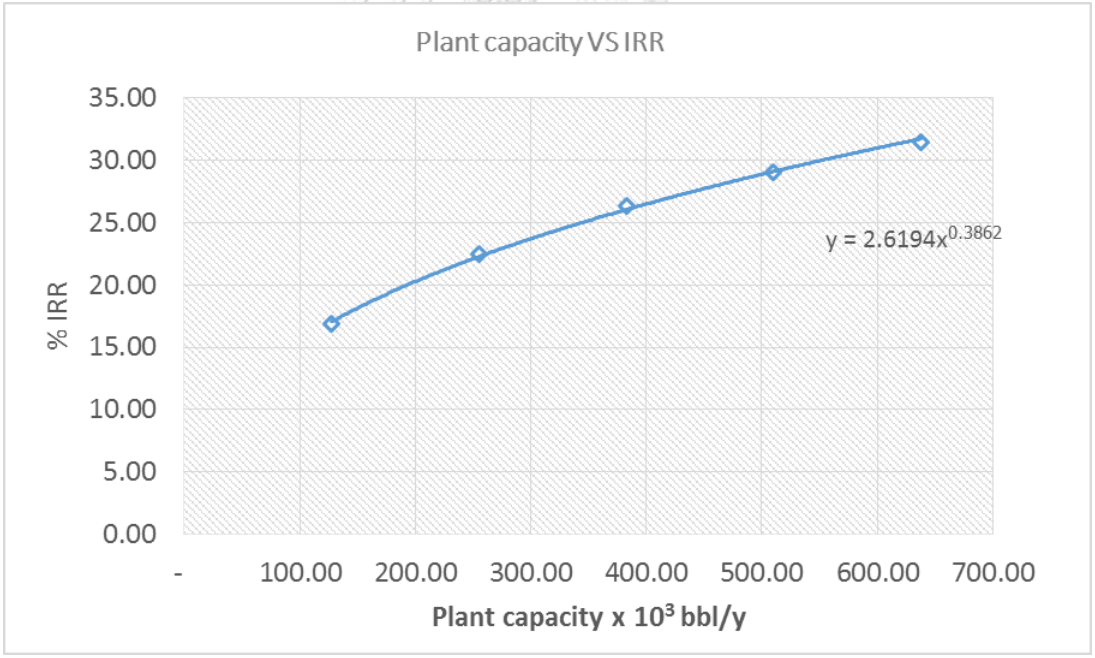

Figure 34 Effect of plant capacity on IRR

CHAPTER 5 CONCLUSION

This study showed the BHD production process from crude palm oil and the modification of the existing BHD process to produce bio-jet fuel. For the deoxygenation reaction of CPO to BHD, the packed bed reactor was selected, and the simulation was run by conversion reactor at 370 °C and 55.2 barg. The process consumed hydrogen of 0.052 kg per kg product. The produced BHD composition, which is mainly n-hexadecane and n-octadecane, was used as a raw material for bio-jet fuel production. Hydrocracking/isomerization reactor was added to the existing BHD process to produce bio-jet fuel with a reaction temperature of 360 °C and pressure of 29 barg operating in a packed bed reactor. The alkane mixture product was separated by fractional distillation. A cut point was determined at n-tetradecane having boiling point temperature at 253.58 °C. Bio-jet fuel product had the main composition of n-octadecane and their isomer. In the case of biodiesel composition, the major component was n-pentadecane and i-pentadecane. The HHV at 15 °C of bio-jet fuel estimated by Aspen plus were found to be 43.53 MJ/kg. The overall product yield of bio-jet fuel/biodiesel plant was bio-jet fuel 37.7% and biodiesel 29.7%. The by-product gases obtained are mainly propane with a purity of 91.73 %mol. Hydrogen consumption of bio-jet fuel/biodiesel plant was 0.107 kg per kg product, which was 52% higher than BHD based case process.

The economic analysis and feasibility study of each process were also performed. The fixed capital investment of the bio-jet fuel/biodiesel plant was two times higher than BHD plant, and manufacturing cost was increased by 17% due to higher hydrogen consumption. Therefore, the BHD plant is still more attractive for investment because of higher NPV and IRR. Moreover, the payback period was shorter. The IRR of the bio-jet fuel/biodiesel plant was 16.90%, which can be increased depending on the market situation. To achieve greater IRR, the bio-jet fuel/biodiesel plant capacity was adjusted to 279,870 bbl/y of bio-jet fuel and 230,511 bbl/y of biodiesel. IRR was increased to 29.07% because of the lower cost of equipment per unit capacity; thus the project was more attractive. For future work, a higher yield of bio-jet fuel catalyst should be investigated in order to elevate the economic attractiveness.

REFERENCES

1. Letcher, T.M., *1 - Why do we have global warming?*, in *Managing Global Warming*, T.M. Letcher, Editor. 2019, Academic Press. p. 3-15.
2. *Chapter 1 - Review and outlook of world energy development*, in *Non-Fossil Energy Development in China*, Y. Zhang, et al., Editors. 2019, Academic Press: Oxford. p. 1-36.
3. Othman, M.F., et al., *Green fuel as alternative fuel for diesel engine: A review.* Renewable and Sustainable Energy Reviews, 2017. **80**: p. 694-709.
4. Voloshin, R.A., et al., *Review: Biofuel production from plant and algal biomass.* International Journal of Hydrogen Energy, 2016. **41**(39): p. 17257-17273.
5. Gaurav, N., et al., *Utilization of bioresources for sustainable biofuels: A Review.* Renewable and Sustainable Energy Reviews, 2017. **73**: p. 205-214.
6. Joshi, G., et al., *Challenges and opportunities for the application of biofuel.* Renewable and Sustainable Energy Reviews, 2017. **79**: p. 850-866.
7. Kiatkittipong, W., et al., *Diesel-like hydrocarbon production from hydroprocessing of relevant refining palm oil.* Fuel Processing Technology, 2013. **116**: p. 16-26.
8. Srifa, A., et al., *Production of bio-hydrogenated diesel by catalytic hydrotreating of palm oil over NiMoS2/γ-Al2O3 catalyst.* Bioresource Technology, 2014. **158**: p. 81-90.
9. Yoosuk, B., et al., *Hydrodeoxygenation of oleic acid and palmitic acid to hydrocarbon-like biofuel over unsupported Ni-Mo and Co-Mo sulfide catalysts.* Renewable Energy, 2019. **139**: p. 1391-1399.
10. Bezergianni, S., et al., *Refinery co-processing of renewable feeds.* Progress in Energy and Combustion Science, 2018. **68**: p. 29-64.
11. Hsu, K.-H., W.-C. Wang, and Y.-C. Liu, *Experimental studies and techno-economic analysis of hydro-processed renewable diesel production in Taiwan.* Energy, 2018. **164**: p. 99-111.
12. Khan, S., et al., *A review on deoxygenation of triglycerides for jet fuel range hydrocarbons.* Journal of Analytical and Applied Pyrolysis, 2019. **140**: p. 1-24.
13. Corporation, N.O. *Neste Oil's second renewable diesel plant commissioned at Porvoo*. 2009 [cited 2020 29 Aug 20]; Available from: https://www.neste.com/neste-oils-second-renewable-diesel-plant-commissioned-porvoo.
14. Plazas-González, M., C.A. Guerrero-Fajardo, and J.R. Sodré, *Modelling and simulation of hydrotreating of palm oil components to obtain green diesel.* Journal of Cleaner Production, 2018. **184**: p. 301-308.
15. de Sousa, F.P., C.C. Cardoso, and V.M.D. Pasa, *Producing hydrocarbons for green diesel and*

jet fuel formulation from palm kernel fat over Pd/C. Fuel Processing Technology, 2016. **143**: p. 35-42.

16. Edwards, T., J. Stricker, and W.J.H.o.A.F.P. Harrison III, 3rd Edition, SAE, *Coordinating support of fuels and lubricant research and development (R&D) 2.* 2004.
17. Blakey, S., L. Rye, and C.W. Wilson, *Aviation gas turbine alternative fuels: A review.* Proceedings of the Combustion Institute, 2011. **33**(2): p. 2863-2885.
18. Lin, C.-H., Y.-K. Chen, and W.-C. Wang, *The production of bio-jet fuel from palm oil derived alkanes.* Fuel, 2020. **260**: p. 116345.
19. Wang, W.-C., *Techno-economic analysis of a bio-refinery process for producing Hydro-processed Renewable Jet fuel from Jatropha.* Renewable Energy, 2016. **95**: p. 63-73.
20. Lorenz T. Biegler, I.E.G., Arthur W. Westerberg, *systematic Medthods of Chemical Process Design*. Pretice Hall International Series in the Physical and Chemical Engineering Sciences.
21. Turton, R., et al., *Analysis, synthesis and design of chemical processes*. 2008: Pearson Education.
22. Martinez-Hernandez, E., et al., *Process simulation and techno-economic analysis of bio-jet fuel and green diesel production — Minimum selling prices.* Chemical Engineering Research and Design, 2019. **146**: p. 60-70.
23. Tunpaiboon, N., *Biodiesel*, in *THAILAND INDUSTRY OUTLOOK 2017-19*. 2017.
24. J.W. Thybaut, G.B.M., *Advances in Catalysis*. Multiscale Aspects in Hydrocracking: From Reaction Mechanism Over Catalysts to Kinetics and Industrial Application. Vol. Volume 59. 2016: Elsevier Inc.
25. Levenspiel, O., *Chemical Reaction Engineering*. 3rd ed. 1999: John Wiley&Sons.
26. Geankoplis, C.J., *Transport Processes and Separation Process Principles (Includes Unit Operations)*. Fourth edition ed. 2003: Pearson Education, Inc.
27. *Industry Indicators : Biodiesel, Palm oil price*. 2020, Krungsri research.
28. Brown, T., *The cost of hydrogen: Platts launches Hydrogen Price Assessment*. 2019, S&P Global Platts press release, S&P Global Platts Launches World's First Hydrogen Price Assessments.
29. Mont Belvieu, T.P.S.P.F., *Propane Daily Price*. US Energy Information Administration.
30. Leland Blank, A.T., *Basics of Engineering Economy*. 2014, McGraw-Hill, a business unit of The McGraw-Hill Companies, Inc.

VITA

NAME	Nattamon Munkong
DATE OF BIRTH	28 January 1991
PLACE OF BIRTH	Phetchabun
INSTITUTIONS ATTENDED	School: Protpittayapayat Bachelor degree: Department of Chemical Engineering, Faculty of Engineering, King Mongkut's Institute of Technology Ladkrabang
HOME ADDRESS	112/6 Kumkloa village, Kumkloa road, Lamplatiew, Lat Krabang. Bangkok,10520
PUBLICATION	-
AWARD RECEIVED	-

APPENDIX A Bio-hydrogenated Diesel Process

The reaction occurred in the deoxygenation reactor are determined based on palm oil compositions as Table 6. The main reaction pathway is Hydrogenation, Hydrogenolysis, HDO, DCO, DCO_2, cracking, and methanation.

a) Hydrogenation; Convert unsaturated triglyceride to saturated triglyceride. Triolein (18:1), $C_{57}H_{104}O_6$ reacts with 3 moles of hydrogen to form tristearin (18:0), $C_{57}H_{110}O_6$ and triolein (18:2), $C_{57}H_{98}O_6$ react with 6 moles of hydrogen to form tristearin as equation A1 - A2

$$C_{57}H_{104}O_6 + 3H_2 \longrightarrow C_{57}H_{110}O_6 \quad \text{A1.}$$

$$C_{57}H_{98}O_6 + 6H_2 \longrightarrow C_{57}H_{110}O_6 \quad \text{A2.}$$

b) Hydrogenolysis; Convert saturated triglyceride to a fatty acid. By this reaction, the saturated triglyceride such as tripalmitin (16:0), $C_{51}H_{98}O_6$, tristearin (18:0), $C_{57}H_{110}O_6$ and triarachidin (20:0), $C_{63}H_{122}O_6$ react with 3 moles of hydrogen to obtain 3 moles of their fatty acid including palmatic acid ($C_{16}H_{32}O_2$), stearic acid ($C_{18}H_{36}O_2$) and arachidic acid ($C_{20}H_{40}O_2$), respectively. Propane is by-product of this reaction. The hydrogenolysis reactions are shown as equation A3 – A5.

$$C_{51}H_{98}O_6 + 3H_2 \longrightarrow 3C_{16}H_{32}O_2 + C_3H_8 \quad \text{A3.}$$

$$C_{57}H_{110}O_6 + 3H_2 \longrightarrow 3C_{18}H_{36}O_2 + C_3H_8 \quad \text{A4.}$$

$$C_{63}H_{112}O_6 + 3H_2 \longrightarrow 3C_{20}H_{40}O_2 + C_3H_8 \quad \text{A5.}$$

c) Hydrodeoxygenation; Convert fatty acid to n-alkane by remove water. The n-alkane product from this reaction will have a number of carbon atoms equal to the primary fatty acid as express in equation A6 - A8, while 2 moles of water are removed.

$$C_{16}H_{32}O_2 + 3H_2 \longrightarrow C_{16}H_{34} + 2H_2O \quad \text{A6.}$$

$$C_{18}H_{36}O_2 + 3H_2 \longrightarrow C_{18}H_{38} + 2H_2O \quad \text{A7.}$$

$$C_{20}H_{40}O_2 + 3H_2 \longrightarrow C_{20}H_{42} + 2H_2O \quad \text{A8.}$$

d) Decarbonylation; Convert fatty acid to n-alkane by removing carbon monoxide and water. The n-alkane products with one carbon atom lower than their fatty acid feed are produced as equation A9 – A11.

$$C_{16}H_{32}O_2 + H_2 \longrightarrow C_{15}H_{32} + CO + 2H_2O \quad \text{A9.}$$

$$C_{18}H_{36}O_2 + H_2 \longrightarrow C_{17}H_{36} + CO + 2H_2O \quad \text{A10}$$

$$C_{20}H_{40}O_2 + H_2 \longrightarrow C_{19}H_{40} + CO + 2H_2O \quad \text{A11.}$$

e) Decarboxylation; Convert fatty acid to n-alkane by removing carbon dioxide and water. This reaction is not required hydrogen to convert fatty acid to n-alkane, which one carbon atom lower than the original compound as equation A12 – A14.

$$C_{16}H_{32}O_2 \longrightarrow C_{15}H_{32} + CO_2 \quad \text{A12.}$$

$C_{18}H_{36}O_2 \longrightarrow C_{17}H_{36} + CO_2$ A13.

$C_{20}H_{40}O_2 \longrightarrow C_{19}H_{40} + CO_2$ A14.

f) Cracking; Convert n-alkane to shorter hydrocarbon by reacting with hydrogen. All possible cracking reactions according to lab-scale product composition are expressed in equation A15- A23.

$C_3H_8 + H_2 \longrightarrow CH_4 + C_2H_6$ A15.

$C_{15}H_{32} + H_2 \longrightarrow C_{12}H_{26} + C_3H_8$ A16.

$C_{16}H_{34} + H_2 \longrightarrow C_{13}H_{28} + C_3H_8$ A17.

$C_{16}H_{34} + 2H_2 \longrightarrow C_{11}H_{24} + C_3H_8 + C_2H_6$ A18.

$C_{17}H_{36} + 2H_2 \longrightarrow C_{14}H_{30} + C_3H_8$ A19.

$C_{17}H_{36} + H_2 \longrightarrow C_9H_{20} + C_8H_{18}$ A20.

$C_{18}H_{38} + H_2 \longrightarrow C_{15}H_{32} + C_3H_8$ A21.

$C_{18}H_{38} + H_2 \longrightarrow C_{10}H_{22} + C_8H_{18}$ A22.

$C_{18}H_{38} + H_2 \longrightarrow C_{16}H_{34} + C_2H_6$ A23.

g) Methanation and water gas shift; the gases product from HDO, DCO, and DCO_2 such as H_2O, CO and CO_2 can further react with H_2 in the gas phase as equation A24- A26.

$CO + 3H_2 \longrightarrow CH_4 + H_2O$ A24.

$CO_2 + 4H_2 \longrightarrow CH_4 + 2H_2O$ A25.

$CO + H_2O \longrightarrow H_2 + CO_2$ A26.

Materials balance of the BHD process is clarified in Figure 35. It was the base case before process improvement to produce jet fuel. Crude palm oil 2,107.72 kg/h reacted hydrogen 88.59 kg/h giving product 2,196.31 kg/h. Hydrogen stream is fed at H_2 to oil ratio at 550 Ncm^3/cm^3. Product including light gas, BHD, and water were separated by a flash drum. A process flow diagram of the BHD production process for simulation is shown in Figure 21. The composition of the input and output stream was interpreted in Table 27 and Table 28.

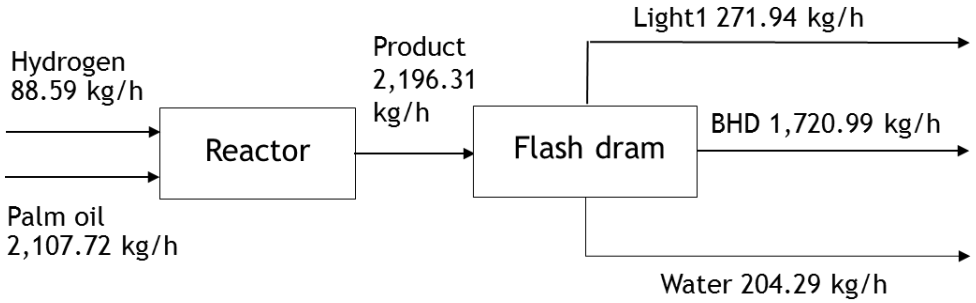

Figure 35 Block flow diagram for BHD process

Table 27 Stream mass flowrate and conditions of BHD process

	Units	PALM	H2-1	PRODUCT1	LIGHT1	LIQ1 (BHD)	WATER
Phase		Liquid	Vapor	Liquid	Vapor	Liquid	Liquid
Temperature	C	30.00	30.00	370.00	40.00	40.00	40.00
Pressure	barg	1.01	42.00	55.16	8.52	8.52	8.52
Mass Vapor Fraction		0.00	1.00	0.00	1.00	0.00	0.00
Mass Flows	kg/hr	2107.72	88.59	2196.31	271.94	1720.09	204.29
C15	kg/hr	0.00	0.00	242.94	0.00	242.94	0.00
C16	kg/hr	0.00	0.00	781.50	0.00	781.49	0.00
C17	kg/hr	0.00	0.00	66.28	0.00	66.28	0.00
C18	kg/hr	0.00	0.00	207.87	0.00	207.87	0.00
C19	kg/hr	0.00	0.00	7.24	0.00	7.24	0.00
C20	kg/hr	0.00	0.00	30.49	0.00	30.49	0.00
TRIPALM	kg/hr	927.40	0.00	0.00	0.00	0.00	0.00
TRISTEAR	kg/hr	84.31	0.00	0.00	0.00	0.00	0.00
TRIOLE	kg/hr	843.09	0.00	0.00	0.00	0.00	0.00
TRILINO	kg/hr	210.77	0.00	0.00	0.00	0.00	0.00
ARACHI	kg/hr	42.15	0.00	0.00	0.00	0.00	0.00
TRIARACH	kg/hr	0.00	0.00	0.00	0.00	0.00	0.00
H2	kg/hr	0.00	88.59	22.00	21.91	0.09	0.00
CO	kg/hr	0.00	0.00	17.07	16.88	0.19	0.00

Table 27 Stream mass flowrate and conditions of BHD process (continue)

	Units	PALM	H2-1	PRODUCT1	LIGHT1	LIQ1 (BHD)	WATER
CO2	kg/hr	0.00	0.00	56.33	51.72	4.61	0.00
H2O	kg/hr	0.00	0.00	210.98	2.67	4.03	204.29
METHANE	kg/hr	0.00	0.00	10.80	10.50	0.30	0.00
ETHANE	kg/hr	0.00	0.00	51.29	45.35	5.95	0.00
PROPANE	kg/hr	0.00	0.00	173.03	122.40	50.63	0.00
C8	kg/hr	0.00	0.00	34.56	0.37	34.19	0.00
C9	kg/hr	0.00	0.00	13.86	0.05	13.80	0.00
C10	kg/hr	0.00	0.00	27.68	0.04	27.63	0.00
C11	kg/hr	0.00	0.00	17.47	0.01	17.45	0.00
C12	kg/hr	0.00	0.00	82.55	0.02	82.53	0.00
C13	kg/hr	0.00	0.00	4.12	0.00	4.12	0.00
C14	kg/hr	0.00	0.00	138.26	0.00	138.26	0.00
Volume Flow	l/min	28.78	438.12	184.81	801.47	40.22	3.43

Table 28 Stream mole flowrate and conditions of BHD process

	Units	PALM	H2-1	PRODUCT1	LIGHT1	LIQ1 (BHD)	WATER
Phase		Liquid	Vapor	Liquid	Vapor	Liquid	Liquid
Temperature	C	30.00	30.00	370.00	40.00	40.00	40.00
Pressure	barg	1.01	42.00	55.16	8.52	8.52	8.52
Molar Vapor Fraction		0.00	1.00	0.00	1.00	0.00	0.00
Mole Flows	kmol/hr	2.57	43.95	38.56	17.74	9.48	11.34
C15	kmol/hr	0.00	0.00	1.14	0.00	1.14	0.00
C16	kmol/hr	0.00	0.00	3.45	0.00	3.45	0.00
C17	kmol/hr	0.00	0.00	0.28	0.00	0.28	0.00
C18	kmol/hr	0.00	0.00	0.82	0.00	0.82	0.00
C19	kmol/hr	0.00	0.00	0.03	0.00	0.03	0.00
C20	kmol/hr	0.00	0.00	0.11	0.00	0.11	0.00
TRIPALM	kmol/hr	1.15	0.00	0.00	0.00	0.00	0.00
TRISTEAR	kmol/hr	0.09	0.00	0.00	0.00	0.00	0.00
TRIOLE	kmol/hr	0.95	0.00	0.00	0.00	0.00	0.00
TRILINO	kmol/hr	0.24	0.00	0.00	0.00	0.00	0.00
ARACHI	kmol/hr	0.13	0.00	0.00	0.00	0.00	0.00
TRIARACH	kmol/hr	0.00	0.00	0.00	0.00	0.00	0.00
H2	kmol/hr	0.00	43.95	10.91	10.87	0.05	0.00
CO	kmol/hr	0.00	0.00	0.61	0.60	0.01	0.00

Table 28 Stream mole flowrate and conditions of BHD process (continue)

	Units	PALM	H2-1	PRODUCT1	LIGHT1	LIQ1 (BHD)	WATER
CO2	kmol/hr	0.00	0.00	1.28	1.18	0.10	0.00
H2O	kmol/hr	0.00	0.00	11.71	0.15	0.22	11.34
METHANE	kmol/hr	0.00	0.00	0.67	0.65	0.02	0.00
ETHANE	kmol/hr	0.00	0.00	1.71	1.51	0.20	0.00
PROPANE	kmol/hr	0.00	0.00	3.92	2.78	1.15	0.00
C8	kmol/hr	0.00	0.00	0.30	0.00	0.30	0.00
C9	kmol/hr	0.00	0.00	0.11	0.00	0.11	0.00
C10	kmol/hr	0.00	0.00	0.19	0.00	0.19	0.00
C11	kmol/hr	0.00	0.00	0.11	0.00	0.11	0.00
C12	kmol/hr	0.00	0.00	0.48	0.00	0.48	0.00
C13	kmol/hr	0.00	0.00	0.02	0.00	0.02	0.00
C14	kmol/hr	0.00	0.00	0.70	0.00	0.70	0.00
Volume Flow	l/min	28.78	438.12	184.81	801.47	40.22	3.43

The simulation results of BHD stream was compared with the product compositions from Hsu et al report [11], it was found that the difference was less than 3%. The data was interpreted in Table 29 and Table 30. Therefore it can be concluded that the simulation data was validated.

Table 29 Comparison of BHD from simulation and experimental result by Hsu et al

Composition	Experimental result (% Weight)	Simulation result (% Weight)	% Difference
n-C_8-C_{14}	20.20	18.49	1.71
C_{15}	14.37	14.12	0.25
C_{16}	45.74	45.43	0.31
C_{17}	3.79	3.85	-0.06
C_{18}	12.63	12.08	0.55
C_{19}-C_{20}	3.43	2.19	1.24

Table 30 Comparison of gas product from simulation and experimental result by Hsu et al

Composition	Simulation result (% Weight)	Experimental result (% Weight)	% Difference
CO_2	22.0	19.02	2.98
H_2	6.0	8.06	-2.06
C_2H_6	17.0	16.68	0.32
CH_4	5.0	3.86	1.14
CO	8.0	6.21	1.79
C_3H_8	42.0	45.01	-3.01

APPENDIX B Improving of BHD process and validation of jet fuel production from BHD

A hydrocracker unit is used to convert it to a jet fuel product. It is a typical process in the petroleum refinery. Cracking reaction converts high-boiling point constituent hydrocarbons to valuable fuel such as gasoline and jet fuel. This result applied R-Equil and R-Stoic reactor model in Aspen Plus V9 to find cracking reaction and their conversion then verify data by comparing simulation results with C.-H. Lin et al research [18]. They recommended the reaction temperature at 360 ℃, the pressure of 3 MPa (29 barg), the LHSV of 1 h^{-1}, and the hydrogen/oil molar ratio of 13.6 were the optimal condition for hydrocracking/isomerization over the NiAg/SAPO-11 catalyst. Figure 36 and Table 31 were showing raw material, product stream, and their composition. The verification on the simulation result was illustrated in Table 32.

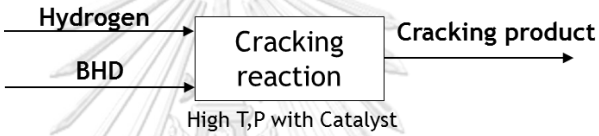

Figure 36 Block flow diagram for cracking process

Table 31 Composition of raw material and product stream of cracking process

	Units	BHD	H2	PRODUCT
Mole Flows	kmol/hr	1.00	13.60	14.60
Mass Flows	kg/hr	231.36	27.42	258.77
Mass Fractions				
CH_4		0.00	0.00	0.01
C_2H_6		0.00	0.00	0.03
C_3H_8		0.00	0.00	0.07
C_8		0.00	0.00	0.09
C_9		0.00	0.00	0.10
C_{10}		0.00	0.00	0.09
C_{11}		0.00	0.00	0.06
C_{12}		0.00	0.00	0.02
C_{13}		0.00	0.00	0.04
C_{14}		0.00	0.00	0.03
C_{15}		0.14	0.00	0.16
C_{16}		0.56	0.00	0.12

	Units	BHD	H2	PRODUCT
Mole Flows	kmol/hr	1.00	13.60	14.60
Mass Flows	kg/hr	231.36	27.42	258.77
Mass Fractions				
C_{17}		0.05	0.00	0.06
C_{18}		0.25	0.00	0.02
H_2		0.00	1.00	0.10

Table 32 Comparing of cracking production distribution between paper based and simulation.

Cracking Product fraction	C.-H. Lin	Simulation result	%Difference
C_8	0.12	0.117	2.79%
C_9	0.12	0.120	-0.39%
C_{10}	0.11	0.110	-0.30%
C_{11}	0.07	0.072	-2.79%
C_{12}	0.03	0.030	-0.50%
C_{13}	0.05	0.051	-2.35%
C_{14}	0.04	0.040	-0.39%
C_{15}	0.2	0.203	-1.28%
C_{16}	0.15	0.148	1.25%
C_{17}	0.08	0.078	2.10%
C_{18}	0.03	0.030	-0.38%
Total	1.000	1.000	

Isomerization was spontaneous occur together with hydrocracking reaction over the NiAg/SAPO-11 catalyst. The simulation was run by using the R-Stioc reactor model. The stoichiometry and fractional conversion were required input. The potential reactions were shown in Table 33.

Process flow diagram and materials balance of bio-jet fuel production illustrated Figure 37. The BHD, 1,720.99 kg/h from the deoxygenation section, entered to hydrocracking /isomerization reactor and reacted with hydrogen 70.46 kg/h. The cracking product 1,790.55 kg/h was sent to a flash drum to separated light gas. The liquid product 1,542.10 kg/h was distilled to derive 854.68kg/h of bio-jet fuel and 632.36 kg/h of bio-diesel. Propane at a flow rate of 6.68 kg/h was the by-product. The compositions of each stream were shown in Table 34 and Table 35. The abbreviation of each component was listed in Table 36.

Table 33 Isomerization reaction used in R-Stioc reactor medel.

Carbon	n-alkane	Mono brach isomer	Conversion
C_8	Octane	4-METHYLHEPTANE	0.15
		3-Methylheptane	0.15
		2-METHYLHEPTANE	0.15
		3-Ethylhexane	0.15
C_9	Nonane	2-Methyloctane	0.15
		3-METHYLOCTANE	0.15
		4-METHYLOCTANE	0.15
		3-ETHYLHEPTANE	0.15
C_{10}	Decane	3-METHYLNONANE	0.15
		2-METHYLNONANE	0.15
		4-METHYLNONANE	0.15
		5-METHYLNONANE	0.15
C_{11}	Undecane	3-METHYLDECANE	0.3
		2-METHYLDECANE	0.3
C_{12}	Dodecane	3-METHYLUNDECANE	0.3
		2-METHYLUNDECANE	0.3
C_{13}	Tridecane	3-METHYLDODECANE	0.3
		2-METHYLDODECANE	0.3
C_{14}	Tetradecane	3-METHYLTRIDECANE	0.2
		3-ETHYLDODECANE	0.2
		2-METHYLTRIDECANE	0.2
C_{15}	Pentadecane	6-METHYLTETRADECANE	0.075
		2-METHYLTETRADECANE	0.075
		6-PROPYLDODECANE	0.075
		4-METHYLTETRADECANE	0.075
		5-METHYLTETRADECANE	0.075
		TRIDECANE,-3-ETHYL-	0.075
		TETRADECANE,-3-METHYL-	0.075
		7-METHYLTETRADECANE	0.075

Table 33 Isomerization reaction used in R-Stioc reactor medel. (Continue)

Carbon	n-alkane	Mono brach isomer	Conversion
C_{16}	Hexadecane	3-ETHYLTETRADECANE	0.06
		2-METHYLPENTADECANE	0.06
		PENTADECANE,-3-METHYL-	0.06
		7-METHYLPENTADECANE	0.06
		6-METHYLPENTADECANE	0.06
		PENTADECANE,-5-METHYL-	0.06
		4-METHYLPENTADECANE	0.06
		TRIDECANE,-7-PROPYL-	0.06
		8-METHYLPENTADECANE	0.06
		6-PENTYLUNDECANE	0.06
C_{17}	Heptadecane	7-BUTYLTRIDECANE	0.075
		6-PENTYLDODECANE	0.075
		HEXADECANE,-4-METHYL-	0.075
		HEXADECANE,-5-METHYL-	0.075
		7-METHYLHEXADECANE	0.075
		14-METHYLHEXADECANE	0.075
		15-METHYLHEXADECANE	0.075
		4-PROPYLTETRADECANE	0.075
C_{18}	Octadecane	16-METHYLHEPTADECANE	0.1
		HEPTADECANE,-4-METHYL-	0.1
		HEPTADECANE,-5-METHYL-	0.1
		9-METHYLHEPTADECANE	0.1
		HEPTADECANE,-3-METHYL-	0.1
		8-PROPYLPENTADECANE	0.1

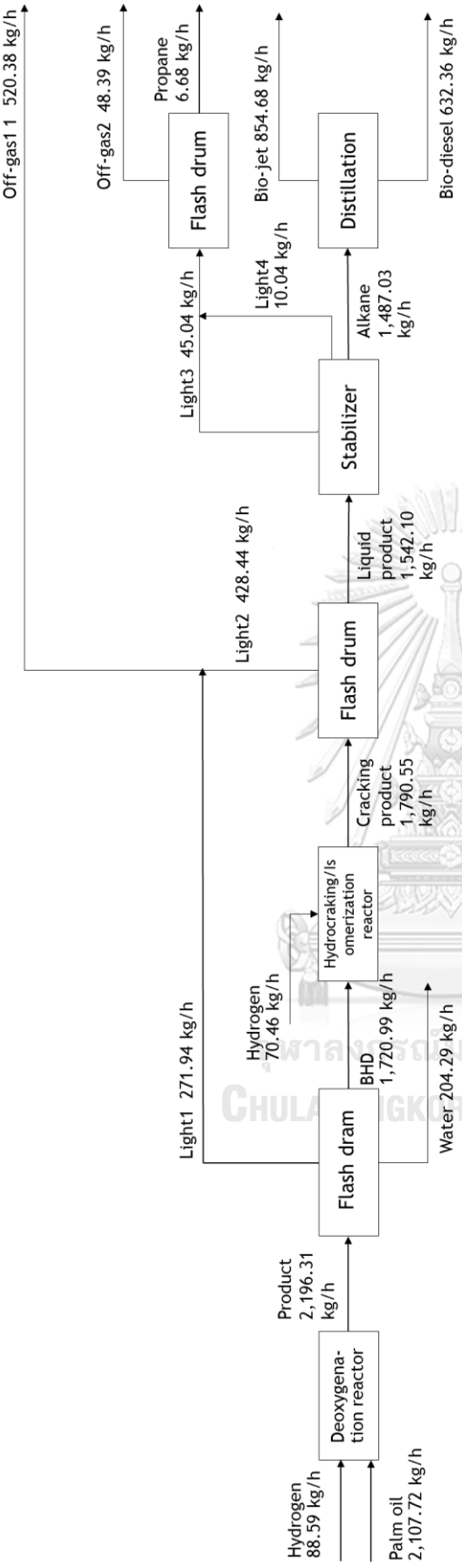

Figure 37 Block flow diagram for Bio-jet fuel production from BHD

Table 34 Stream mass flowrate and conditions of bio-jet fuel/biodiesel production process

	Units	LIQ1	H2-2	LIGHT1	WATER	PRODUCT2	PRODUCT3	LIQ4	LIGHT2	N-ALKANE	LIGHT3	LIGHT4	OFFGAS2	BIODIESE	BIOJET	PROPANE	OFFGAS1
Phase		Liquid	Vapor	Vapor	Liquid	Vapor	Vapor	Liquid	Vapor	Liquid	Vapor	Liquid	Vapor	Liquid	Liquid	Liquid	Vapor
Temperature	C	40.00	30.00	40.00	40.00	360.00	360.00	50.00	50.00	372.77	37.79	37.79	0.00	317.77	169.77	0.00	45.65
Pressure	barg	8.52	28.99	8.52	8.52	28.99	28.99	20.00	20.00	18.50	18.00	18.00	5.50	1.50	1.00	5.50	8.52
Mass Vapor Fraction		0.00	1.00	1.00	0.00	1.00	1.00	0.00	1.00	0.00	1.00	0.00	1.00	0.00	0.00	0.00	1.00
Mass Flows	kg/hr	1720.1	70.46	271.94	204.29	1790.6	1790.6	1542.1	248.44	1487.0	45.04	10.04	48.39	632.36	854.68	6.68	520.38
PALMITIC	kg/hr	0.00	0.00	0.00	0.00	0.00	0.00	0.00	0.00	0.00	0.00	0.00	0.00	0.00	0.00	0.00	0.00
STEARIC	kg/hr	0.00	0.00	0.00	0.00	0.00	0.00	0.00	0.00	0.00	0.00	0.00	0.00	0.00	0.00	0.00	0.00
OLEIC	kg/hr	0.00	0.00	0.00	0.00	0.00	0.00	0.00	0.00	0.00	0.00	0.00	0.00	0.00	0.00	0.00	0.00
LINOLEIC	kg/hr	0.00	0.00	0.00	0.00	0.00	0.00	0.00	0.00	0.00	0.00	0.00	0.00	0.00	0.00	0.00	0.00
C15	kg/hr	242.94	0.00	0.00	0.00	272.33	145.96	145.95	0.00	145.95	0.00	0.00	0.00	145.94	0.01	0.00	0.01
C16	kg/hr	781.49	0.00	0.00	0.00	182.51	98.30	98.30	0.00	98.30	0.00	0.00	0.00	98.30	0.00	0.00	0.00
C17	kg/hr	66.28	0.00	0.00	0.00	40.31	21.60	21.60	0.00	21.60	0.00	0.00	0.00	21.60	0.00	0.00	0.00
C18	kg/hr	207.87	0.00	0.00	0.00	22.11	11.75	11.75	0.00	11.75	0.00	0.00	0.00	11.75	0.00	0.00	0.00
C19	kg/hr	7.24	0.00	0.00	0.00	7.24	7.24	7.24	0.00	7.24	0.00	0.00	0.00	7.24	0.00	0.00	0.00
C20	kg/hr	30.49	0.00	0.00	0.00	30.49	30.49	30.49	0.00	30.49	0.00	0.00	0.00	30.49	0.00	0.00	0.00
TRIPALM	kg/hr	0.00	0.00	0.00	0.00	0.00	0.00	0.00	0.00	0.00	0.00	0.00	0.00	0.00	0.00	0.00	0.00
TRISTEAR	kg/hr	0.00	0.00	0.00	0.00	0.00	0.00	0.00	0.00	0.00	0.00	0.00	0.00	0.00	0.00	0.00	0.00
TRIOLE	kg/hr	0.00	0.00	0.00	0.00	0.00	0.00	0.00	0.00	0.00	0.00	0.00	0.00	0.00	0.00	0.00	0.00
TRILINO	kg/hr	0.00	0.00	0.00	0.00	0.00	0.00	0.00	0.00	0.00	0.00	0.00	0.00	0.00	0.00	0.00	0.00
ARACHI	kg/hr	0.00	0.00	0.00	0.00	0.00	0.00	0.00	0.00	0.00	0.00	0.00	0.00	0.00	0.00	0.00	0.00
TRIARACH	kg/hr	0.00	0.00	0.00	0.00	0.00	0.00	0.00	0.00	0.00	0.00	0.00	0.00	0.00	0.00	0.00	0.00
H2	kg/hr	0.09	70.46	21.91	0.00	57.94	57.94	0.29	57.65	0.00	0.29	0.00	0.29	0.00	0.00	0.00	79.56
CO	kg/hr	0.19	0.00	16.88	0.00	0.19	0.19	0.00	0.19	0.00	0.00	0.00	0.00	0.00	0.00	0.00	17.06
CO2	kg/hr	4.61	0.00	51.72	0.00	4.61	4.61	0.40	4.20	0.00	0.39	0.02	0.40	0.00	0.00	0.01	55.93
H2O	kg/hr	4.03	0.00	2.67	204.29	4.03	4.03	2.40	1.63	2.24	0.09	0.08	0.09	0.00	2.24	0.08	4.29

	Units	LIQ1	H2-2	LIGHT1	WATER	PRODUCT2	PRODUCT3	LIQ4	LIGHT2	N-ALKANE	LIGHT3	LIGHT4	OFFGAS2	BIODIESE	BIOJET	PROPANE	OFFGAS1
METHANE	kg/hr	0.30	0.00	10.50	0.00	18.77	18.77	0.57	18.20	0.00	0.56	0.01	0.57	0.00	0.00	0.00	28.71
ETHANE	kg/hr	5.95	0.00	45.35	0.00	54.40	54.40	6.57	47.83	0.00	6.00	0.57	6.32	0.00	0.00	0.25	93.18
PROPANE	kg/hr	50.63	0.00	122.40	0.00	161.39	161.39	47.14	114.25	0.07	37.71	9.36	40.73	0.00	0.07	6.34	236.65
C8	kg/hr	34.19	0.00	0.37	0.00	171.51	89.53	88.27	1.26	88.27	0.00	0.00	0.00	0.00	88.27	0.00	1.63
C9	kg/hr	13.80	0.00	0.05	0.00	113.26	59.12	58.80	0.32	58.80	0.00	0.00	0.00	0.00	58.80	0.00	0.38
C10	kg/hr	27.63	0.00	0.04	0.00	154.13	80.46	80.28	0.17	80.28	0.00	0.00	0.00	0.00	80.28	0.00	0.21
C11	kg/hr	17.45	0.00	0.01	0.00	107.86	52.85	52.80	0.05	52.80	0.00	0.00	0.00	0.00	52.80	0.00	0.06
C12	kg/hr	82.53	0.00	0.02	0.00	119.68	58.64	58.62	0.02	58.62	0.00	0.00	0.00	0.00	58.62	0.00	0.04
C13	kg/hr	4.12	0.00	0.00	0.00	82.53	40.44	40.44	0.01	40.44	0.00	0.00	0.00	0.01	40.42	0.00	0.01
C14	kg/hr	138.26	0.00	0.00	0.00	185.26	94.85	94.85	0.01	94.85	0.00	0.00	0.00	76.84	18.01	0.00	0.01
4-MET-01	kg/hr	0.00	0.00	0.00	0.00	0.00	25.73	25.23	0.50	25.23	0.00	0.00	0.00	0.00	25.23	0.00	0.50
3-MET-01	kg/hr	0.00	0.00	0.00	0.00	0.00	21.87	21.46	0.41	21.46	0.00	0.00	0.00	0.00	21.46	0.00	0.41
2-MET-01	kg/hr	0.00	0.00	0.00	0.00	0.00	18.59	17.88	0.71	17.88	0.00	0.00	0.00	0.00	17.88	0.00	0.71
3-ETH-01	kg/hr	0.00	0.00	0.00	0.00	0.00	15.80	15.50	0.30	15.50	0.00	0.00	0.00	0.00	15.50	0.00	0.30
2-MET-02	kg/hr	0.00	0.00	0.00	0.00	0.00	16.99	16.87	0.12	16.87	0.00	0.00	0.00	0.00	16.87	0.00	0.12
3-MET-02	kg/hr	0.00	0.00	0.00	0.00	0.00	14.44	14.33	0.11	14.33	0.00	0.00	0.00	0.00	14.33	0.00	0.11
4-MET-02	kg/hr	0.00	0.00	0.00	0.00	0.00	12.28	12.18	0.10	12.18	0.00	0.00	0.00	0.00	12.18	0.00	0.10
3-ETH-02	kg/hr	0.00	0.00	0.00	0.00	0.00	10.43	10.35	0.08	10.35	0.00	0.00	0.00	0.00	10.35	0.00	0.08
3-MET-03	kg/hr	0.00	0.00	0.00	0.00	0.00	23.12	23.05	0.07	23.05	0.00	0.00	0.00	0.00	23.05	0.00	0.07
2-MET-03	kg/hr	0.00	0.00	0.00	0.00	0.00	19.65	19.59	0.06	19.59	0.00	0.00	0.00	0.00	19.59	0.00	0.06
4-MET-03	kg/hr	0.00	0.00	0.00	0.00	0.00	16.70	16.65	0.05	16.65	0.00	0.00	0.00	0.00	16.65	0.00	0.05
5-MET-01	kg/hr	0.00	0.00	0.00	0.00	0.00	14.20	14.15	0.05	14.15	0.00	0.00	0.00	0.00	14.15	0.00	0.05
3-MET-04	kg/hr	0.00	0.00	0.00	0.00	0.00	32.36	32.33	0.03	32.33	0.00	0.00	0.00	0.00	32.33	0.00	0.03
2-MET-04	kg/hr	0.00	0.00	0.00	0.00	0.00	22.65	22.63	0.02	22.63	0.00	0.00	0.00	0.00	22.63	0.00	0.02
3-MET-05	kg/hr	0.00	0.00	0.00	0.00	0.00	35.90	35.89	0.02	35.89	0.00	0.00	0.00	0.00	35.89	0.00	0.02
2-MET-05	kg/hr	0.00	0.00	0.00	0.00	0.00	25.13	25.12	0.01	25.12	0.00	0.00	0.00	0.00	25.12	0.00	0.01
3-MET-06	kg/hr	0.00	0.00	0.00	0.00	0.00	24.76	24.76	0.00	24.76	0.00	0.00	0.00	0.00	24.75	0.00	0.00

	Units	LIQ1	H2-2	LIGHT1	WATER	PRODUCT2	PRODUCT3	LIQ4	LIGHT2	N-ALKANE	LIGHT3	LIGHT4	OFFGAS2	BIODIESE	BIOJET	PROPANE	OFFGAS1
2-MET-06	kg/hr	0.00	0.00	0.00	0.00	0.00	17.33	17.33	0.00	17.33	0.00	0.00	0.00	0.00	17.33	0.00	0.00
3-MET-07	kg/hr	0.00	0.00	0.00	0.00	0.00	37.05	37.05	0.00	37.05	0.00	0.00	0.00	3.69	33.36	0.00	0.00
3-ETH-03	kg/hr	0.00	0.00	0.00	0.00	0.00	29.64	29.64	0.00	29.64	0.00	0.00	0.00	5.53	24.11	0.00	0.00
2-MET-07	kg/hr	0.00	0.00	0.00	0.00	0.00	23.71	23.71	0.00	23.71	0.00	0.00	0.00	1.83	21.88	0.00	0.00
6-MET-01	kg/hr	0.00	0.00	0.00	0.00	0.00	20.42	20.42	0.00	20.42	0.00	0.00	0.00	20.22	0.20	0.00	0.00
2-MET-08	kg/hr	0.00	0.00	0.00	0.00	0.00	18.89	18.89	0.00	18.89	0.00	0.00	0.00	18.86	0.03	0.00	0.00
6-PRO-01	kg/hr	0.00	0.00	0.00	0.00	0.00	17.48	17.47	0.00	17.47	0.00	0.00	0.00	7.33	10.14	0.00	0.00
4-MET-04	kg/hr	0.00	0.00	0.00	0.00	0.00	16.17	16.16	0.00	16.16	0.00	0.00	0.00	16.13	0.03	0.00	0.00
5-MET-02	kg/hr	0.00	0.00	0.00	0.00	0.00	14.95	14.95	0.00	14.95	0.00	0.00	0.00	14.92	0.03	0.00	0.00
TRIDE-01	kg/hr	0.00	0.00	0.00	0.00	0.00	13.83	13.83	0.00	13.83	0.00	0.00	0.00	13.80	0.03	0.00	0.00
TETRA-01	kg/hr	0.00	0.00	0.00	0.00	0.00	12.79	12.79	0.00	12.79	0.00	0.00	0.00	12.79	0.01	0.00	0.00
7-MET-01	kg/hr	0.00	0.00	0.00	0.00	0.00	11.83	11.83	0.00	11.83	0.00	0.00	0.00	11.82	0.01	0.00	0.00
3-ETH-04	kg/hr	0.00	0.00	0.00	0.00	0.00	10.95	10.95	0.00	10.95	0.00	0.00	0.00	10.95	0.00	0.00	0.00
2-MET-09	kg/hr	0.00	0.00	0.00	0.00	0.00	10.29	10.29	0.00	10.29	0.00	0.00	0.00	10.29	0.00	0.00	0.00
PENTA-01	kg/hr	0.00	0.00	0.00	0.00	0.00	9.68	9.68	0.00	9.68	0.00	0.00	0.00	9.68	0.00	0.00	0.00
7-MET-02	kg/hr	0.00	0.00	0.00	0.00	0.00	9.10	9.10	0.00	9.10	0.00	0.00	0.00	9.10	0.00	0.00	0.00
6-MET-02	kg/hr	0.00	0.00	0.00	0.00	0.00	8.55	8.55	0.00	8.55	0.00	0.00	0.00	8.55	0.00	0.00	0.00
PENTA-02	kg/hr	0.00	0.00	0.00	0.00	0.00	8.04	8.04	0.00	8.04	0.00	0.00	0.00	8.04	0.00	0.00	0.00
4-MET-05	kg/hr	0.00	0.00	0.00	0.00	0.00	7.55	7.55	0.00	7.55	0.00	0.00	0.00	7.55	0.00	0.00	0.00
TRIDE-02	kg/hr	0.00	0.00	0.00	0.00	0.00	7.10	7.10	0.00	7.10	0.00	0.00	0.00	7.10	0.00	0.00	0.00
8-MET-01	kg/hr	0.00	0.00	0.00	0.00	0.00	6.68	6.68	0.00	6.68	0.00	0.00	0.00	6.67	0.00	0.00	0.00
6-PEN-01	kg/hr	0.00	0.00	0.00	0.00	0.00	6.27	6.27	0.00	6.27	0.00	0.00	0.00	6.26	0.01	0.00	0.00
7-BUT-01	kg/hr	0.00	0.00	0.00	0.00	0.00	3.02	3.02	0.00	3.02	0.00	0.00	0.00	3.02	0.00	0.00	0.00
6-PEN-02	kg/hr	0.00	0.00	0.00	0.00	0.00	2.80	2.80	0.00	2.80	0.00	0.00	0.00	2.80	0.00	0.00	0.00
HEXAD-01	kg/hr	0.00	0.00	0.00	0.00	0.00	2.59	2.59	0.00	2.59	0.00	0.00	0.00	2.59	0.00	0.00	0.00
HEXAD-02	kg/hr	0.00	0.00	0.00	0.00	0.00	2.39	2.39	0.00	2.39	0.00	0.00	0.00	2.39	0.00	0.00	0.00
7-MET-03	kg/hr	0.00	0.00	0.00	0.00	0.00	2.21	2.21	0.00	2.21	0.00	0.00	0.00	2.21	0.00	0.00	0.00

	Units	LIQ1	H2-2	LIGHT1	WATER	PRODUCT2	PRODUCT3	LIQ4	LIGHT2	N-ALKANE	LIGHT3	LIGHT4	OFFGAS2	BIODIESE	BIOJET	PROPANE	OFFGAS1
14-ME-01	kg/hr	0.00	0.00	0.00	0.00	0.00	2.05	2.05	0.00	2.05	0.00	0.00	0.00	2.05	0.00	0.00	0.00
15-ME-01	kg/hr	0.00	0.00	0.00	0.00	0.00	1.89	1.89	0.00	1.89	0.00	0.00	0.00	1.89	0.00	0.00	0.00
4-PRO-01	kg/hr	0.00	0.00	0.00	0.00	0.00	1.75	1.75	0.00	1.75	0.00	0.00	0.00	1.75	0.00	0.00	0.00
16-ME-01	kg/hr	0.00	0.00	0.00	0.00	0.00	2.21	2.21	0.00	2.21	0.00	0.00	0.00	2.21	0.00	0.00	0.00
HEPTA-01	kg/hr	0.00	0.00	0.00	0.00	0.00	1.99	1.99	0.00	1.99	0.00	0.00	0.00	1.99	0.00	0.00	0.00
HEPTA-02	kg/hr	0.00	0.00	0.00	0.00	0.00	1.79	1.79	0.00	1.79	0.00	0.00	0.00	1.79	0.00	0.00	0.00
9-MET-01	kg/hr	0.00	0.00	0.00	0.00	0.00	1.61	1.61	0.00	1.61	0.00	0.00	0.00	1.61	0.00	0.00	0.00
HEPTA-03	kg/hr	0.00	0.00	0.00	0.00	0.00	1.45	1.45	0.00	1.45	0.00	0.00	0.00	1.45	0.00	0.00	0.00
8-PRO-01	kg/hr	0.00	0.00	0.00	0.00	0.00	1.31	1.31	0.00	1.31	0.00	0.00	0.00	1.31	0.00	0.00	0.00
Volume Flow	l/min	40.22	496.49	801.47	3.43	1291.6	1292.4	37.15	731.07	69.86	22.34	0.36	69.49	19.29	23.40	0.21	2403.5

Table 35 Stream mole flowrate and conditions of bio-jet fuel/biodiesel production process

	Units	LIQ1	H2-2	LIGHT1	WATER	PRODUCT2	PRODUCT3	LIQ4	LIGHT2	N-ALKANE	LIGHT3	LIGHT4	OFFGAS2	BIODIESE	BIOJET	PROPANE	OFFGAS1
Phase		Liquid	Vapor	Vapor	Liquid	Vapor	Vapor	Liquid	Vapor	Liquid	Vapor	Liquid	Vapor	Liquid	Liquid	Liquid	Vapor
Temperature	C	40.00	30.00	40.00	40.00	360.00	360.00	50.00	50.00	372.77	37.79	37.79	0.00	317.77	169.77	0.00	45.65
Pressure	barg	8.52	28.99	8.52	8.52	28.99	28.99	20.00	20.00	18.50	18.00	18.00	5.50	1.50	1.00	5.50	8.52
Molar Vapor Fraction		0.00	1.00	1.00	0.00	1.00	1.00	0.00	1.00	0.00	1.00	0.00	1.00	0.00	0.00	0.00	1.00
Mole Flows	kmol/hr	9.48	34.95	17.74	11.34	44.44	44.44	10.29	34.14	8.81	1.25	0.24	1.33	2.87	5.94	0.16	51.88
PALMITIC	kmol/hr	0.00	0.00	0.00	0.00	0.00	0.00	0.00	0.00	0.00	0.00	0.00	0.00	0.00	0.00	0.00	0.00
STEARIC	kmol/hr	0.00	0.00	0.00	0.00	0.00	0.00	0.00	0.00	0.00	0.00	0.00	0.00	0.00	0.00	0.00	0.00
OLEIC	kmol/hr	0.00	0.00	0.00	0.00	0.00	0.00	0.00	0.00	0.00	0.00	0.00	0.00	0.00	0.00	0.00	0.00
LINOLEIC	kmol/hr	0.00	0.00	0.00	0.00	0.00	0.00	0.00	0.00	0.00	0.00	0.00	0.00	0.00	0.00	0.00	0.00
C15	kmol/hr	1.14	0.00	0.00	0.00	1.28	0.69	0.69	0.00	0.69	0.00	0.00	0.00	0.69	0.00	0.00	0.00
C16	kmol/hr	3.45	0.00	0.00	0.00	0.81	0.43	0.43	0.00	0.43	0.00	0.00	0.00	0.43	0.00	0.00	0.00
C17	kmol/hr	0.28	0.00	0.00	0.00	0.17	0.09	0.09	0.00	0.09	0.00	0.00	0.00	0.09	0.00	0.00	0.00
C18	kmol/hr	0.82	0.00	0.00	0.00	0.09	0.05	0.05	0.00	0.05	0.00	0.00	0.00	0.05	0.00	0.00	0.00
C19	kmol/hr	0.03	0.00	0.00	0.00	0.03	0.03	0.03	0.00	0.03	0.00	0.00	0.00	0.03	0.00	0.00	0.00
C20	kmol/hr	0.11	0.00	0.00	0.00	0.11	0.11	0.11	0.00	0.11	0.00	0.00	0.00	0.11	0.00	0.00	0.00
TRIPALM	kmol/hr	0.00	0.00	0.00	0.00	0.00	0.00	0.00	0.00	0.00	0.00	0.00	0.00	0.00	0.00	0.00	0.00
TRISTEAR	kmol/hr	0.00	0.00	0.00	0.00	0.00	0.00	0.00	0.00	0.00	0.00	0.00	0.00	0.00	0.00	0.00	0.00
TRIOLE	kmol/hr	0.00	0.00	0.00	0.00	0.00	0.00	0.00	0.00	0.00	0.00	0.00	0.00	0.00	0.00	0.00	0.00
TRILINO	kmol/hr	0.00	0.00	0.00	0.00	0.00	0.00	0.00	0.00	0.00	0.00	0.00	0.00	0.00	0.00	0.00	0.00
ARACHI	kmol/hr	0.00	0.00	0.00	0.00	0.00	0.00	0.00	0.00	0.00	0.00	0.00	0.00	0.00	0.00	0.00	0.00
TRIARACH	kmol/hr	0.00	0.00	0.00	0.00	0.00	0.00	0.00	0.00	0.00	0.00	0.00	0.00	0.00	0.00	0.00	0.00
H2	kmol/hr	0.05	34.95	10.87	0.00	28.74	28.74	0.14	28.60	0.00	0.14	0.00	0.14	0.00	0.00	0.00	39.47
CO	kmol/hr	0.01	0.00	0.60	0.00	0.01	0.01	0.00	0.01	0.00	0.00	0.00	0.00	0.00	0.00	0.00	0.61
CO2	kmol/hr	0.10	0.00	1.18	0.00	0.10	0.10	0.01	0.10	0.00	0.01	0.00	0.01	0.00	0.00	0.00	1.27

	Units	LIQ1	H2-2	LIGHT1	WATER	PRODUCT2	PRODUCT3	LIQ4	LIGHT2	N-ALKANE	LIGHT3	LIGHT4	OFFGAS2	BIODIESE	BIOJET	PROPANE	OFFGAS1
H2O	kmol/hr	0.22	0.00	0.15	11.34	0.22	0.22	0.13	0.09	0.12	0.00	0.00	0.00	0.00	0.12	0.00	0.24
METHANE	kmol/hr	0.02	0.00	0.65	0.00	1.17	1.17	0.04	1.13	0.00	0.03	0.00	0.04	0.00	0.00	0.00	1.79
ETHANE	kmol/hr	0.20	0.00	1.51	0.00	1.81	1.81	0.22	1.59	0.00	0.20	0.02	0.21	0.00	0.00	0.01	3.10
PROPANE	kmol/hr	1.15	0.00	2.78	0.00	3.66	3.66	1.07	2.59	0.00	0.86	0.21	0.92	0.00	0.00	0.14	5.37
C8	kmol/hr	0.30	0.00	0.00	0.00	1.50	0.78	0.77	0.01	0.77	0.00	0.00	0.00	0.00	0.77	0.00	0.01
C9	kmol/hr	0.11	0.00	0.00	0.00	0.88	0.46	0.46	0.00	0.46	0.00	0.00	0.00	0.00	0.46	0.00	0.00
C10	kmol/hr	0.19	0.00	0.00	0.00	1.08	0.57	0.56	0.00	0.56	0.00	0.00	0.00	0.00	0.56	0.00	0.00
C11	kmol/hr	0.11	0.00	0.00	0.00	0.69	0.34	0.34	0.00	0.34	0.00	0.00	0.00	0.00	0.34	0.00	0.00
C12	kmol/hr	0.48	0.00	0.00	0.00	0.70	0.34	0.34	0.00	0.34	0.00	0.00	0.00	0.00	0.34	0.00	0.00
C13	kmol/hr	0.02	0.00	0.00	0.00	0.45	0.22	0.22	0.00	0.22	0.00	0.00	0.00	0.00	0.22	0.00	0.00
C14	kmol/hr	0.70	0.00	0.00	0.00	0.93	0.48	0.48	0.00	0.48	0.00	0.00	0.00	0.39	0.09	0.00	0.00
4-MET-01	kmol/hr	0.00	0.00	0.00	0.00	0.00	0.23	0.22	0.00	0.22	0.00	0.00	0.00	0.00	0.22	0.00	0.00
3-MET-01	kmol/hr	0.00	0.00	0.00	0.00	0.00	0.19	0.19	0.00	0.19	0.00	0.00	0.00	0.00	0.19	0.00	0.00
2-MET-01	kmol/hr	0.00	0.00	0.00	0.00	0.00	0.16	0.16	0.01	0.16	0.00	0.00	0.00	0.00	0.16	0.00	0.01
3-ETH-01	kmol/hr	0.00	0.00	0.00	0.00	0.00	0.14	0.14	0.00	0.14	0.00	0.00	0.00	0.00	0.14	0.00	0.00
2-MET-02	kmol/hr	0.00	0.00	0.00	0.00	0.00	0.13	0.13	0.00	0.13	0.00	0.00	0.00	0.00	0.13	0.00	0.00
3-MET-02	kmol/hr	0.00	0.00	0.00	0.00	0.00	0.11	0.11	0.00	0.11	0.00	0.00	0.00	0.00	0.11	0.00	0.00
4-MET-02	kmol/hr	0.00	0.00	0.00	0.00	0.00	0.10	0.09	0.00	0.09	0.00	0.00	0.00	0.00	0.09	0.00	0.00
3-ETH-02	kmol/hr	0.00	0.00	0.00	0.00	0.00	0.08	0.08	0.00	0.08	0.00	0.00	0.00	0.00	0.08	0.00	0.00
3-MET-03	kmol/hr	0.00	0.00	0.00	0.00	0.00	0.16	0.16	0.00	0.16	0.00	0.00	0.00	0.00	0.16	0.00	0.00
2-MET-03	kmol/hr	0.00	0.00	0.00	0.00	0.00	0.14	0.14	0.00	0.14	0.00	0.00	0.00	0.00	0.14	0.00	0.00
4-MET-03	kmol/hr	0.00	0.00	0.00	0.00	0.00	0.12	0.12	0.00	0.12	0.00	0.00	0.00	0.00	0.12	0.00	0.00
5-MET-01	kmol/hr	0.00	0.00	0.00	0.00	0.00	0.10	0.10	0.00	0.10	0.00	0.00	0.00	0.00	0.10	0.00	0.00
3-MET-04	kmol/hr	0.00	0.00	0.00	0.00	0.00	0.21	0.21	0.00	0.21	0.00	0.00	0.00	0.00	0.21	0.00	0.00
2-MET-04	kmol/hr	0.00	0.00	0.00	0.00	0.00	0.14	0.14	0.00	0.14	0.00	0.00	0.00	0.00	0.14	0.00	0.00
3-MET-05	kmol/hr	0.00	0.00	0.00	0.00	0.00	0.21	0.21	0.00	0.21	0.00	0.00	0.00	0.00	0.21	0.00	0.00

	Units	LIQ1	H2-2	LIGHT1	WATER	PRODUCT2	PRODUCT3	LIQ4	LIGHT2	N-ALKANE	LIGHT3	LIGHT4	OFFGAS2	BIODIESE	BIOJET	PROPANE	OFFGAS1
2-MET-05	kmol/hr	0.00	0.00	0.00	0.00	0.00	0.15	0.15	0.00	0.15	0.00	0.00	0.00	0.00	0.15	0.00	0.00
3-MET-06	kmol/hr	0.00	0.00	0.00	0.00	0.00	0.13	0.13	0.00	0.13	0.00	0.00	0.00	0.00	0.13	0.00	0.00
2-MET-06	kmol/hr	0.00	0.00	0.00	0.00	0.00	0.09	0.09	0.00	0.09	0.00	0.00	0.00	0.00	0.09	0.00	0.00
3-MET-07	kmol/hr	0.00	0.00	0.00	0.00	0.00	0.19	0.19	0.00	0.19	0.00	0.00	0.00	0.02	0.17	0.00	0.00
3-ETH-03	kmol/hr	0.00	0.00	0.00	0.00	0.00	0.15	0.15	0.00	0.15	0.00	0.00	0.00	0.03	0.12	0.00	0.00
2-MET-07	kmol/hr	0.00	0.00	0.00	0.00	0.00	0.12	0.12	0.00	0.12	0.00	0.00	0.00	0.01	0.11	0.00	0.00
6-MET-01	kmol/hr	0.00	0.00	0.00	0.00	0.00	0.10	0.10	0.00	0.10	0.00	0.00	0.00	0.10	0.00	0.00	0.00
2-MET-08	kmol/hr	0.00	0.00	0.00	0.00	0.00	0.09	0.09	0.00	0.09	0.00	0.00	0.00	0.09	0.00	0.00	0.00
6-PRO-01	kmol/hr	0.00	0.00	0.00	0.00	0.00	0.08	0.08	0.00	0.08	0.00	0.00	0.00	0.03	0.05	0.00	0.00
4-MET-04	kmol/hr	0.00	0.00	0.00	0.00	0.00	0.08	0.08	0.00	0.08	0.00	0.00	0.00	0.08	0.00	0.00	0.00
5-MET-02	kmol/hr	0.00	0.00	0.00	0.00	0.00	0.07	0.07	0.00	0.07	0.00	0.00	0.00	0.07	0.00	0.00	0.00
TRIDE-01	kmol/hr	0.00	0.00	0.00	0.00	0.00	0.07	0.07	0.00	0.07	0.00	0.00	0.00	0.06	0.00	0.00	0.00
TETRA-01	kmol/hr	0.00	0.00	0.00	0.00	0.00	0.06	0.06	0.00	0.06	0.00	0.00	0.00	0.06	0.00	0.00	0.00
7-MET-01	kmol/hr	0.00	0.00	0.00	0.00	0.00	0.06	0.06	0.00	0.06	0.00	0.00	0.00	0.06	0.00	0.00	0.00
3-ETH-04	kmol/hr	0.00	0.00	0.00	0.00	0.00	0.05	0.05	0.00	0.05	0.00	0.00	0.00	0.05	0.00	0.00	0.00
2-MET-09	kmol/hr	0.00	0.00	0.00	0.00	0.00	0.05	0.05	0.00	0.05	0.00	0.00	0.00	0.05	0.00	0.00	0.00
PENTA-01	kmol/hr	0.00	0.00	0.00	0.00	0.00	0.04	0.04	0.00	0.04	0.00	0.00	0.00	0.04	0.00	0.00	0.00
7-MET-02	kmol/hr	0.00	0.00	0.00	0.00	0.00	0.04	0.04	0.00	0.04	0.00	0.00	0.00	0.04	0.00	0.00	0.00
6-MET-02	kmol/hr	0.00	0.00	0.00	0.00	0.00	0.04	0.04	0.00	0.04	0.00	0.00	0.00	0.04	0.00	0.00	0.00
PENTA-02	kmol/hr	0.00	0.00	0.00	0.00	0.00	0.04	0.04	0.00	0.04	0.00	0.00	0.00	0.04	0.00	0.00	0.00
4-MET-05	kmol/hr	0.00	0.00	0.00	0.00	0.00	0.03	0.03	0.00	0.03	0.00	0.00	0.00	0.03	0.00	0.00	0.00
TRIDE-02	kmol/hr	0.00	0.00	0.00	0.00	0.00	0.03	0.03	0.00	0.03	0.00	0.00	0.00	0.03	0.00	0.00	0.00
8-MET-01	kmol/hr	0.00	0.00	0.00	0.00	0.00	0.03	0.03	0.00	0.03	0.00	0.00	0.00	0.03	0.00	0.00	0.00
6-PEN-01	kmol/hr	0.00	0.00	0.00	0.00	0.00	0.03	0.03	0.00	0.03	0.00	0.00	0.00	0.03	0.00	0.00	0.00
7-BUT-01	kmol/hr	0.00	0.00	0.00	0.00	0.00	0.01	0.01	0.00	0.01	0.00	0.00	0.00	0.01	0.00	0.00	0.00
6-PEN-02	kmol/hr	0.00	0.00	0.00	0.00	0.00	0.01	0.01	0.00	0.01	0.00	0.00	0.00	0.01	0.00	0.00	0.00

	Units	LIQ1	H2-2	LIGHT1	WATER	PRODUCT2	PRODUCT3	LIQ4	LIGHT2	N-ALKANE	LIGHT3	LIGHT4	OFFGAS2	BIODIESE	BIOJET	PROPANE	OFFGAS1
HEXAD-01	kmol/hr	0.00	0.00	0.00	0.00	0.00	0.01	0.01	0.00	0.01	0.00	0.00	0.00	0.01	0.00	0.00	0.00
HEXAD-02	kmol/hr	0.00	0.00	0.00	0.00	0.00	0.01	0.01	0.00	0.01	0.00	0.00	0.00	0.01	0.00	0.00	0.00
7-MET-03	kmol/hr	0.00	0.00	0.00	0.00	0.00	0.01	0.01	0.00	0.01	0.00	0.00	0.00	0.01	0.00	0.00	0.00
14-ME-01	kmol/hr	0.00	0.00	0.00	0.00	0.00	0.01	0.01	0.00	0.01	0.00	0.00	0.00	0.01	0.00	0.00	0.00
15-ME-01	kmol/hr	0.00	0.00	0.00	0.00	0.00	0.01	0.01	0.00	0.01	0.00	0.00	0.00	0.01	0.00	0.00	0.00
4-PRO-01	kmol/hr	0.00	0.00	0.00	0.00	0.00	0.01	0.01	0.00	0.01	0.00	0.00	0.00	0.01	0.00	0.00	0.00
16-ME-01	kmol/hr	0.00	0.00	0.00	0.00	0.00	0.01	0.01	0.00	0.01	0.00	0.00	0.00	0.01	0.00	0.00	0.00
HEPTA-01	kmol/hr	0.00	0.00	0.00	0.00	0.00	0.01	0.01	0.00	0.01	0.00	0.00	0.00	0.01	0.00	0.00	0.00
HEPTA-02	kmol/hr	0.00	0.00	0.00	0.00	0.00	0.01	0.01	0.00	0.01	0.00	0.00	0.00	0.01	0.00	0.00	0.00
9-MET-01	kmol/hr	0.00	0.00	0.00	0.00	0.00	0.01	0.01	0.00	0.01	0.00	0.00	0.00	0.01	0.00	0.00	0.00
HEPTA-03	kmol/hr	0.00	0.00	0.00	0.00	0.00	0.01	0.01	0.00	0.01	0.00	0.00	0.00	0.01	0.00	0.00	0.00
8-PRO-01	kmol/hr	0.00	0.00	0.00	0.00	0.00	0.01	0.01	0.00	0.01	0.00	0.00	0.00	0.01	0.00	0.00	0.00
Volume Flow	l/min	40.22	496.49	801.47	3.43	1291.64	1292.40	37.15	731.07	69.86	22.34	0.36	69.49	19.29	23.40	0.21	2403.55

Table 36 Component abbreviation in the simulation

Carbon	n-alkane	Mono branch isomer	Name	Alias
C_8	Octane	4-METHYLHEPTANE	4-MET-01	C8H18-4
		3-Methylheptane	3-MET-01	C8H18-3
		2-METHYLHEPTANE	2-MET-01	C8H18-2
		3-Ethylhexane	3-ETH-01	C8H18-11
C_9	Nonane	2-Methyloctane	2-MET-02	C9H20-D1
		3-METHYLOCTANE	3-MET-02	C9H20-D2
		4-METHYLOCTANE	4-MET-02	C9H20-D3
		3-ETHYLHEPTANE	3-ETH-02	C9H20-E5
C_{10}	Decane	3-METHYLNONANE	3-MET-03	C10H22-E3
		2-METHYLNONANE	2-MET-03	C10H22-E2
		4-METHYLNONANE	4-MET-03	C10H22-E4
		5-METHYLNONANE	5-MET-01	C10H22-E5
C_{11}	Undecane	3-METHYLDECANE	3-MET-04	C11H24-N45
		2-METHYLDECANE	2-MET-04	C11H24-N5
C_{12}	Dodecane	3-METHYLUNDECANE	3-MET-05	C12H26-D1
		2-METHYLUNDECANE	2-MET-05	C12H26-N9
C_{13}	Tridecane	3-METHYLDODECANE	3-MET-06	C13H28-N9
		2-METHYLDODECANE	2-MET-06	C13H28-N1
C_{14}	Tetradecane	3-METHYLTRIDECANE	3-MET-07	C14H30-N7
		3-ETHYLDODECANE	3-ETH-03	C14H30-D1
		2-METHYLTRIDECANE	2-MET-07	C14H30-N1
C_{15}	Pentadecane	6-METHYLTETRADECANE	6-MET-01	C15H32-N9
		2-METHYLTETRADECANE	2-MET-08	C15H32-N1
		6-PROPYLDODECANE	6-PRO-01	C15H32-N16
		4-METHYLTETRADECANE	4-MET-04	C15H32-N7
		5-METHYLTETRADECANE	5-MET-02	C15H32-N8
		TRIDECANE,-3-ETHYL-	TRIDE-01	C15H32-N5
		TETRADECANE,-3-METHYL-	TETRA-01	C15H32-N6
		7-METHYLTETRADECANE	7-MET-01	C15H32-N3
C_{16}	Hexadecane	3-ETHYLTETRADECANE	3-ETH-04	C16H34-N19
		2-METHYLPENTADECANE	2-MET-09	C16H34-N1
		PENTADECANE,-3-METHYL-	PENTA-01	C16H34-N5

Carbon	n-alkane	Mono branch isomer	Name	Alias
C_{16}	Hexadecane	7-METHYLPENTADECANE	7-MET-02	C16H34-N7
		6-METHYLPENTADECANE	6-MET-02	C16H34-N9
		PENTADECANE,-5-METHYL-	PENTA-02	C16H34-N14
		4-METHYLPENTADECANE	4-MET-05	C16H34-N4
		TRIDECANE,-7-PROPYL-	TRIDE-02	C16H34-N15
		8-METHYLPENTADECANE	8-MET-01	C16H34-N12
		6-PENTYLUNDECANE	6-PEN-01	C16H34-N8
C_{17}	Heptadecane	7-BUTYLTRIDECANE	7-BUT-01	C17H36-N5
		6-PENTYLDODECANE	6-PEN-02	C17H36-N8
		HEXADECANE,-4-METHYL-	HEXAD-01	C17H36-N11
		HEXADECANE,-5-METHYL-	HEXAD-02	C17H36-N12
		7-METHYLHEXADECANE	7-MET-03	C17H36-N15
		14-METHYLHEXADECANE	14-ME-01	C17H36-N10
		15-METHYLHEXADECANE	15-ME-01	C17H36-N1
		4-PROPYLTETRADECANE	4-PRO-01	C17H36-N3
C_{18}	Octadecane	16-METHYLHEPTADECANE	16-ME-01	C18H38-N1
		HEPTADECANE,-4-METHYL-	HEPTA-01	C18H38-N11
		HEPTADECANE,-5-METHYL-	HEPTA-02	C18H38-N12
		9-METHYLHEPTADECANE	9-MET-01	C18H38-N6
		HEPTADECANE,-3-METHYL-	HEPTA-03	C18H38-N4
		8-PROPYLPENTADECANE	8-PRO-01	C18H38-N7

APPENDIX C Equipment sizing

C.1 Reactor

To estimate the actual size of the reactor, the laboratory results from Hsu et al. and C.H. Lin et al. were used. All parameters using for reactor sizing and process simulation in the deoxygenation process and hydrocracking/isomerization process was presented in Table 37

Table 37 Parameters for deoxygenation process and hydrocracking/isomerization process

Parameters	Unit	Deoxygenation process	hydrocracking/ isomerization process
Catalyst		NiMo/γ-Al_2O_3	NiAg/SAPO-11
Temperature	℃	370	360
Pressure	barg	55.2	29
H_2/Oil ratio		254.3 (Ncm^3/cm^3)	13.6 (Molar ratio)
WHSV	h^{-1}	3	-
LHSV	h^{-1}	-	1
Weight of catalyst	g	5	5
Reactor inner diameter	cm	3.0	1.3
Reactor length	cm	40.0	40.0
Total reactor volume	cm^3	282.74	50.67
Volume of catalyst bed	cm^3	184.00	32.94
%Volume of catalyst bed	% of total volume	65	65
Bulk density	g/cm^3	0.027	0.152

a) Calculation of deoxygenation process reactor

Weight of catalyst used = WHSV x mass flow rate of palm oil
= 3 (h^{-1}) x 2,107.72 (kg/h)
= 702.57 kg

Bulk density of catalyst = volume of catalyst bed x weight of catalyst [lab scale]
= 184 (cm^3) x 5 (g)
= 0.027 g/cm^3

Volume of catalyst bed = weight of catalyst used x bulk density of catalyst
= 702.57 (kg) / (0.027 (g/cm^3) x 1,000)
= 25.85 m^3

Total volume of reactor = volume of catalyst bed / %of volume of catalyst bed

= 25.85 (m^3) / 65.08%

= 39.73 m^3 or 40 m^3

b) Calculation of hydrocracking/isomerization process reactor

Total volume of reactor = volume flow rate of BHD / LHSV

= 3.93 (m^3/h) x 1 (h^{-1})

= 3.93 m^3 or 4 m^3

Bulk density of catalyst = weight of catalyst [lab scale] / volume of catalyst bed

= 5 (g) / 32.94 (cm^3)

= 0.152 g/cm^3

Volume of catalyst bed = Total volume of reactor x %of volume of catalyst bed

= 3.93 m^3 x 65%

= 2.55 m^3

Weight of catalyst used = Volume of catalyst bed x Bulk density of catalyst

= 2.55 (m^3) x 0.152 (g/cm^3) x 1000

= 387.73 kg

C2. Column

To determine distillate rate, reflux ratio and number of stages, DSTWU column model was performed and it needed to define cut point of distillation. For the lighter fraction, the cut point represents the end point, or temperature below which all of the light fraction components boil. For the heavier fraction, the cut point represents initial boiling point or temperature above which all of the heavier fraction's components boil. Table 38 showing the boiling point of pure component. The cut point of stabilizer column (T-201) set between propane and 2-methylheptane (i-C_8H_{18}) and for distillation column set between n-tetradecane (n-$C_{14}H_{30}$) and n-pentadecane (n-$C_{15}H_{32}$). Running result from DSTWU model was in Table 39 then they will be used as input parameters for Radfrac column model.

Table 38 Boiling point of component in the simulation

Component	Boiling point (°C)	Component	Boiling point (°C)	Component	Boiling point (°C)
H2	-252.76	C13	235.47	14-ME-01	295.34
CO	-191.45	2-MET-07	247.90	HEXAD-01	295.62
METHANE	-161.49	3-ETH-03	247.95	15-ME-01	296.75
ETHANE	-88.60	3-MET-07	248.40	C17	302.15
CO2	-78.45	6-PRO-01	251.62	HEPTA-01	308.68
PROPANE	-42.04	C14	253.58	HEPTA-02	309.17
H2O	100.00	6-MET-01	261.18	8-PRO-01	310.53
2-MET-01	117.65	5-MET-02	263.15	16-ME-01	311.21
4-MET-01	117.71	TRIDE-01	263.89	HEPTA-03	311.34
3-ETH-01	118.54	4-MET-04	264.03	C18	316.71
3-MET-01	118.93	6-PEN-01	264.60	9-MET-01	318.13
C8	125.68	2-MET-08	265.31	C19	329.90
4-MET-02	142.44	TETRA-01	266.28	C20	343.78
3-ETH-02	143.20	7-MET-01	266.55		
2-MET-02	143.30	C15	270.69		
3-MET-02	144.23	TRIDE-02	273.25		
C9	150.82	6-MET-02	277.31		
5-MET-01	165.15	8-MET-01	277.71		
4-MET-03	165.70	PENTA-02	278.13		
2-MET-03	167.00	3-ETH-04	280.42		
3-MET-03	167.80	7-MET-02	280.79		
C10	174.16	4-MET-05	281.13		
2-MET-04	189.20	2-MET-09	284.08		
3-MET-04	190.90	PENTA-01	284.28		
C11	195.93	7-BUT-01	285.06		
2-MET-05	210.00	C16	286.86		
3-MET-05	211.20	7-MET-03	288.32		
C12	216.32	4-PRO-01	288.32		
2-MET-06	229.50	6-PEN-02	292.93		
3-MET-06	230.20	HEXAD-02	294.47		

Table 39 Input parameter for Radfrac column model

Parameter	Unit	Stabilizer (T-201)	Distillation column (T-202)
Minimum reflux ratio	-	0.42	1.18
Actual reflux ratio	-	2	5
Number of stages	-	14	40
Feed stage	-	5	20
Distillate rate	kmol/h	1.483	6.638

C3. Heat exchanger

To calculate heat exchanger area of countercurrent shell and tube heat exchanger, heat duty must be known. It can obtain from energy balance in Aspen plus then heat exchanger area was calculated using

$$Q = UA\Delta T_{lm} \tag{9}$$

where heat duty (Q) is known by energy balance from simulation, the log mean temperature (ΔT_{lm}) is given by

$$\Delta T_{lm} = [(T_1 - t_2) - (T_2 - t_1)]/ln\{(T_1 - t_2)/(T_2 - t_1)\} \tag{10}$$

The temperature in equation (10) are define as Figure 38. Overall heat transfer coefficient was obtained form Lorenz T. Biegler and team [20]. The calculation result was shown in *Table 40*

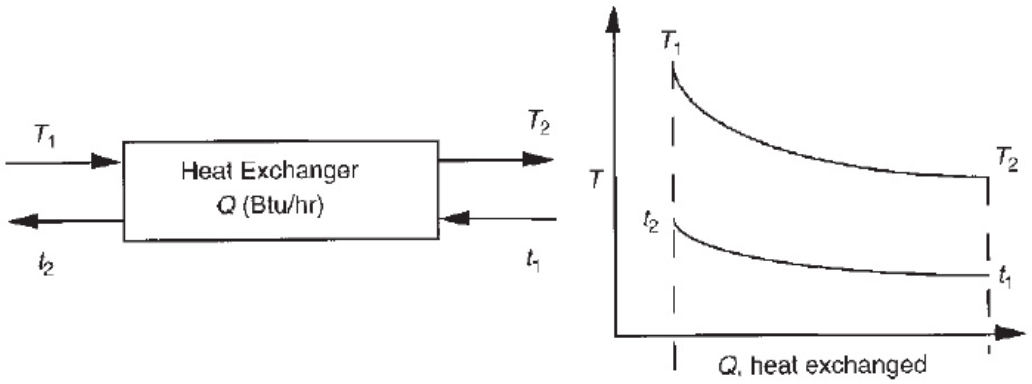

Figure 38 Heat exchanger temperature

Table 40 Heat transfer area calculation

	T_1 (°C)	T_2 (°C)	t_1 (°C)	t_2 (°C)	ΔT_{lm} (°C)	U (kcal/h m2 °C)	Q (kcal/h)	A (m^2)	A +20% (m^2)
E-103	370	40	30	40	92	317	576,921	19.9	24
E-203	360	50	30	40	108	146	485,844	30.7	37
E-204	49	38	30	40	8	390	10,687	3.2	4
E-206	224	170	30	40	161	146	491,551	20.9	26

C4. Flash drum

Selected D-202 volume (V) based on a five-minute liquid hold up time with an equal volume added for vapor flows. D-102 and D-203 volume was estimated by Aspen plus

$$V = 2[\frac{F_L \tau}{\rho_l}] \quad \text{C1.}$$

Where F_L = liquid flow rate leaving the vessel

ρ_l = Liquid density

τ = residence time, typically set to five minute

Table 41 Flash drum sizing calculation

List	**F_L** (kg/min)	τ (min)	ρ_l (kg/m^3)	**V** (m^3)	**V +20%** (m^3)
D-202	25.70	5	23.09	11.13	14

APPENDIX D ECONOMIC ANALYSIS AND FEASIBILITY STUDY

The evaluation of fixed capital cost and manufacturing costs was performed. Firstly, The BHD plant with a capacity of 120,229 bbl/y was compared with bio-jet and biodiesel plant with total capacity 127,595 bbl/y. The economic analysis of both cases was also considered, then the feasibility study was executed.

D1. Fixed capital investment calculation

The equipment module costing technique [21] was used for estimating the fixed capital investment in this research. This method calculated the purchased cost of equipment, which evaluated for a based condition then multiply by a factor to the other condition depending on equipment type, system pressure, and material for construction. The bare module cost for each piece of equipment, C_{BM}, was determined by equation D.1. The based case conditions were using carbon steel (CS) for fabrication material and unit operated at near-ambient temperature

$$C_{BM} = C^0_p F_{BM} = C^0_p (B_1 + B_2 F_M F_P) \quad \text{D1.}$$

where, C_{BM} = bare module equipment cost: direct and indirect costs for each unit

C^0_p = purchased cost for base condition

F_{BM} = bare module factor for the equipment

B_1. B_2 = bare module factor for equipment

F_M = material factor

F_P = Pressure factor

Purchased cost of the equipment, at ambient operating pressure and using carbon steel construction estimated by equation D2

$$\log_{10} C^0_P = K_1 + K_2 \log_{10}(A) + K_3 [\log_{10}(A)]^2 \quad \text{D2.}$$

where A = capacity or size parameter for equipment

K_1, K_2, K_3, = parameter given in The calculated **purchased costs of the equipment and corresponding parameters were interpreted in Table 44 to Table 47**

Table 42 (Depending on equipment)

The pressure factor is calculated by equation D3, which is a pressure factor for process vessel and equation D4 for other process equipment. The material factor was determined by Turton. [21]

$$F_{P,vessel} = \frac{\frac{(P+1)D}{2[850-0.6(P+1)]} + 0.00315}{0.0063} \quad \text{for } t_{vessel} > 0.0063 \text{ m} \quad \text{D3}$$

If F_p, vessel < 1 (corresponding to t_{vessel} < 0.0063m), then F_p, vessel = 1, For Pressure < -0.5 barg, Fp vessel = 1.25 where P= pressure and D = diameter

$$\log_{10} F_p = C_1 + C_2 \log_{10} P + C_3 (\log_{10} P)^2 \quad \text{D4}$$

where, parameter C_1, C_2, and C_3 used in this research were listed in *Table 43*

The calculated purchased costs of the equipment and corresponding parameters were interpreted in Table 44 to Table 47

Table 42 Equipment cost data

Equipment	**K_1**	**K_2**	**K_3**	**Capacity, Unit**	**Min size**	**Max size**
Heat exchanger - fixed tube type	4.3247	-0.303	0.1634	Area, m2	10	1000
Heat exchanger - double pipe	3.3444	0.2745	-0.0472	Area, m2	1	10
Heat exchanger - U-tube	4.1884	-0.2503	0.1974	Area, m2	10	1000
Furnaces - Nonreactive fired heater	7.3488	-1.1666	0.2028	Duty, kW	1000	100000
Furnaces - Reformer furnaces	3.068	0.6597	0.0194	Duty, kW	3000	100,000
Process vessel - Vertical	3.4974	0.4485	0.1074	Volume, m3	0.3	520
Tower - Tray and packed	3.4979	0.4485	0.1074	Volume, m3	0.3	520
Trays - sieve	2.9949	0.4465	0.3961	Area, m2	0.07	12.3
Pumps - Centrifugal	3.3892	0.0536	0.1538	Shaft power, kW	1	300
Compressor - centrifugal	2.2897	1.3604	-0.1027	Fluid power, kW	450	3000

Table 43 Pressure factor for process equipment

Equipment type	**C_1**	**C_2**	**C_3**	**P range (barg)**
Heat exchanger - fixed tube type	0	0	0	P<5
	0.03881	-0.11272	0.08183	5<P<140
Heat exchanger - double pipe	0	0	0	P<40
Heat exchanger - U-tube	0	0	0	P<5
	0.03881	-0.11272	0.08183	5<P<140
Process vessel - Vertical	see equation D3			
Tower - Tray and packed	see equation D3			
Trays - sieve	0	0	0	-
Pumps - Centrifugal	0	0	0	P<10
	-0.3935	0.3957	-0.00226	10<P<100
Compressor - centrifugal	0	0	0	-
Furnances	0	0	0	P<10
	0.1347	-0.2368	0.1021	10<P<200

Table 44 Purchased cost for BHD plant and Bio-jet fuel/biodiesel plant

Equipment	Type	Cap.	$\log_{10}(A)$	$[\log_{10}(A)]^2$	$\log_{10}C^0_p$	C^0_p ($)	THB
Heater1 (E-101)	Non reactive furnance	469	2.671172843	7.13516436	5.67962109	478,213	15,595,950
Heater2 (E-102)	Non reactive furnance	110	2.041392685	4.1672841	5.81243651	649,287	21,175,187
Heater3 (E-201)	Non reactive furnance	427	2.630427875	6.91915081	5.68334662	482,333	15,730,313
Heater4 (E-202)	Non reactive furnance	94	1.973127854	3.89323353	5.83649681	686,273	22,381,416
Heat exchanger (E-103)	Fixed tube	24	1.380211242	1.90498307	4.21777023	16,511	538,469
Heat exchanger (E-203)	Fixed tube	37	1.568201724	2.45925665	4.25137741	17,839	581,793
STABILIZ-cond	Double pipe	4	0.602059991	0.36247623	4.20150444	15,904	518,675
DISTIL-cond	Fixed tube	26	1.414973348	2.00214958	4.22311432	16,715	545,136
STABILIZ-reb	Non reactive furnance	411	2.614190386	6.83399137	5.68501895	484,193	15,791,002
DISTIL-reb	Non reactive furnance	373	2.571662256	6.61344676	5.68990581	489,673	15,969,693
Flash1 (D-102)	Vertical	3	0.477121255	0.22764469	3.73583792	5,443	177,512
Flash2 (D-202)	Vertical	14	1.146128036	1.31360947	4.15252008	14,208	463,352
Flash3 (D-203)	Vertical	3	0.477121255	0.22764469	3.73583792	5,443	177,512
STABILIZ-tower	Tray and packed	5	0.698970004	0.48855907	3.86385929	7,309	238,369
DISTIL-tower	Tray and packed	25	1.397940009	1.95423627	4.33476107	21,615	704,939
Reactor 1 (D-101)	packed bed	40	1.602059991	2.56659622	4.49157634	31,015	1,011,503
Reactor 2 (D-201)	packed bed	4	0.602059991	0.36247623	3.80635385	6,403	208,807
Pump1 (P-101)	Centrifugal	13	1.113943352	1.24086979	3.63975314	4,363	284,560.02
Pump2 (P-201)	Centrifugal	5	0.698970004	0.48855907	3.50180518	3,175	207,121.85
STABILIZ-reflux pump	Centrifugal	1	0	0	3.3892	2,450	159,816.18
DISTIL-reflux pump	Centrifugal	2	0.301029996	0.09061906	3.41927242	2,626	171,274.68
Compressor	Centrifugal	13	1.113943352	1.24086979	3.63975314	4,363	284,560.02
Tray-STABILIZ	Sieve	0.291864	-0.534820202	0.28603265	3.40452546	45,688	1,490,008
Tray-DISTL	Sieve	0.656693	-0.182637684	0.03335652	3.38454085	133,323	4,348,048
Sum						3,624,363	118,755,018

Table 45 Bare module for BHD plant and Bio-jet fuel/biodiesel plant

Equipment	Type	B_1	B_2	F_M	F_P	$B_1 + B_2F_MF_P$	C_{BM} ($)	THB
Heater1 (E-101)	Non reactive furnance	-	-	-	1	2.1	1,004,247	32,751,496
Heater2 (E-102)	Non reactive furnance	-	-	-	1.07604134	2.1	1,363,502	44,467,893
Heater3 (E-201)	Non reactive furnance	-	-	-	1.01567794	2.1	1,012,898	33,033,658
Heater4 (E-202)	Non reactive furnance	-	-	-	1.01567794	2.1	1,441,173	47,000,973
Heat exchanger (E-103)	Fixed tube	1.63	1.66	1	1.23165229	3.6745428	60,670	1,978,628.63
Heat exchanger (E-203)	Fixed tube	1.63	1.66	1	1.11936257	3.48814187	62,226	2,029,375.00
STABILIZ-cond	Double pipe	1.74	1.55	1	1	3.29	52,324	1,706,440
DISTIL-cond	Fixed tube	1.63	1.66	1	1	3.29	54,993	1,793,498
STABILIZ-reb	Non reactive furnance	-	-	-	0.99734673	2.1	1,016,806	33,161,105
DISTIL-reb	Non reactive furnance	-	-	-	1	2.1	1,028,312	33,536,355
Flash1 (D-102)	Vertical	2.25	1.82	1	5.81253104	12.8288065	69,827	2,277,272
Flash2 (D-202)	Vertical	2.25	1.82	1	3.42354867	8.48085857	120,492	3,929,621
Flash3 (D-203)	Vertical	2.25	1.82	1	2.44737945	6.7042306	36,491	1,190,084
STABILIZ-tower	Tray and packed	2.25	1.82	1	1.82764668	5.57631696	40,757	1,329,222
DISTIL-tower	Tray and packed	2.25	1.82	1	0.79391907	3.69493271	79,867	2,604,704
Reactor 1 (D-101)	packed bed	2.25	1.82	1	0.73959901	3.59607021	111,533	3,637,435
Reactor 2 (D-201)	packed bed	2.25	1.82	1	0.61080329	3.36166199	21,523	701,938
Pump1 (P-101)	Centrifugal	1.89	1.35	1.55	1.99071643	6.05557413	26,419	861,587.15
Pump2 (P-201)	Centrifugal	1.89	1.35	1.55	1.34685067	4.70828503	14,951	487,594.36
STABILIZ-reflux pump	Centrifugal	1.89	1.35	1.55	1.34685067	4.70828503	11,536	376,230.06
DISTIL-reflux pump	Centrifugal	1.89	1.35	1.55	1	3.9825	10,458	341,050.71
Compressor	Centrifugal	-	-	-	-	2.75	11,997	391,270.03
Tray-STABILIZ	Sieve	-	-	-	-	1	45,688	1,490,008
Tray-DISTL	Sieve	-	-	-	-	1	133,323	4,348,048
Sum							7,832,014	255,425,486

Table 46 Pressure factor for process vessel in BHD plant and Bio-jet fuel/biodiesel plant

Equipment	Type	Pressure (P)	Diameter (D)	P+1	$F_{p,vessel}$
Flash1 (D-102)	Vertical	58.60552	0.9144	59.6055192	5.81253104
Flash2 (D-202)	Vertical	32.43421	0.9144	33.4342108	3.42354867
Flash3 (D-203)	Vertical	21.44746	0.9144	22.4474608	2.44737945
STABILIZ-tower	Tray and packed	21.94746	0.6096	22.9474608	1.82764668
DISTIL-tower	Tray and packed	2.434211	0.9144	3.4342108	0.79391907
Reactor 1	packed bed	0	2.56429408	1	0.73959901
Reactor 2	packed bed	0	1.185865553	1	0.61080329

Table 47 Pressure factor for process equipment in BHD plant and Bio-jet fuel/biodiesel plant

Equipment	Type	Pressure (P)	Diameter (D)	C_1	C_2	C_3	$\log_{10}P$	$(\log_{10}P)^2$	$C_2\log_{10}P$	$C_3(\log_{10}P)^2$	$\log_{10}F_p$	F_p
Heater1 (E-101)	Non reactive furnace	1.00	-	0	0	0	0	0	0	0	0	1
Heater2 (E-102)	Non reactive furnace	55.00	-	0.1347	-0.2368	0.1021	1.740362689	3.028862291	-0.41212	0.30924684	0.031829	1.076041
Heater3 (E-201)	Non reactive furnace	29.00	-	0.1347	-0.2368	0.1021	1.462397998	2.138607904	-0.3463	0.21835187	0.006756	1.015678
Heater4 (E-202)	Non reactive furnace	29.00		0.1347	-0.2368	0.1021	1.462397998	2.138607904	-0.3463	0.21835187	0.006756	1.015678
Heat exchanger (E-103)	Fixed tube	55.00		0.03881	-0.11272	0.08183	1.740362689	3.028862291	-0.19617	0.2478518	0.090488	1.231652
Heat exchanger (E-203)	Fixed tube	29.00		0.03881	-0.11272	0.08183	1.462397998	2.138607904	-0.16484	0.17500228	0.048971	1.119363
STABILIZ-cond	Double pipe	21.49	-	0	0	0	1.332154001	1.774634282	0	0	0	1
DISTIL-cond	Fixed tube	2.43	-	0	0	0	0.386358185	0.149272647	0	0	0	1
STABILIZ-reb	Non reactive furnace	19.00	-	0.1347	-0.2368	0.1021	1.278753601	1.635210772	-0.30281	0.16695502	-0.00115	0.997347
DISTIL-reb	Non reactive furnace	2.00	-	0	0	0	0.301029996	0.090619058	0	0	0	1
Pump1	Centrifugal	58.60552	-	-0.3935	0.3957	-0.00226	1.767938518	3.125606603	0.699573	-0.0070639	0.299009	1.990716
Pump2	Centrifugal	21.44746	-	-0.3935	0.3957	-0.00226	1.331375883	1.772561742	0.526825	-0.004006	0.129319	1.346851
STABILIZ-reflux pump	Centrifugal	21.44746	-	-0.3935	0.3957	-0.00226	1.331375883	1.772561742	0.526825	-0.004006	0.129319	1.346851
DISTIL-reflux pump	Centrifugal	2.434211	-	0	0	0	0.386358185	0.149272647	0	0	0	1
Compressor	Centrifugal	58.60552	-	0	0	0	1.767938518	3.125606603	0	0	0	1
Tray-STABILIZ	Sieve	21.94746	-	0	0	0	1.341384282	1.799311791	0	0	0	1
Tray-DISTL	Sieve	2.434211	-	0	0	0	0.386358185	0.149272647	0	0	0	1

Purchased equipment cost was affected by time; thus, the equation D5 was used for convert cost at reference year to specify the year.

$$C_2 = C_1\left(\frac{I_2}{I_1}\right) \quad \text{D5}$$

where, C = Purchased cost

I = Cost index, CEPCI (Chemical Engineering Plant Cost Index) was used

Subscript: 1 = refers to base time when cost is known (2001)

Subscript: 2 = refers to time when cost is desired (2017)

Table 48 Effect of time on purchased equipment cost

Year	CEPCI	Cost (Baht)
2001	397	255,425,486
2017	562.1	361,649,032

D2. Manufacturing cost

Manufacturing cost can be estimated from the cost of fixed capital investment (FCI), operating labor (C^{OL}), Cost of utilities (C_{UT}), Cost of waste treatment (C_{WT}), and Cost of raw materials (C_{RM}) by Turton method [21]. Manufacturing cost of bio-jet fuel/biodiesel plant was shown in *Table 49*, and the manufacturing cost of the BHD plant was shown in *Table 50*

Table 49 Manufacturing cost of bio-jet/biodiesel plant

Cost item	
1. Direct manufacturing cost	MB/Y
a. Raw materials	347.17
b. Waste treatment	2.98
c. Utilities	13.70
d. Operating labor	27.38
e. Direct supervisory and clerical labor	4.93
f. Maintenance and repairs	21.70
g. Operating supplies	3.25
h. Laboratory charges	4.11
i. Patents and royalties	18.71
Total direct manufacturing cost	**443.91**
2. Fixed manufacturing cost	
a. Local taxes and insurance	11.57
b. Plant overhead	32.40
Total Fixed manufacturing cost	**43.97**
3. General manufacturing expenses	
a. Administration cost	8.10
b. Distribution and selling costs	68.59
c. Research and development	31.18
Total General manufacturing costs	**107.86**
Total costs	**595.75**

Table 50 Manufacturing cost of BHD plant

Cost item	
1. Direct manufacturing cost	MB/Y
a. Raw materials	347.17
b. Waste treatment	2.98
c. Utilities	13.70
d. Operating labor	27.38
e. Direct supervisory and clerical labor	4.93
f. Maintenance and repairs	21.70
g. Operating supplies	3.25
h. Laboratory charges	4.11
i. Patents and royalties	18.71
Total direct manufacturing cost	**443.91**
2. Fixed manufacturing cost	
a. Local taxes and insurance	11.57
b. Plant overhead	32.40
Total Fixed manufacturing cost	**43.97**
3. General manufacturing expenses	
a. Administration cost	8.10
b. Distribution and selling costs	68.59
c. Research and development	31.18
Total General manufacturing costs	**107.86**
Total costs	**595.75**

D.3 Feasibility study

The feasibility study of bio-jet fuel/biodiesel plant was an example for calculation, showing in Table 51 to Table 58

Table 51 Assumption for calculation

1	Selling price (US/liter)	:	Bio-jet fuel	Biodiesel	Propane	
		:	1.21	0.92	0.17	
2	Production day	:	7,920	hour/year		
3	Insurance	:	0.15	% of fixed asset		
4	Raw material	:	Palm oil (Baht/kg)	Hydrogen (baht/kg)	$NiMo/Y\text{-}Al_2O_3$ ($/kg)	NiAg/SAPO-11 ($/kg)
			18.318	32.613	4.38	114.7
5	Interest					
	- MLR	:	5.58	%		
	- MOR	:	5.95	%		
6	Exchange rate	:	32.613	Baht/USD		
7	Depreciation	:	Straight-line depreciation during 15 years			
8	Corporate income tax rate	:	20	%		
9	Debt to Equity ratio	:	1.17	:1		

Table 52 Investment cost

Description	Cost		Total Cost
	M USD	M THB	M THB
Fixed capital investment	11.1	361.6	361.6
Contingency 18%			65.10
Interest During Construction			4.92
Total Investment			**431.67**

Table 53 project benefit

	Description	**Production (liter/h)**	**Price (US/liter)**	**Benefit (MB/Y)**
1	Bio-jet fuel product	1,404.28	1.21	438.89
2	Biodiesel product	1,157.09	0.92	274.96
3	Propane product	12.62	0.17	0.56
	Total benefit			**714.41**

Table 54 Projected income statement and EBITDA (Unit: MB)

	Description	Year 0	Year 1	Year 2	Year 3	Year 4	Year 5	Year 6	Year 7	Year 8	Year 9	Year 10	Year 11	Year 12	Year 13	Year 14	Average
1	Production Cost Saving	-	-	-	714.4	714.4	714.4	714.4	714.4	714.4	714.4	714.4	714.4	714.4	714.4	714.4	571.53
2	Incremental Insurance Expense	(0.5)	(0.5)	(0.5)	(0.5)	(0.5)	(0.5)	(0.5)	(0.5)	(0.5)	(0.5)	(0.5)	(0.5)	(0.5)	(0.5)	(0.5)	(0.54)
3	**Net Benefit**	**(0.5)**	**(0.5)**	**(0.5)**	**713.9**	**713.9**	**713.9**	**713.9**	**713.9**	**713.9**	**713.9**	**713.9**	**713.9**	**713.9**	**713.9**	**713.9**	**570.99**
4	Manufacturing cost	-	-	-	(595.8)	(595.8)	(595.8)	(595.8)	(595.8)	(595.8)	(595.8)	(595.8)	(595.8)	(595.8)	(595.8)	(595.8)	(476.60)
8	Depreciation Expenses	(28.8)	(28.8)	(28.8)	(28.8)	(28.8)	(28.8)	(28.8)	(28.8)	(28.8)	(28.8)	(28.8)	(28.8)	(28.8)	(28.8)	(28.8)	(14.39)
9	**Net Profit before Interest and Tax**	**(29.3)**	**(29.3)**	**(29.3)**	**89.3**	**89.3**	**89.3**	**89.3**	**89.3**	**89.3**	**89.3**	**89.3**	**89.3**	**89.3**	**89.3**	**89.3**	**65.61**
10	Interest Expenses	(2.9)	(4.9)	(3.7)	(2.6)	(1.4)	(0.3)	-	-	-	-	-	-	-	-	-	(1.05)
11	**Net Profit before Tax**	**(32.2)**	**(34.2)**	**(33.0)**	**86.8**	**87.9**	**89.1**	**89.3**	**89.3**	**89.3**	**89.3**	**89.3**	**89.3**	**89.3**	**89.3**	**89.3**	**64.56**
12	Corporate Income Tax - 20%	-	-	-	(17.4)	(17.6)	(17.8)	(17.9)	(17.9)	(17.9)	(17.9)	(17.9)	(17.9)	(17.9)	(17.9)	(17.9)	(14.24)
13	**Net Profit/ (Loss) after Tax**	**(32.2)**	**(34.2)**	**(33.0)**	**69.4**	**70.3**	**71.2**	**71.5**	**71.5**	**71.5**	**71.5**	**71.5**	**71.5**	**71.5**	**71.5**	**71.5**	**50.32**
14	EBITDA	(0.54)	(0.54)	(0.54)	118.12	118.12	118.12	118.12	118.12	118.12	118.12	118.12	118.12	118.12	118.12	118.12	101.17
15	EBITDA on Total Investment	0%	0%	0%	27%	27%	27%	27%	27%	27%	27%	27%	27%	27%	27%	27%	23.4%

Table 55 Projected cash flow statement, IRR and NPV calculation (Unit: MB)

Description	Year 0	Year 1	Year 2	Year 3	Year 4	Year 5	Year 6	Year 7	Year 8	Year 9	Year 10	Year 11	Year 12	Year 13	Year 14
Cash Outflows															
Fixed Assets Investment	(74)	(255)	(103)	-	-	-	-	-	-	-	-	-	-	-	-
Total Cash Outflows	**(74)**	**(255)**	**(103)**	**-**	**-**	**-**	**-**	**-**	**-**	**-**	**-**	**-**	**-**	**-**	**-**
Cash Inflows															
Net Profit/ (Loss) after Tax	(32)	(34)	(33)	69	70	71	71	71	71	71	71	71	71	71	71
+ Depreciation	29	29	29	29	29	29	29	29	29	29	29	29	29	29	29
+ Interest Expenses	3	5	4	3	1	0	-	-	-	-	-	-	-	-	-
+ Tax Shield	(0.6)	(1.0)	(0.7)	(0.5)	(0.3)	(0.1)	-	-	-	-	-	-	-	-	-
+ Salvage value				-	-	-	-	-	-	-	-	-	-	-	28.8
Total Cash Inflows	**(1)**	**(1.5)**	**(1.3)**	**100.3**	**100.3**	**100.3**	**100.3**	**100.3**	**100.3**	**100.3**	**100.3**	**100.3**	**100.3**	**100.3**	**129.0**
Net Cash Flow	**(75)**	**(256.3)**	**(104.2)**	**100.3**	**100.3**	**100.3**	**100.3**	**100.3**	**100.3**	**100.3**	**100.3**	**100.3**	**100.3**	**100.3**	**129.0**

NPV @ WACC 12.5%	=	99.79	MB		
IRR	=	16.90%			
Payback Period	=	7	Years	4	Months

Table 56 Interest expenses calculation (Unit: MB)

Fixed Assets	432	MB
Total Investment	**432**	**MB**
Debt to Equity ratio	1.17	: 1
Equity	328.9	MB
Total Debt	**102.7**	**MB**
Initial incremental working capital	0	MB
Long term Loan for Fixed Assets Investment	**102.7**	**MB**

			Year 0	Year 1	Year 2	Year 3	Year 4	Year 5	Year 6	Year 7	Year 8	Year 9
Long Term Loan												
Beginning Balance				92.5	71.9	51.4	30.8	10.3				
1st payment				(10.3)	(10.3)	(10.3)	(10.3)	(10.3)				
Mid-year balance			102.7	82.2	61.6	41.1	20.5	(0.0)				
2nd payment			(10.3)	(10.3)	(10.3)	(10.3)	(10.3)					
Ending balance			92.5	71.9	51.4	30.8	10.3					
Long Term Interest Expenses	**5.58%**	**MLR**	**2.9**	**4.9**	**3.7**	**2.6**	**1.4**	**0.3**				
TOTAL INTERST EXPENSES			**2.9**	**4.9**	**3.7**	**2.6**	**1.4**	**0.3**	-	-	-	-

Table 57 Depreciation calculation (Unit: MB)

Description	Total Investment	Estimated Life (Year)	Total	Year 0 1	Year 1 2	Year 2 3	Year 3 4	Year 4 5	Year 5 6	Year 6 7	Year 7 8	Year 8 9	Year 9 10	Year 10 11	Year 11 12	Year 12 13	Year 13 14	Year 14 15
Machine and Equipment	431.7	15.0	431.7	28.8	28.8	28.8	28.8	28.8	28.8	28.8	28.8	28.8	28.8	28.8	28.8	28.8	28.8	28.8
Net Operating Assets				402.9	374.1	345.3	316.6	287.8	259.0	230.2	201.4	172.7	172.7	143.9	115.1	86.3	57.6	28.78

Table 58 Interest during construction calculation (Unit: MB)

Details	Investment	Payment	Amount	Debt	Duration (month)	IDC	Equity
1 Fixed capital investment	362	20%	72.3	20.5	25	2.4	51.8
		70%	253.2	71.9	7	2.3	181.2
		10%	36.2	10.3	4	0.2	25.9
Sub Total Fixed Assets Investment	362		361.649	102.7		4.9	258.9
1 Contingency 18%	65						65
2 Interest During Construction	4.9						4.92
Total Fixed Assets Investment	432			102.73			328.93
3 Working Capital	0			0			
Total Investment	**432**			**102.73**			**328.93**